University of Cape Town,

Hydrometallurgy Laboratory

Department of Chemical Engineering

An investigation of cyanide-based heap leaching for extracting precious metals from Platreef ore

By:

James Malumbo Mwase

Supervisor:

Prof. Jochen Petersen

2016

Submitted in fulfilment of the requirements for the award of the

degree of Doctorate in Chemical Engineering

Acknowledgements

Praises to my heavenly Father and Lord and saviour Jesus Christ, everything comes from you and all I do is for your honour.

To my family, my parents Frank and Julie Mwase, my elder brother Frank, my elder sisters Patricia and Thoko, my nieces Sammy and Nandi and my nephews Nthato and Frank Jnr. Thank you for your support and love, I will always love you all.

Thanks to my supervisor Professor Jochen Petersen for your supervision and support.

I would like to acknowledge Lonmin Plc for providing the funding for this project and the test material.

Thanks to Professor Jacques Eksteen for his support without which this project would not have been funded.

My thanks to the various members of the Centre of Bioprocess Engineering Research for all the support provided, technical and administrative. Especially the Biominerals discussion group

For their technical support, my thanks to the Centre for Minerals Research (CMR) and the Crystallization and Precipitation Unit (CPU).

Declaration

I, **James Malumbo Mwase**, hereby declare that the work on which this thesis is based is my original work (except where acknowledgements indicate otherwise) and that neither the whole work nor any part of it has been, is being, or is to be submitted for another degree in this or any other university. I authorise the University to reproduce for the purpose of research either the whole or any portion of the contents in any manner whatsoever.

Signature: Date: 15/04/2016

Signed by candidate

Symbol

Al: Aluminium

Ca: Calcium

Co: Cobalt

Cr: Chromium

Cu: Copper

Fe: Iron

g: Grams

kg: Kilograms

L: Litres

m: Metres

M: Molar

Mg: Magnesium

mg: Milligrams

Ni: Nickel

Pd: Palladium

Pt: Platinum

Rh: Rhodium

Ru: Ruthenium

s: Seconds

Si: Silicon

µg: micrograms

ppm: parts per million

ppb: parts per billion

BSTR: Batch stirred tank reactor

PGMs: Platinum Group Metals

BMs: Base Metals

PMR: Precious Metals Refinery

BMR: Base Metals Refinery

PLS: Pregnant Leach Solution

Summary

Cyanide heap leaching had been proposed as an alternative to the classic crush-mill-float-smelt-refine route for processing platinum group metals (PGMs) from the Platreef ore body. Overall the process includes two stages of leaching. The first stage involves the thermophile bioleaching of the base metal (BM) sulphide minerals and acts as a form of pre-treatment to oxidise sulphur compounds and recovery valuable metals such as Cu, Ni and Co. The second stage focuses on cyanide-based heap leaching for the recovery of precious metals (PGMs + gold) from the solid residue of the first stage. Exploration and optimisation of this second stage in the context of a whole ore Platreef material is the focus of the present study.

The first part of the study used a series of laboratory tests simulating heap leaching, conducted on coarse ore. The initial tests showed high recoveries of base metals (Cu, Ni and Co) could be achieved in a pre-treatment bioleach process, while in the second stage cyanide leach high levels of Pd and Au were extracted, but only 58% of the Pt after 60 days from the whole ore. It was observed that during the 60 day leaching period the rate of Pt leaching decreased considerably after 35 days. From the trajectory of the Pt leach curve from the 35 day mark onwards, it was observed that the leaching would not cease even after 60 days but would likely proceed but at that slow pace which indicated further Pt extraction would not be commercially viable in the long run. Mineralogical analysis has indicated that a significant component of the Pt in the ore is in the form a mineral sperrylite ($PtAs_2$), which appears to leach slowly in cyanide as compared to other mineral forms such as certain tellurides and sulphides in the ore.

Subsequently, efforts were made to investigate methods to improve the second stage leach process, in terms of Pt leaching from sperrylite, through further work on a pure mineral sample. The key focus was on finding a suitable oxidant that can be used in cyanide solutions, from among air, oxygen and ferricyanide, to facilitate the dissolution. Various tests using sperrylite mineral samples micronized to 5 µm in batch stirred tank reactors (BSTR) at 50°C were conducted. It was found that a combination of ferricyanide with cyanide extracted as much as 16 times more Pt than tests using only cyanide. The presence of air or pure oxygen did not contribute significantly to the amount of Pt leached in this system and made no difference at all in the leach tests using only cyanide. Further bench-scale studies focused on characterising the leaching mechanism of sperrylite in cyanide-ferricyanide solutions. It was found that the reaction, after proceeding at appreciable rates initially, tended to cease after 1 day, indicating

some form of surface passivation, tentatively related to some form of solution equilibrium being achieved. However after re-leaching the sample with fresh solution, the Pt dissolution improved tremendously. This was further investigated in continuous leaching of a sample of the mineral using a small bed of sperrylite fixed in mini-columns. The results from the mini-columns showed the same leaching pattern as the experiments using BSTRs. It was eventually revealed that a suitable wash of the sperrylite sample using water removes the inhibiting layer and facilitates further and improved leaching. Unlike the cyanide-only system where the passivation was attributed to As build-up at the surface, in the cyanide-ferricyanide system it was attributed to adsorption of unknown reaction products on the mineral surface.

Residual samples from batch leach experiments were analysed using X-ray photoelectron spectroscopy and showed samples from the cyanide-ferricyanide tests had less As on the surface than the untreated sample and the sample leached in cyanide. To some degree this supported the hypothesis that Pt leaching is eventually hindered by As passivation in a cyanide system. The presence of ferricyanide serves to oxidise As and thereby release more Pt in solution. Additionally, electrochemical techniques using a sperrylite electrode were employed to further understand the redox reaction under varying oxidation conditions. While the tests indicated a weak current under mildly oxidising conditions in cyanide solutions, this became rapidly limiting at potentials expected in a ferricyanide solution, indicating a form of surface passivation. An attempt was made to determine the number of electrons transferred during Pt dissolution to indicate the primary reaction mechanism through a long-term test held at constant potential, but dissolution rates were too small to be conclusive.

Hence the study has shown that the cyanide-based heap leaching of PGMs from Platreef type ores is feasible in principle, but the dissolution of $PtAs_2$ remains limited. While the study has given valuable pointers to understanding this observation, the conclusion is that $PtAs_2$ is refractory in the given context and further development of this process remains promising through further investigation into the use of the cyanide-ferricyanide combination.

Contents

List of Figures

List of Tables

1. Chapter 1: Introduction

As much as 90% of the entire world's known primary platinum group metal (PGM) reserves can be found in the Republic of South Africa, mostly in the area known as the Bushveld Igneous Complex (British Geological Survey, 2009). Currently the PGMs are mostly sourced from three ore bodies namely the Merensky Reef, the Upper Group 2 (UG2) and the Platreef. Aside from the vast reserves of PGMs, these ore bodies house significant quantities of base metals (BMs), namely copper, nickel and cobalt, mostly in the form of sulphide minerals and an appreciable amount of gold. The industry currently relies heavily on the conventional crush-mill-float-concentrate-smelt-refine route to obtain PGMs (Crudwell et al., 2011). This in turn relies on the mineralogy of the ore being suitable for this process. The PGMs must either be in sulphide mineral form or deport to the sulphide minerals (copper, nickel and iron) present in more significant quantities, which are liberated by crushing and milling and concentrated via flotation. The high grade concentrate can then be treated by a smelter for further concentration and the resulting matte is refined by a series of pressure leach (sulphate and chloride based) and purification stages to produce the BMs and PGMs.

However, there are many instances where this process may not be feasible. The study focused specifically on the case of the Platreef ore body whose unique mineralogy presents a challenge for processing via the conventional route (Shackleton et al., 2007a; Shackleton et al., 2007b; Shamaila and O'Connor, 2008). In this regard heap leaching presents an alternative process route that may have lower costs and be more economically viable. Unlike the copper and gold industries which have made use of percolation leaching methods, such as heap, dump and vat leaching, for low-grade or mineralogically challenging ores, the PGM industry is yet to apply these alternative methods that are direct and cost less.

Previous studies have investigated the feasibility of using heap leaching to extract PGMs from PGM bearing concentrates from Merensky, UG2 and Platreef ore (Mwase et al., 2012a; Mwase, 2009). The process was conducted in two stages with encouraging results. In the first stage a high temperature (65°C) bioleach achieved high extractions of BMs and in principle acted as a pre-treatment for the second stage. In the second stage the residual material was treated with cyanide at an elevated temperature (50°C) achieving high extractions of Pd and Au, but only about 35% of Pt in a similar period of time.

The success of this conceptual process on a concentrate material gave rise to the present study in which high temperature cyanide leaching was applied to coarse Platreef ore in columns, simulating heap leaching, subsequent to the ore being pre-treated with a bioleaching process (Mwase et al., 2012b). Residual materials from the test work underwent extensive mineralogical analyses using tools such as Mineral Liberation Analyser (MLA) and Quantitative Evaluation of Minerals by Scanning Electron Microscopy (QEMSCAN) to determine the influence that the mineralogy of the ore had on the success of the process. These methods aided in identifying the presence of the mineral called sperrylite ($PtAs_2$) as being a bottleneck in successfully heap leaching the Platreef ore. The MLA analysis excluded lack of contact with solution as the cause for low Pt extraction as the sperrylite mineral grains in both studies were liberated. It was therefore concluded that sperrylite was resistant to cyanide leaching under the conditions explored in the primary study.

The second study aimed both at providing a better understanding of the conditions limiting the leaching of sperrylite in plain cyanide solutions as well as exploring opportunities for using alternate cyanide based lixiviants to improve its dissolution.

Although the mineral had never been studied before, research on gold arsenides provided some insight, which suggests that the presence of an oxidant stronger than oxygen in air could aid in the dissolution process. In this case ferricyanide was chosen over a number of options due to its compatibility with cyanide and the promising results it has thus far achieved on gold minerals that are similarly resistant to cyanide leaching.

2. Chapter 2: Literature Review

2.1. PGMs: An Overview of the Metals and the Industry

Platinum group metals (PGMs), namely platinum (Pt); palladium (Pd); rhodium (Rh); ruthenium (Ru); iridium (Ir) and osmium (Os) are rare in the earth's crust. Pt and Pd have an abundance of 5 parts per billion (ppb) while Rh, Ir and Ru are at 1 ppb. However in ultramafic lithologies Pt and Pd can be present in concentrations of 10-20 ppb. The six elements can be found in group VIII of the periodic table along with Fe, Co, Cu, Ni, Au and Ag. They are often grouped in threes specifically Ru-Rh-Pd and Os-Ir-Pt due to the similarities of atomic weights of elements in each group. PGMs are referred to as precious metals because they are rare and very high value commodities. This is due to their various useful physical and chemical properties (Table 1), amongst which are (Crudwell et al., 2011):

1. their ability to catalyse chemical reactions;
2. their ability to resist corrosion;
3. their attractive visual appeal;
4. the ease with which they can be worked and
5. their high conductivities, densities and melting points.

Table 1: Selected properties of the PGMs adapted from British Geological Survey (2009)

	Pt	**Pd**	**Rh**	**Ir**	**Ru**	**Os**
Atomic weight	195.08	106.42	102.91	192.22	101.07	190.23
Atomic number	78	46	45	77	44	76
Density (g/cm^3)	21.45	12.02	12.41	22.65	12.45	22.61
Melting point (°C)	1769	1554	1960	2443	2310	3050
Electrical resistivity (μΩcm at 0°C)	9.85	9.93	4.33	4.71	6.8	8.12
Hardness (Mohs)	4-4.5	4.75	5.5	6.5	6.5	7

With the exception of Os which emits a toxic gas when exposed to air in powder form, the PGMs, find wide application in a variety of industries such as car and truck emission-control catalysts, electronics, jewellery, investment (bars and coins), medical (dental, anticancer drugs,

implant components), chemical industry (catalysts), glass industry and many other applications (Crudwell et al., 2011). The most commercially significant of the six are by far Pt and Pd, with Rh and Ir also finding a market followed by Ru. The biggest consumers of PGMs are Europe, Japan, North America, China (in differing order dependent on the application and PGM) followed by the rest of the world. The most demand for PGMs is in the manufacture of autocatalysts and jewellery (Johnson Matthey, 2015). Table 2 shows the prices of the PGMs as of 13-January-2016. The most economically significant metals are Pt and Pd due to their uses and abundance compared to the others.

Table 2: Trading prices of the PGMs[1]

Metal	Price (US$/troy ounce)
Pt	837
Pd	487
Rh	520
Ir	640
Ru	42
Os	400

By far the largest producers of PGMs in the world are South Africa followed by Russia as seen in Table 3 (Johnson Matthey, 2015). Russia dominates in the supply of Pd while South Africa is responsible for most of the overall combined supply of the worlds PGMs. Zimbabwe, Canada and the United States round off the list of top 5 PGM producers in the world, while other notable producers include Australia, China and Colombia.

Further still, only a few corporations are responsible for as much as 78% of the world's PGM supply; namely Anglo American Platinum, Norilsk Nickel, Impala Platinum and Lonmin plc (Table 4).

[1] Prices from https://www.quandl.com/collections/markets/platinum

Table 3: Supply and demand '000 oz in 2015

Supply	Pt	Pd	Rh
South Africa	4, 237	2, 480	584
Russia	696	2, 600	80
Others	874	1, 323	62
Total Supply	5, 807	6, 403	726
Gross Demand			
Autocatalyst	3, 695	7, 457	851
Jewellery	2, 862	245	146
Industrial	1, 836	2, 074	997
Investment	-88	-400	584
Total Gross Demand	8, 305	9, 376	80

Table 4: Top producing PGM companies in the world in 2014[2]

	Pt ('000 oz)	Pd ('000 oz)	Rh ('000 oz)
Anglo American Platinum	1, 890	1, 230	229
Impala Platinum	1, 180	710	157
Norilsk Nickel	657	2, 749	91
Lonmin plc	436	210	78
Stillwater Mining	285	667	34
Northam Platinum Ltd	241	117	31
Aquarius Platinum	184	110	28
Vale SA	182	398	
Glencore plc	91	-	15
Asahi Holdings	44	126	
North American Palladium	-	174	-
African Rainbow Minerals			35

[2] From http://metals.about.com/od/Top-10-Producers/tp/The-10-Biggest-Rhodium-Producers-2014.htm

2.2. PGMs: A Brief Overview of Geology and Mineralogy

As discussed by Vermaak (2005) the distribution of PGMs in an ore body is related to the type of ore and subsequently determines the PGM mineralogy in the ore. The ores can be classified as:

1. Stratabound Layered Intrusions: These ore bodies contain the world's largest reserves of PGMs and PGM mineralisation plays an important role in the economic importance of the deposits given that the PGM concentrations range from 1-15 g/t.

2. Alluvial Ores: Are composed of liberated minerals and individual particles of rock and contain almost no sulphides.

3. Magmatic Nickel Sulphide Deposits: These types of ores account for nearly 60% of the world's Ni production and can be divided into two types; sulphide-rich deposits which are primarily exploited for the Ni and Cu with PGMs being a secondary or "by-product", and the sulphide-poor which are principally exploited for PGMs (Schultz et al., 2010).

PGMs in nature rarely occur in native metal form but are commonly in alloy form (with each other or other metals), or bonded to a variety of ligands such as sulphur, tellurium, arsenic, antimony and selenium to form minerals. Table 5 is a selection of platinum group minerals, with the most common ones highlighted, using data from Cabri (2002) and British Geological Survey (2009). Vermaak (2005) reports that sperrylite is the most abundant platinum group mineral in the world and can be found in every type of geological environment. Platinum group minerals are mostly hosted in sulphide minerals with pentlandite [$(Fe,Ni)_9S_8$] being the most dominant carrier followed by pyrrhotite ($Fe_{1-x}S$), and finally pyrite (FeS_2) and chalcopyrite ($CuFeS_2$) which both do not hold significant quantities. Vermaak (2005) has also reported that PGMs are hosted in oxides (such as $FeCr_2O_4$ and Fe_3O_4), silicates, sulpharsenides (e.g. CoAsS), arsenides and tellurides.

Table 5: Selection of Platinum Group Minerals

Group	Mineral	Formula	Group	Mineral	Formula
Alloys	Atokite	$(Pd,Pt)_3Sn$	**Arsenides**	Sperrylite	$PtAs_2$
	Isoferroplatinum	Pt_3Fe		Stillwaterite	Pd_8As_3
	Osmiridium	OsIr	**Antimonides**	Genkinite	$(Pt,Pd,Rh)_4Sb_3$
	Polarite	PdHg		Isomertieite	$Pd_{11}As_2Sb_2$
	Rustenburgite	$(Pt,Pd)_3Sn$		Stibiopalladinite	Pd_5Sb_2
	Tulameenite	Pt_2FeCu		Sudburyite	(Pd,Ni)Sb
Sulphides	Braggite	(Pt,Pd)S		Geversite	$Pt(Sb,Bi)_2$
	Cooperite	PtS	**Bismuthides**	Froodite	$PdBi_2$
	Erlichmanite	OsS_2	**Tellurides**	Kotulskite	PdTe
	Hollingworthite	RhAsS		Merenskyite	$(Pd,Pt)(Te,Bi)_2$
	Laurite	$(Ru,Os)S_2$		Michenerite	Pd(Bi,Sb)Te
	Ruarsite	(Ru,Os)AsS		Moncheite	$(Pt,Pd)(Te,Bi)_2$

2.3. World PGM Resources

2.3.1. The Bushveld Igneous Complex (BIC)

South Africa is the foremost primary producer of PGMs in the world largely due to the fact that it contains a vast majority of the worlds' reserves (Cawthorn and Hochreiter, 2000), approximately up to 90%. The PGMs are mostly located in an area known as the Bushveld Igneous Complex (BIC) in the north-western part of the country. The BIC is the largest layered igneous intrusion in the world with a roughly oval shape measuring 400 km by 300 km in diameter. For convenience the BIC is generally divided into three areas, the eastern and western limbs and the Potgietersrus or northern limb (Figure 1). PGM mineralization in the eastern and western limbs is concentrated in the ore bodies known as the Merensky Reef and Upper Group 2 (UG2) layer. At any given location a mining company (large or small) will exploit both these ore bodies at the same time, although the vertical distance between the two can vary from 20 m to 400 m. In the northern limb, the economic exploitation of PGMs is mainly limited to the Platreef ore body (Merkle and McKenzie, 2002). The UG2 is generally considered to be the better ore of three, being denser, and hence cheaper to mine, (von Gruenewaldt, 1977) and having a higher PGM content than the other two. It is more friable (easier to mill/comminute) leading to lower comminution costs (partially offset by the more abrasive nature of the

chromite and lower recovery during flotation). The UG2 also has a higher Rh content and the concentrates generally have a higher PGM content leading to lower smelting costs per unit PGM output (Merkle and McKenzie, 2002). The geology and mineralogy of the BC have been well studied and are explored in several publications and thus will not be explored in detail here, but Table 7, Table 8, Table 9 and Table 10 can be consulted to further highlight the differences between the three ore bodies. The typical PGM grade for ores mined in the BIC is 1-10 g/t (Crudwell et al., 2011; Seymour and O'Farrelly, 2001; British Geological Survey, 2009) depending on which of the three ore bodies it is mined from. The average grades of the three ore bodies compiled from data from Seymour and O'Farrelly, 2001 and Merkle and McKenzie, 2002 can be seen in Table 6.

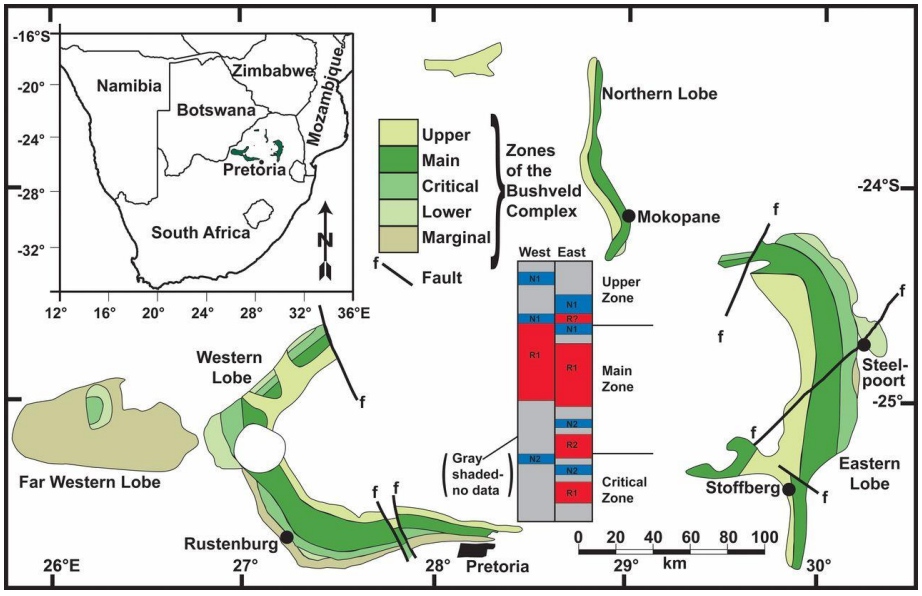

Figure 1: Map of the three economically important limbs of the BC taken from http://geology.gsapubs.org/content/41/6/687/F1.large.jpg

Table 6: Average grades of PGMs in ore bodies of the BIC in g/t

	Merensky	UG2	Platreef
Pt	3.25	2.46	1.26
Pd	1.38	2.04	1.38
Ru	0.44	0.72	0.12
Rh	0.17	0.54	0.09
Ir	0.06	0.11	0.02
Os	0.04	0.10	0.02
Au	0.18	0.02	0.10

Table 7: A brief geological and mineralogical overview of the BC (Eksteen, 2010)

Property	**Merensky Reef**	**UG2**	**Platreef**
Geology	Stratiform (layered), Narrow reef, Mineralization fairly uniform within reef. Pyroxenite rock-type	Stratiform (layered), Narrow reef, Mineralization fairly uniform within reef. Chromatite rock type.	Stratabound (bounded by layers), Thick reef Mineralization highly variable, intrusions of extraneous material occurs often (Calc-silicate xenoliths)
PGM mineralization	Mostly as Pt and Pd sulphides and minor quantities of PGM alloys. PGM mineralization associated with base metal sulphides (BMS). PGM liberation easy.	Mostly Pt, Pd, & Rh sulphides and alloys. Significant part of mineralization associated with silicates. PGM liberation easy.	Mostly Pd, Pt Bismuth-Tellurides and Pt, Pd Arsenides. Fine intergrowth textures of PGM's on grain boundaries between silicates and BMS.
PGM relative content	Pt > Pd > Ru > Au Little to no Rh	Pt > Pd > Ru > Rh Little to no Au	Pd ≈ Pt > Au, Ag Very little Rh, Ru, Ir

Table 8: Mill and flotation behaviour (Eksteen, 2010)

Property	Merensky	UG2	Platreef
Base Metal Sulphide content	Moderate	Very low	High (for PGM ore bodies)
Pyrrhotite (FeS) Content	Moderate, easy to depress during flotation	Low, easy to depress during flotation	Very high, difficult to depress with lower PGM recovery
Ore Hardness	Moderate & Consistent	Moderate & Consistent	Hard, but highly variable
Ease of PGM liberation during milling	Easy	Easy	Difficult
Mass pull required	Moderately low	Very Low	High
Upgrade Factor with flotation	Moderate (x40-50)	Very High (x90-100)	Low (x15-20)
Concentrate Grade	Moderate (160 g/t)	High (300-400 g/t)	Low (60-70 g/t)
Mineralogical feed Consistency	Consistent per location	Consistent per location	Inconsistent / highly variable

Table 9: Conventional smelting requirements (Eksteen, 2010)

Property	Merensky	UG2	Platreef
Matte fall	Moderate (15-20%)	Low (5-10%)	Very High (30-55%)
Environmental: SO_2 release and mitigation	Moderate (Acid manufacture possible when economy of scale sufficient and acid market in close proximity	Low (Acid manufacture uneconomic and scrubbing required).	High SO_2 production, but clients for sulphuric acid far away – high logistical cost for low value material
Matte & slag temperatures	Moderate	High	Moderate
Chromite content	Insignificant	High	Insignificant
Aisle logistical demand	Moderate	Low	High High quantities of furnace matte, converter slag
Potential for smelter accidents, stability	Low potential for problems, stable feed	High matte & slag temperatures makes smelting more risky	Large mineralogical variability gives large variation in matte fall and furnace matte levels, making matte runouts a significant risk

Table 10: Mineralization and mineral associations (Eksteen, 2010)

Mineral type	Merensky	UG2	Platreef
	%	%	%
Pt, Pd alloys	6.4	0.2	1.0
Au-Ag alloy	4.2	-	9.5
Pt-Arsenide	50.3	1.2	17.3
Ru-Sulphide	-	10.2	-
Pt-Pd Sulphide	17.1	84.9	14
Rh-Sulphides	-	3.3	-
Pt-Pd Tellurides	21.1	0.2	58.1
PGMs in BM Sulphides	28	-	-
PGM on grain boundaries	41	84	31
PGM assoc. with silicates	28	11	69
PGMs assoc. with chromite	-	5	-

2.3.2. Other PGM Resources

Although the BIC contains the vast majority of the worlds PGM reserves, there are several other deposits and ore body types worldwide of economic significance. These include:

The Great Dyke, Zimbabwe: This area contains the second largest reserves of PGMs in the world after the BIC in neighbouring South Africa (Oberthür, 2002). Like the ore bodies in the BIC the Great Dyke is a layered intrusion stratabound ore. The PGMs are associated with chromites (lower economic importance) and sulphides (most economic importance). The Great Dyke PGM also has deposits of sub-economic concentrations in the Lower Sulphide Zone ten metres below the MSZ, the Böhmke Reef and the Dream Reef (Oberthür, 2002). The presence of PGMs has also been detected in alluvial sediments of rivers draining the Great Dyke (Oberthür et al., 1998).

The Stillwater Complex, Montana, USA: Is one of the world's notable layered, ultramafic to mafic intrusions housing economic concentrations of PGMs, Cu, Ni, Ti and Cr (Zientek et al., 2002).

Ni-Cu-PGM ores: These magmatic sulphide ores are the most important source of Ni worldwide. The most significant deposits being Noril'sk-Talnakh, Russia; Sudbury, Ontario, Canada and Jinchuan, China (British Geological Survey, 2009).

Further, a selection of types of other PGM resources worldwide can be found in British Geological Survey (2009).

2.3.3. Other Sources of PGMs

The recycling of spent catalysts (automobile and industrial) is another source of PGMs (Jha et al., 2013; Polinares, 2012; Baghalha et al., 2009; Cao et al., 2006; Grumett, 2003). This is done by PGM producers with smelter capacity or companies specializing in this field (Crundwell et al., 2011). Copper anodic slimes produced in electrorefining plants are also a secondary source of PGMs (Kruyswijk, 2009; Biswas et al., 1998).

2.4. Current PGM Processing Technology

2.4.1. The Conventional Process Route

Although complex and diverse, the metallurgical operations in the South African PGM industry consist of the following five steps outlining what will be referred to from herein as the conventional route/process:

1. Mining of PGM bearing ores

2. Comminution which involves crushing then milling of the ore to micron size particles

3. Concentration which involves separating the PGMs associated with BM sulphides from the bulk of the ore to produce a much lower volume higher grade PGM concentrate.

4. Smelting and converting, to create a Ni-Cu-PGM sulphide rich matte which is again much higher in PGM grade and lower volume.

5. Refining, which involves several stages of usually high temperature and pressure leaching, and several purification and separation processes like precipitation, crystallisation, reduction, solvent extraction, and electrowinning to recover BMs and PGMs in whatever forms required by the markets. Whether high purity metals or intermediate products such as sulphide powders or sulphate crystals

Without doubt major PGM producers outside South Africa also recover their PGMs in similar circuits. As a matter of interest it must be noted that South African companies are the only ones in the world that classify themselves as PGM producers with PGMs being their main business. With the exception of Zimbabwe, major producers outside South Africa are primarily BM producers with PGMs being a "by-product". This is owing to the fact that the BMs are often processed first, owing to their chemical properties allowing this, leaving behind a low volume PGM rich material.

Despite all producers having the above steps and order in their process flowsheets there is no generic circuit among South African PGM producers (or the rest of the world). This is a reflection of the variability in ore mineralogy discussed in the section prior to this one. Merkle and McKenzie (2002) report that the challenge of designing an optimal processing circuit starts with a detailed understanding of ore mineralogy. The economic value of the PGMs makes maximum recovery at each stage in the process an imperative. Historically this was done empirically, but with time, increase in production costs and need for improvement, emphasis has been placed on fundamental understanding of the behaviour of the ores at different stages in the whole process (Merkle and McKenzie, 2002). Table 11 shows a breakdown of what each major step contributes to the operating costs of processing PGMs.

Table 11: Breakdown of operating costs in PGM processing

Operation	Contribution to cost (%) (Crundwell et al., 2011)	Contribution to cost (%) (Merkle and McKenzie, 2002)
Mining	70	65-75
Comminution and Concentration	10	9-10
Smelting/converting	10	6
BM Refining	-	7
PGM Refining	10	4-5

Figure 2 shows a generalised flowsheet of the conventional process combining elements from different operations of PGM producers in South Africa.

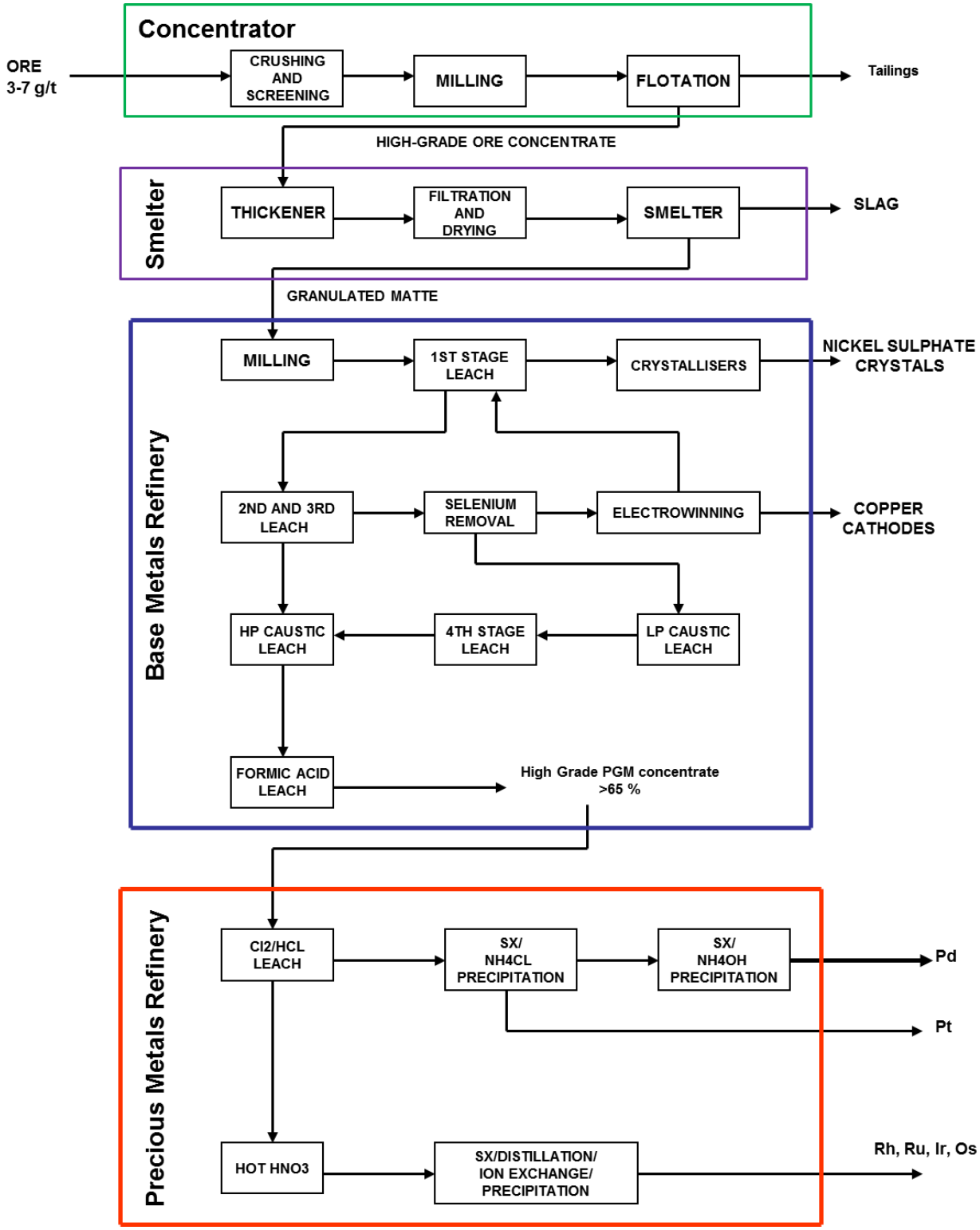

Figure 2: General PGM processing flow diagram for Lonmin Plc [adapted from Mwase (2009)]

2.4.1.1. Mining of PGM ores

Merkle and Mckenzie (2002) provide a detailed discussion on this topic summarised herein. Mining practices in the BIC vary between organisations and within the organisation on the same mining operation. They can be either small-tonnage opencast operations or large tonnage mechanized underground operations. Typically only the most economically attractive portion of an ore body will be mined. As expected opencast mining is naturally practiced by smaller organisations with limited means; but the larger organisations have of late been known to initially opencast strip-mine the mineralized horizons of a site to help reduce the development time of a mine and provide some initial and quick returns on capital. When opencast mining is no longer viable due to increased depth, sub-surface mining commences first via inclined shafts and later by vertical shafts. These large underground multi-level operations, serviced by a network of shafts allow for maximum mining depth to be achieved. Figure 3 shows some images of open pit and underground PGM mining.

Current operations favour dip mining (extracting ore against or in the direction of the dip) to breast mining techniques (consisting faces and ore scrapping gullies). Dip-mining allows for better geological and cost control. A typical mining operation consists of pre-development, manual drilling and charging, blasting and either manual or mechanized ore clearing. Particularly in cases where the reef is narrow, trackless mining methods (use of earth moving vehicles, dump trucks, etc. on permanent roads instead of rail tracks and carts) are used (Merkle and Mckenzie, 2002).

Anglo Platinum, Mogalakwena open pit platinum mine

Lonmin, Marikana Karee underground mine

Figure 3: Examples of open pit and underground PGM mining

2.4.1.2. Comminution (milling and crushing)

As the names state the purpose of these operations is size reduction of ore with the aim of liberating PGMs and more specifically sulphide minerals that host them from the bulk gangue minerals (silicates, quartz, etc). Operations in the BIC vary in type and configuration but they all essentially use jaw or cone crushers as the primary crushers. The crushed ore is then sent through the milling circuit which once again differs with different operations.

Typical mills used are the standard rod or ball mills (semi-autogenous-use of grinding media like iron/steel balls) or autogenous mills (self-grinding, ore acts as grinding media). The milling circuits can either be open or closed. Of late there has been some interest in the application of high pressure grinding rolls (HPGR) on PGM ores (Solomon, 2010) for better liberation and reduced energy consumption. Crundwell et al. (2011) report that HPGRs have been installed in the place of gyratory crushers at several PGM mining locations in South Africa for these very reasons. Similar interest has been shown in the IsaMill™ for the same reasons (Chaponda, 2011). Milling is done up to a point with over-milling being avoided. If excessive fine material is generated, difficulty in recovering the PGMs through flotation may result. Operations among South Africa PGM producers typically configure the circuits to be closed and incorporate mills with stages of screening and flotation in-between to optimize liberation and prevent overgrinding (Barratt and Sherman, 2002). Some authors often discuss comminution with flotation as they usually constitute an integrated operation; the perfect example being the MF2 (mill-float-mill-float) circuit used at many UG2 concentrators (Merkle and Mckenzie, 2002). Other modifications to the comminution circuit that are known are the use of dense media separators between primary crushing and milling. These are used to remove lighter silicate from the denser chromite and PGMs before milling. In so doing the volume of the ore is reduced by up to 20% by mass, without reducing PGM recoveries (Merkle and Mckenzie, 2002). Finally, gravity concentration/separation methods can be used to remove as much as 20% of the PGMs after primary crushing with the aid of cyclones as practiced in some Anglo Platinum circuits (University of Cape Town-Anglo Platinum, 2007). This technique exploits the much higher density of certain platinum bearing minerals than the host rock. The gravity concentrate produced can be sent directly to the precious metals refinery by-passing the other stages of the conventional process. Figure 4 shows some images of types of mills and crushers used in the industry.

Due to the variability in mineralogy, Merensky and UG2 ores are processed separately (Merkle and Mckenzie, 2002) with some exceptions where they can be blended with Platreef (Rapson, 1997) which due to its lower grade and different mineralogy (discussed later and a focus of this study) may sometimes not be economically processed through the current circuit.

Figure 4: Mills and crushers used in the PGM industry

2.4.1.3. Concentration (via flotation)

In this process, the PGM bearing minerals as liberated particles or more commonly attached to BM sulphide mineral particles are separated from the bulk of the ore. The milled ore is mixed with water and treated with an assortment of chemicals, specifically collectors, activators, frothers and depressants. These collectors promote hydrophobicity-the property of particles that facilitates their attachment to air bubbles. The activator creates a copper sulphide surface coating on minerals to give strong mineral-collector attachment hence efficient flotation The frother creates strong but short-lived bubble-mineral particle froth at the top of flotation cells, preventing the particles from falling back until the froth overflows and the depressants ensures

that as little of the gangue as possible reports to the concentrate lowering its grade and increasing its volume.

The air bubbles carry the selected particles to the surface of the pulp and form a stabilized froth (Merkle and McKenzie, 2002). The froth is skimmed off and is now a concentrate with a much higher grade of PGM and BM minerals. Ideally this concentrate should represent 2-3% (Mwase et al., 2012a) by mass of the feed ore and contain 85 -90% of the PGMs at a grade of 100-600 g/t (Crundwell et al., 2011; Merkle and McKenzie, 2002). While the hydrophilic particles, being the bulk of the milled ore, settle at the bottom of the vessel; these materials are referred to as tailings. Figure 5 shows a simple schematic diagram of the flotation process and an image of an actual flotation plant at a PGM mine. In a typical circuit there are multiple stages of flotation and the final product is a combination of concentrates from different cells. It starts with one stage of flotation producing concentrate and tailings. The tailings from this stage may go through regrinding/cyclone treatment then sent to another stage of flotation and so forth. A typical circuit has multiple stages of flotation, but these differ from each other and are classified as three types[3]:

1. Roughing: This is a primary stage whose aim is to produce a "rough concentrate" with an emphasis on recovering as much of the valuable mineral as possible and less on the overall quality of the concentrate. This is performed on a coarse particle size to see how much can be recovered before resorting to fine grinding for further liberation.

2. Cleaning: The concentrate from the rougher cells is subjected to pre-treatment (regrinding/ cyclone) and then sent through cleaner cells to produce a "cleaner concentrate" or "final concentrate". The regrinding is normally done using specialized mills such as the IsaMill™ to reduce energy costs.

3. Scavenging: The tailings from the rougher cells will go through scavenger flotation to recover as much of the mineral values still contained in them. This is accomplished by applying more rigorous flotation conditions than the rougher stages and may include pre-treatment in cyclones to separate different particle sizes if the values are proven to be

[3] Compiled using information from https://en.wikipedia.org/wiki/Froth_flotation

associated with a particular particle size or re-grinding for further liberation. The cleaner stage may also be followed by a scavenging stage.

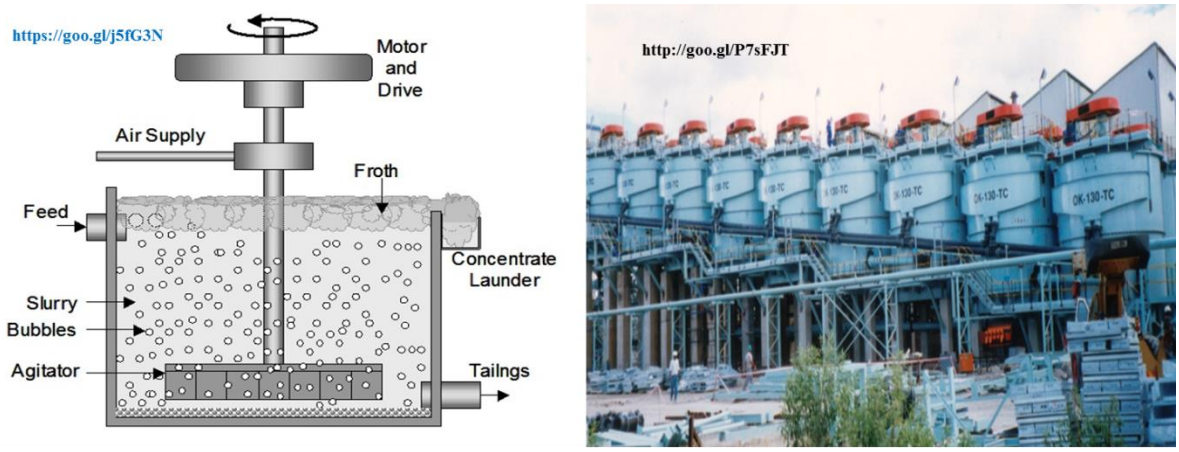

Figure 5: The flotation process and a platinum flotation plant

2.4.1.4. Smelting and Converting

The concentrate from the flotation stage is in the form of slurries and is thickened and spray or fuel-fired flash dried to a water content of less than 0.5%. This is important because the presence of water in an electric furnace can result in a hydrogen explosion (Crundwell et al., 2011).

The dried product is then treated (smelting) in a furnace at temperatures between of 1300-1500°C to produce a molten material with two distinct immiscible phases; a silicate melt (slag) to which the majority of the gangue minerals report and a sulphide melt (matte) to which the PGMs, Ni, Cu, and S report. The matte is completely immiscible in the slag and the two separate due to density differences; the slag having a density of 2.7-3.3 g/cm^3 and the matte matte 4.8-5.3 g/cm^3 (Merkle and McKenzie, 2002). Hence the matte settles at the bottom after some time. Due to the relatively low S content of the concentrate, electric furnaces need to be used for this process. The smelter matte is highly enriched in PGMs ranging from 600-2500 g/t (Crundwell et al., 2011; Merkle and McKenzie, 2002) depending on the ore and the operation. If the slag contains some valuables it can be further treated to recover them. In order to avoid the liquidus temperature and optimize slag viscosity, fluxes (primarily limestone) are added

during smelting. Fluxes also catalyse the desired reactions and chemically bind unwanted impurities and reaction products.

After smelting the next step is converting of the matte which at this stage is referred to as "green matte". This involves the oxidation of iron and sulphur in the matte using air or an air-oxygen mixture to produce an iron and sulphur deficient matte further enriched in PGMs and BMs. This process is highly exothermic with no external heat source required to maintain the operating temperature at 1200-1300°C (Merkle and McKenzie, 2002). If over-heating occurs a cold feed or spillage material is used to cool the temperature back to within range. The most common types of converters used are the Pierce Smith top-blown rotary converters and the Ausmelt continuous converters (Crundwell et al., 2011). The resulting product termed "white matte" is then cast into ingots or granulated before being sent to the base metals refinery (BMR). At this point the PGM grade is in the range of 2000-6000 g/t (Crundwell et al., 2011; Merkle and McKenzie, 2002) depending on the ore and the operation. Anglo Platinum is the exception and treats the white matte through slow cooling (over several days) resulting in the formation of BM sulphide crystals and PGM alloys. The two can be magnetically separated and sent to their respective refineries. The advantage of this is that the PGM production does not depend on BM production.

2.4.1.5. Leaching and Refining

This section will only give the briefest of overviews of the two processes given the extremely wide variation of methods used amongst PGM producers in South Africa and the rest of the world and the numerous steps and complexities of the operations.

It starts in the BMR where the granulated matte is first milled typically to 80% passing 75 µm and leached in three stages with solution from copper electrowinning process. This type of process is known as metathesis and essentially selectively removes Ni from the matte and replaces it with the Cu in the solution; this happens in the first stage at 85°C. Cu and any remaining Ni in the slurry are removed in the second and third stages using pressure leaching with H_2SO_4 at 140°C and 6 bar. An important step in the process is the removal of selenium and tellurium using sulphur dioxide, sulphurous acid or sodium sulphite prior to Cu recovery using electrowinning. The Ni is recovered as $NiSO_4.6H_2O$ crystals in a two-stage process involving an evaporator then a crystallizer. Lonmin Plc, Stillwater and Northam use this

process (Crundwell et al., 2011). Some modifications made to this process include the addition of ammonia prior to crystallization to remove Fe and additional pressure leaching stages using formic acid to remove magnetite and iron oxides; and using oxygen and caustic to remove selenium, tellurium and arsenic amongst many others (Crundwell et al., 2011). Other PGM producers (Impala Platinum) use a similar flowsheet but the Ni (and Co) is recovered by reduction using hydrogen gas. The leach solution from the acid leaching above is mixed with ammonia and water in an autoclave operating at 190°C and 28 bar. This produces a Ni and Co ammonia salt which can be treated to separate the two and eventually produce a Ni powder of 99.9% purity (Crundwell et al., 2011). Further still others such as Anglo Platinum also use acid leaching but recover Ni and Co as cathodes through electrowinning. Regardless and with the exception of Anglo Platinum, all the above routes result in a low-volume and very high-grade solid residue containing 60-65 % PGMs which is then sent to the precious metals refinery (PMR).

In the PMR this material is dissolved in either *aqua regia* (a mixture of HCl and HNO_3) or as preferred by most PGM producers in a mixture of HCl and chlorine gas creating chloro complexes in solution. The separation of primary (Pt, Pd and Au) and secondary precious metals (Rh, Ru, Ir and Os) is carried using any of the following depending on the producer (Crundwell et al., 2011):

1. Crystallization and Precipitation: The Pt chloro complex can be removed as ammonium hexachloroplatinate [$(NH_4)_2PtCl_6$].

2. Hydrolysis: Used to remove Rh and Ir as $Rh(OH)_4$ and $Ir(OH)_4$.

3. Distillation: Used to remove Ru and Os.

4. Organic Precipitation: Pd can be selectively precipitated with dimethylgloxime while Ir and Rh can be precipitated using diethylene triamine.

5. Solvent Extraction: Pt, Pd, Au and Ir can be separated at high ef iciency using solvent extraction using columns, mixer-settlers and centrifuge-type contactors.

6. Ion Exchange and Molecular-Recognition Technology (MRT): Both are performed in columns and used to separate Pd and Au from the bulk of the PGMs.

The resulting products are then processed to produce more pure and saleable products by direct processing of the compound through metal reduction or smelting, or they are re-dissolved and re-recovered and purified using similar processes to the ones above.

2.4.1.6. The Challenges of Processing Platreef Ore using the Conventional Route

The unique characteristics of the Platreef ore body in terms of PGM mineralogy and deportment, geology and chemical assay, which distinguishes it from its counter-parts, the Merensky and UG2 ore bodies (Schouwstra & Kinloch, 2000) present a challenge to economically process the ore via the conventional route, without the benefit of additional ultra-fine grinding and blending with higher grade concentrates (Newell, 2008), which is standard for Merensky and UG2 ore. The PGMs in Platreef ore occur largely as Pd and Pt tellurides and arsenides (Table 7), which are observed to be slow-floating in comparison to the PGM sulphides (Shackleton et al., 2007a; Shackleton et al., 2007b; Shamaila and O'Connor, 2008; Vermaak, 2005). Further to this, nearly 60% of the PGMs in Platreef deport to silicate minerals or on base metal sulphide-silicate grain boundaries (Bryson, 2008; Bushell 2006) (Table 10). The combined consequence is that the PGMs are not fully recoverable via flotation (Table 8), and portions of PGMs of significant value will report to the tailings. To achieve acceptable PGM recoveries, a higher-than-usual mass pull is needed, but this leads to grade dilution and a poor quality concentrate material, which in turn negatively impacts the smelter operation further downstream (Mogosetsi, 2006; Schay 2009). Due to the high iron and sulphur content and comparatively low PGM grade, the smelting and converting costs (and associated costs of gas handling, acid plants, etc) makes these concentrates economically marginal if a smelting route is followed.

Moreover, there is also high variation in metal grade along the reef (Schouwstra and Kinloch, 2000); whereas some sections of the reef are suitable for up-grade via milling and flotation, significant parts fall below the cut-off grade. Additionally, the Pd to Pt ratio in Platreef is about 1.2:1 (Table 6), while it is more favourable for Merensky and UG2 reefs where it is 2:1 in favour of Pt (Bushell, 2006; Seymour and O'Farrelly, 2001). Although certain outcrops of the Platreef allow opencast mining, the rapid dip west downwards from the outcrop, necessitates

expensive underground mining with backfilling, which adds substantially to operating and capital costs. Platreef ore also contains very little chromite, and the content of Rh, Ir and Ru is much less than that of Merensky or UG2 (Table 6; Seymour and O'Farrelly, 2001). Furthermore, Platreef deposits are located in an arid area of South Africa, with a low skilled labour pool and poor electrical infrastructure.

Aside from the conventional process, there are a number of technologies that have the potential to be used on PGM ores having been tested on gold ores. These include thiosulphate, thiocyanate, iodide, bromide and thiourea leaching systems. However, these will not be discussed. Mpinga et al., (2015) discussed a number of hydrometallurgical technologies developed to treat BM sulphide concentrates as an alternative to smelting. Theoretically, these can also be used to treat PGM concentrates prior to applying the specific processes to leach and recover the PGMs. These will also be excluded from the discussion. Only those that are in use or have been tested (lab or pilot scale) on PGM ore with the primary purpose of extracting PGMs, will be discussed. These methods are all purely hydrometallurgical with the aim of creating a direct route between the production of concentrate and the refinery feed. The benefits of which include reduced treatment charges, lower working capital, better metal winning economy at mine-site scale and greater market flexibility for the product (Milbourne et al., 2003). Hydrometallurgical routes generally have greater flexibility during process scale and control and are making inroads into a field traditionally dominated by smelting (Mpinga et al., 2015). The sections below discuss these various alternative options available for processing Platreef ore.

2.4.2. The Platsol™ Process

Platsol™ (Figure 6) is a single step high pressure oxidation (≈700 kPa O_2, 3200 kPa total pressure); high temperature (>200°C) sulphate based leaching process developed at SGS by International PGM Technologies to leach PGMs, Au and BMs in one step, from a variety of low and high grade materials (ores, concentrates, mattes, autocatalysts and other industrial products) (Mpinga et al., 2015; Fleming, 2002). The addition of NaCl (5-20 g/L) creating a mixture containing sulphuric acid (a result of sulphide mineral oxidation) promotes the co-dissolution of the precious metals (PGMs +Au) (PMs) and the BMs in a single step (Liddell and Adams, 2012; Cole and Joe Ferron, 2012). BM sulphide minerals are oxidized with oxygen

to soluble sulphate complexes and sulphuric acid while the precious metals are dissolved as choloro complexes (Dreisinger 2012, Fleming 2002) as illustrated in the equations below:

$$CuFeS_2 + 17/4O_2 + H_2O \rightarrow CuSO_4 + 1/2Fe_2O_3 + H_2SO_4 \quad (2.1)$$

$$NiS + 2O_2 \rightarrow NiSO_4 \quad (2.2)$$

$$Au + 1/4O_2 + 1/2H_2SO_4 + 4NaCl \rightarrow Na_3AuCl_4 + 1/2Na_2SO_4 + 1/2H_2O \quad (2.3)$$

$$Pt + O_2 + 2H_2SO_4 + 6NaCl \rightarrow Na_2PtCl_6 + 2Na_2SO_4 + 2H_2O \quad (2.4)$$

$$Pd + 1/2O_2 + H_2SO_4 + 4NaCl \rightarrow Na_2PdCl_4 + Na_2SO_4 + H_2O \quad (2.5)$$

While the BMs are recovered by precipitation and SX/EW, the PMs are recovered by such methods as sulphide precipitation, activated carbon adsorption or ion exchange (Liddell and Adams, 2012). However, this process has some disadvantages which include possible incomplete PGM leaching from more refractory minerals (such as cooperite-PtS); carry-over losses of precious metals and BMs at the metals separation and recovery stages due to co-precipitation and adsorption effects and it is difficult to optimize the process conditions independently for each metal value species to maximize their dissolution and recovery (Mpinga et al., 2015; Liddell and Adams, 2012; Ferron et al., 2006). The process is under final feasibility study for application by PolyMet Mining (Dreisinger, 2006) and was recently evaluated in prefeasibility studies by Gold Fields at their deposits at Konttijärvi, Ahmavaara and Suhanko North deposits at the end of 2012 (Gold Fields, 2013).

2.4.3. Kell Process

The Kell process (Figure 7) was developed with the aim of treating low-grade and high chromium content PGM flotation concentrates; such as those originating from UG2 and Platreef ores (Adams et al., 2011). The three major steps that comprise this process are the selective oxidative pressure leach (200-225°C, 3150 kPa, 60 minutes) to extract BMs and convert sulphur to sulphates; the treatment of the residual material via roasting at 900°C to make the PGMs specifically Pt amenable to subsequent leaching; and the chlorination of precious metals using Cl_2 gas and 220 g/L HCl (Adams et al., 2011; Liddell and Adams, 2012).

Although patented and well tested at laboratory and currently pilot scale, the Kell process suffers the disadvantage of requiring special materials of construction owing to the use of the aggressive Cl_2/HCl combination. Furthermore, the long-term materials performance has not been well proven and measures for handling contaminants such as S, Se, Te, Bi, Cr, Hg, Si and Pb have not been well evaluated (Mpinga et al., 2015).

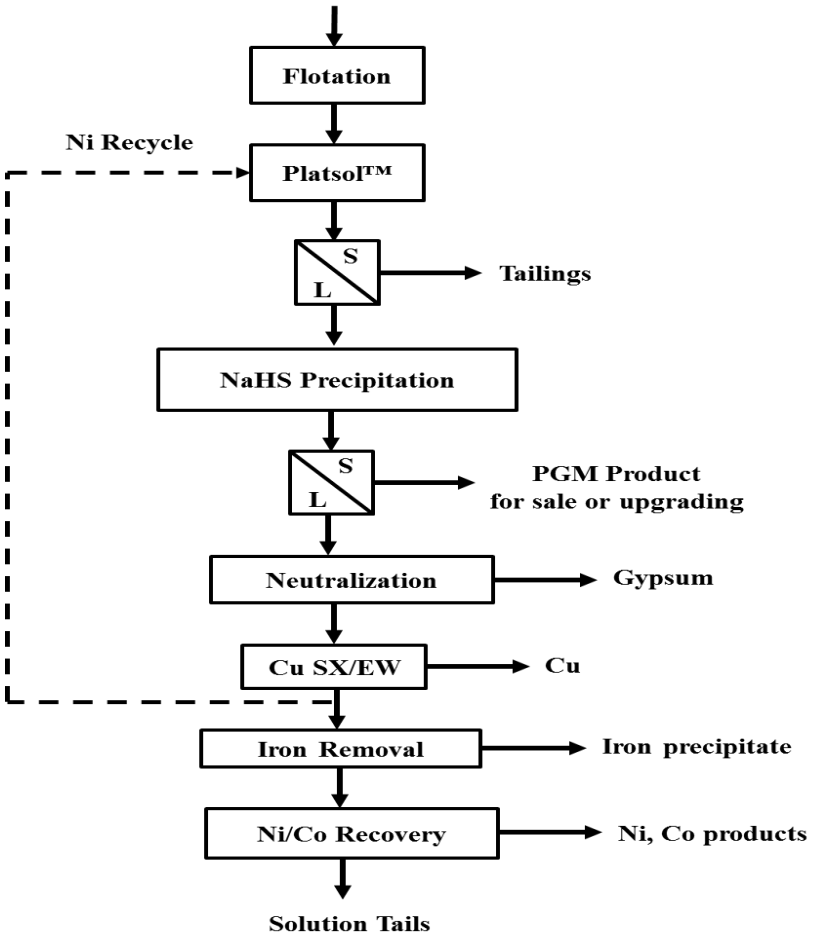

Figure 6: General flowsheet of Platsol™ process [adapted from Fleming (2002)]

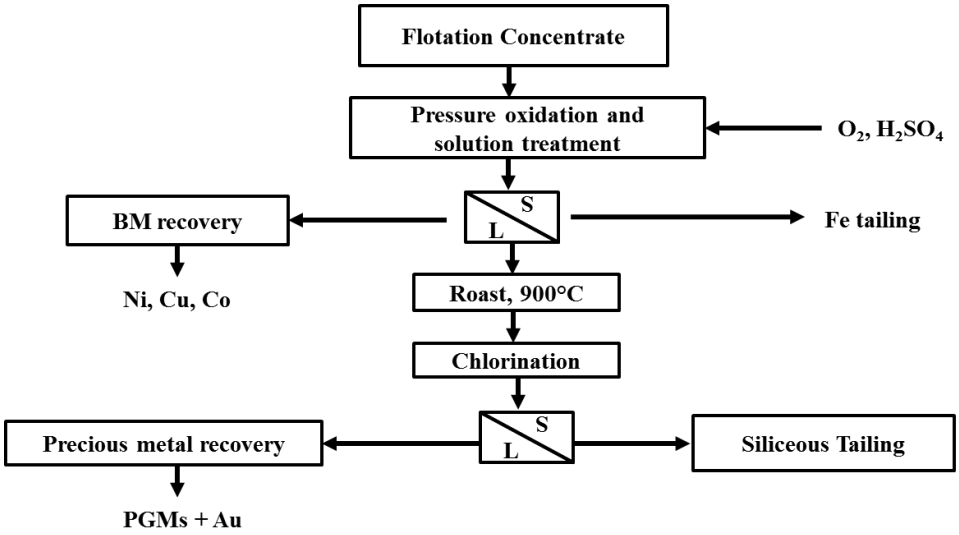

Figure 7: The Kell Process [adapted from Adams et al. (2011)]

2.4.4. Panton Process

This process (Figure 8) was developed by Platinum Australia Limited (PLA) and Lonmin Plc to treat low-grade concentrates by first calcining the concentrate at a low temperature (275-550°C) followed by high temperature cyanidation to leach the PMs and BMs (Snyders et al., 2013). All the metals are then recovered from solution using precipitation to produce high-grade materials that can be directly fed to conventional BM and PM refineries (Mpinga et al., 2015). The disadvantages of this process are the high capital expenditure to build and run a roasting facility, even with relatively low temperatures, and at roasting temperatures higher than 450°C the arsenic from minerals like $PtAs_2$ turns to gaseous state inducing Pt to do the same, hence escaping to the atmosphere as a loss (Mpinga et al., 2015).

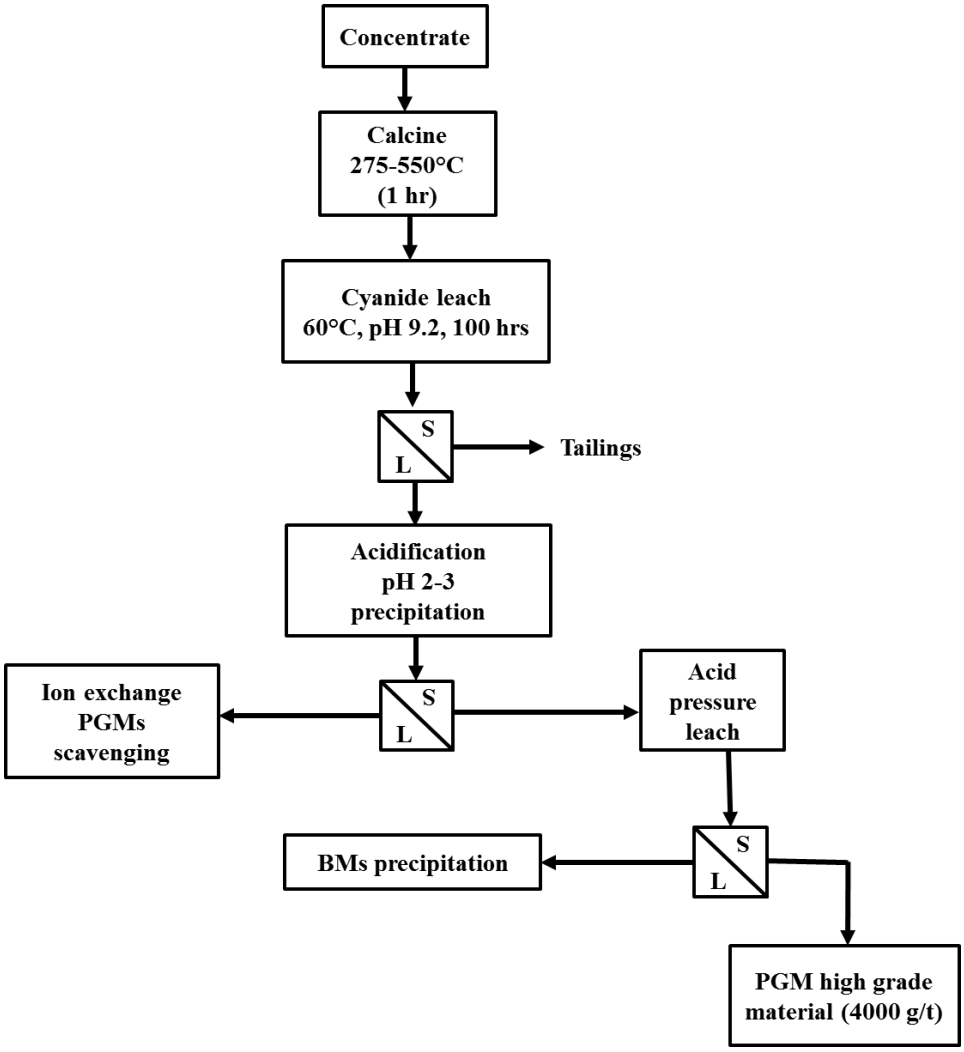

Figure 8: Simplified block flow diagram of Panton process

2.4.5. ConRoast Process

This process was developed by Mintek (South Africa) to process nickel sulphide and PGM concentrates with low sulphur and high chromite content. The ConRoast process has features which address many short comings inherent of current matte-smelter technology (Jones, 2009). Concentrate is first treated using a fluidized-bed roaster to remove all the sulphur, hence eliminating the emission of sulphur dioxide which is a problematic product of matte smelting. The dead roasted concentrate (low sulphur content) is then treated in a DC arc furnace at around 1585°C under strongly reducing conditions. This prevents the formation of magnetite or chromium spinels; a problem common in matte smelting when high chromite concentrate is treated. This produces an iron rich alloy as a collector of the BMs and PMs which is then atomized to fine particles for subsequent recovery of BMs and PMs (Figure 9). However, it

can be seen from Figure 9 that the process still produces sulphur dioxide in the roasting stage which must be scrubbed or neutralized, or converted to sulphuric acid if the scale of the operation permits it. Mintek prioritized the ConRoast process over another technology it was developing in-house to similarly treat high chromite concentrates (Green et al., 2004). The process involved roasting at 800-1000°C, followed by leaching with HCl/chlorine and recovery of PGMs using ion exchange and precipitation (Figure 10). This process was abandoned due to the more favourable economics and technological superiority of the ConRoast process (Green et al., 2004).

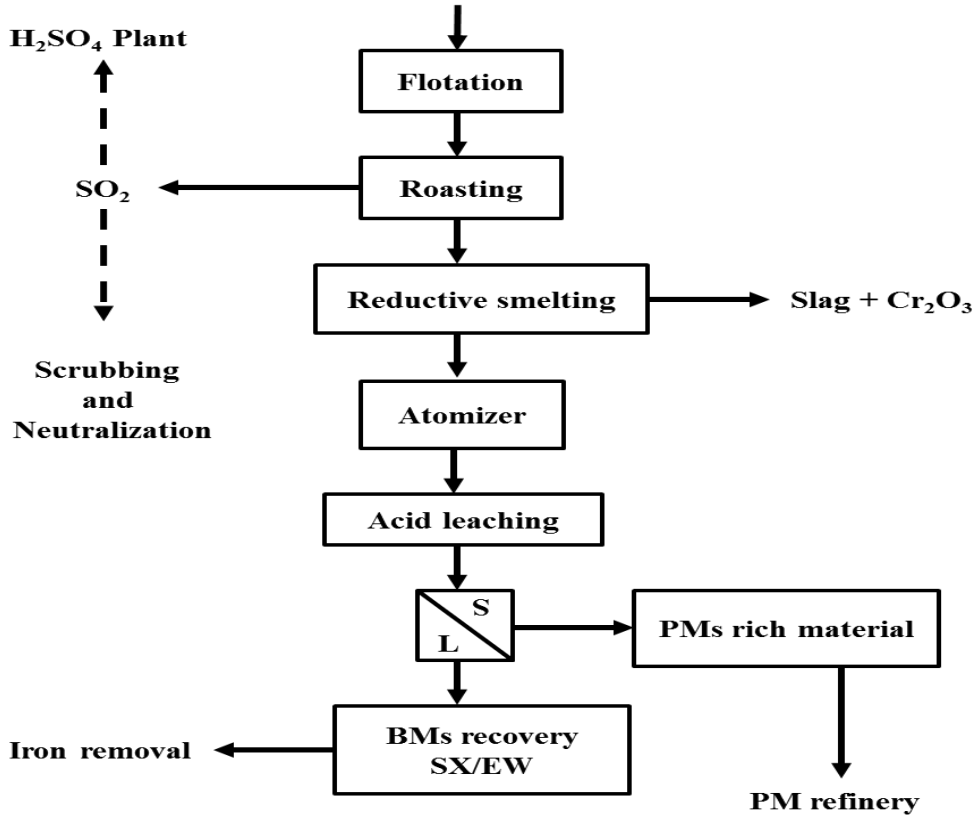

Figure 9: Simplified flow diagram of the ConRoast process

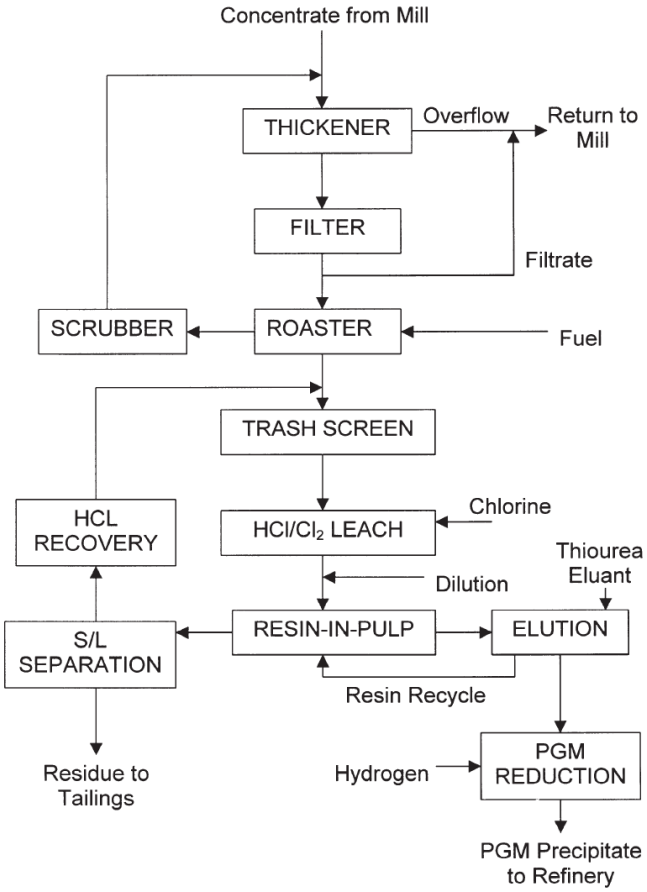

Figure 10: Flow diagram of process reported by Green at al. (2004)

2.4.6. Heap Leaching of PGMs

The above processes are focused on obtaining PGMs from concentrate using extreme temperatures and pressures combined with aggressive hydrometallurgical treatments. For the most part they are intended to bypass the smelter/roasting stage with the exception of a few. Heap leaching on the other hand potentially provides the most direct route to obtaining the PGMs by using less aggressive hydrometallurgical processes on crushed/agglomerated ore thereby bypassing the milling and concentrating stage as well. The sections discuss the process of heap leaching in more detail and eventually how it can be applied to Platreef ore.

2.4.6.1. The Heap Leaching process

Heap leaching is commonly recognized as a low cost method of treating ores that are too low grade or mineralogically challenging to process through conventional methods such as concentrating (crushing-milling-floating), smelting and pressure leaching. It has become

popular over the last 40 years or so due to the lower capital, operating and closure costs associated with a well-designed and operated heap leaching facility (van Zyl et al., 1990). It involves crushing the metal bearing ore and in some cases agglomerating the fines with the coarse particles. The ore is stacked in a heap on an engineered impermeable pad, covered with a plastic liner all tilted at a slight incline. The design of the pad is dependent on various factors such as risk of contaminating the ground water or required regulations of the area. There are various designs available; van Zyl et al. (1990) discussed pads made of either compacted clay or synthetic geomembrane material such as high or low density polyethylene (HDPE or VLDPE) or polyvinylchloride (PVC) although there are many different types of materials that can be used. Possible pad construction using these materials would include a liner, a solution collection system (drain layer and drain piping) and a leakage detection and collection layer typically for double and triple liners (Figure 11).

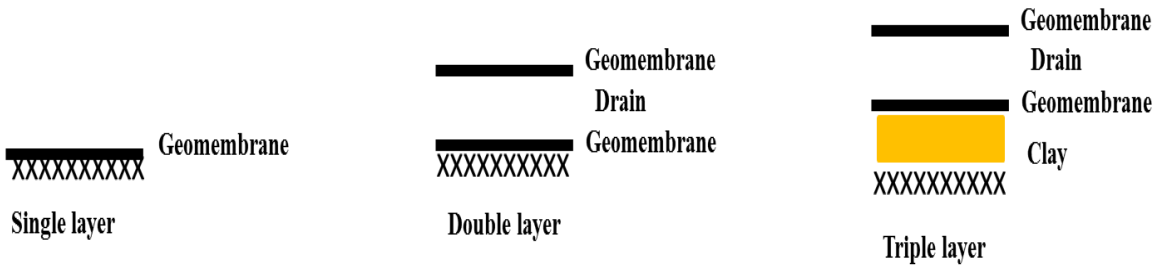

Figure 11: Types of heap pads

Solution is irrigated at the top of the heap and it percolates through the heap, leaching the valuable metals through a series of chemical reactions, sometimes microbially aided. At the bottom of the heap the leachate solution then flows through lined drainage channels to a collection pond and is sent to a processing plant/refinery to recover the metals through the appropriate methods. Figure 12 shows a schematic diagram, while Figure 13 is an actual photograph of a heap leach operation. Table 12 shows some operational data typical of heap leach operations.

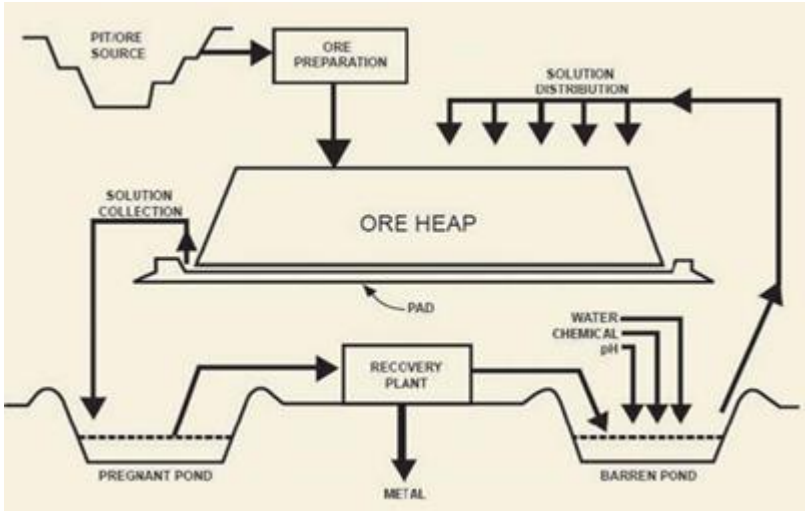

Figure 12: Schematic drawing of a heap leaching operation. Source: http://www.womp-int.com/images/story/2007vol6/013_1.jpg

Figure 13: Photo of actual heap leaching operation. Source: http://www.metallurgium.com/images/OrtizSlide004.jpg

Table 12: Some operational data for heap leaching (adapted from Ghorbani et al., 2015)

Particle size (P_{80} mm)	Crushed	Agglomeration	Irrigation rates ($Lm^{-2}\ h^{-1}$)	Lift height (m)	Leach time (Years)	Recovery (Typical %)
100-5 mm	Yes	Mostly	2-15	2-10 m	Cu: 1-4, Ni: 1-5 U: 1-3, Au: 0.1-2	40-97

To date heap leaching has been mostly exploited by the copper (Scheffel, 2002), gold and silver (Kappes, 2002) mining industries, although there has been some application to uranium extraction and some notable investigation of zinc heap leaching (Petersen and Dixon, 2007).

Like any choice of process route, the option of heap leaching is taken on the basis of finances which may be influenced by any number reasons (Kappes, 2002):

1. Lack of capital to invest in conventional methods of processing ores. This is especially true for smaller companies.

2. Capital risk: the mineral deposit may be located in an undeveloped country which may be politically unstable or may have undesirable socialist leanings.

3. Lack of sufficient reserves to justify the high capital and operating costs of conventional methods, but the deposit may still be profitable if recovered using lower cost methods.

4. In some cases heap leaching may produce equal or better recoveries to conventional process routes due to the mineralogy or specific chemical properties of the ore.

Aside from these, heap leaching offers a number of advantages that can be seen to promote sustainable operations. Heap leaching allows for effective water management and use of leaching reagents. The solid to liquid ratio is around 3:1, which is the opposite for tank leaching where it typically is 1:3 and the pregnant leach solution and spent liquors after recovery processes such as electrowinning and adsorption to carbon, can be recycled back to the heap several times over. It can be argued that because of this closed loop, heap leaching is relatively environmentally benign as waste effluent solution and solid waste are not constantly being discharged to the environment or tailings storage facility. Heap leaching requires low skilled labour and technologies as compared to the standard route; it creates opportunities to engage with local communities (residents, contractors and suppliers) in remote areas where such an operation is likely to be situated. More on this point the transferable skills learned by heap leach personnel include pipe laying, irrigation systems, operating and maintenance of pumps and controls, surveying, earthworks, liner construction and maintenance, slope and erosion control, reclamation and revegetation, and various other aspects of civil construction. All of these have broad applications outside the mineral industry, making a heap leach work force highly employable (Smith, 2004). Further still, heap leaching has the advantages of bypassing the need for capital and energy intensive stages of milling, flotation, smelting and agitated leaching. It does not require solid-liquid separations. No tailings disposal or additional tailings

impoundment is required. Tailings dams and waste dumps are the principal cause of fatalities, not related to direct mine workplace accidents, with an average of 10 fatalities per year caused by tailings and waste dump failures (Smith, 2004). By comparison the history of heap leaching is very good as there have been no significant leach heap slope failures and no failure-related fatalities. Spent heaps are also more stable and easier to reclaim than old tailings deposits because of their self-draining characteristics (Smith 2004). Heap leaching requires quick installation due to it being a relatively simple process with simple equipment. It can be applied to a wide range of low-grade and/or mineralogically challenging ores and easy integration with downstream technologies for metal recovery such as SX/EW, precipitation and adsorption to carbon/resins. All the above advantages make heap leaching a suitable counter to the problems brought by processing Platreef ore through the conventional process (section 2.4.1.).

However it is not without risks and disadvantages which include (Dhawan et al., 2012; Acevedo 2000):

1. Generally lower metal extraction compared to conventional routes,

2. Lack of metallurgical efficiency and control over parameters such as temperature, pH, dissolved oxygen concentration, dissolved carbon dioxide concentration.

3. Slower leach kinetics and longer leach cycles,

4. Larger footprint partly due to the requirement of extensive portions of land,

5. Lengthy pilot test program,

6. Potential environmental release of pregnant leach solution(PLS) and hence shutdown issues,

7. Higher risks of bed permeability decrease as a result of leaching progress,

8. Larger metal and solution inventory in process,

9. Heaps cannot be fixed after construction while a plant can. This is because the mistakes made with the heaps are locked in forever especially during heap building.

Despite seeming like a simple process, the successful design and operation of heap leach requires the inter-disciplinary effort of mining engineers, metallurgists and geologists. They require expertise in the areas of material handling, environmental control, analytical techniques, process chemistry, ore mineralogy, process chemistry and hydrology (Dhawan et al., 2012). Additionally, sufficient test work (laboratory and pilot) must be conducted prior to application, and once established the process must observe best practice for successful operations (Kappes, 2002; Scheffel 2002).

The amount of valuable metal recovered from the ore through heap leaching depends on many factors such as (Dhawan et al., 2012; Zanbak, 2012):

1. climatic conditions of the area-heavy rainfall or extremely low temperatures may not favour certain heap leach operations,

2. crushed ore size-the degree of liberation of the mineral particles,

3. physical characteristics of the ore-the ability of the leaching solution to contact the mineral particles (heap permeability),

4. ore mineralogy-the dissolution potential of the target metal/mineral (leach kinetics) and reagent consumption,

5. in the case of a heap bioleach-microbial activity on sulphide minerals dependent on ideal growth and survival conditions for microorganisms,

6. mass transfer limitations of oxygen or air in the heap.

2.4.6.2. Heap Bioleaching

Heap bioleaching is essentially heap leaching that is assisted by microorganisms. It is currently mostly used in treating secondary copper sulphide mineral bearing ores (covellite and

chalcosite). Primary sulphides such as chalcopyrite and enargite are not currently economically processed via heaps. The majority of operations are located in Chile (Gentina and Acevedo, 2013; Acevedo, 2002; Watling, 2006). Table 13 shows the operations concentrated in Chile and across the globe.

Table 13: Commercial copper heap bioleaching operations around the world (Gentina and Acevedo, 2013)

Plant	Period of Operation
Lo Aguirre, Chile	1982-2001
Cerro Colorado, Chile	1993-present
Quebrada Blanca, Chile	1994-present
La Escondida, Chile	2006-present
Andacollo, Chile	1996-present
Dos Amigos, Chile	1996-present
Ivan-Zar, Chile	1994-present
Zaldivar, Chile	1998-present
Chuquicamata, Chile	1994-present
Andacollo, Chile	1996-present
Los Bronces, Chile	2006-present
Punta del Cobre, Chile	No data
Alliance Copper, Chile	2004-2005
Spence, Chile	2007-present
Cerro Verde, Peru	1998-present
Gunpowder's Mammoth, Australia	1991-present
Mt. Leyson, Australia	1992-1997
Girilambone, Australia	1993-2004
Equatorial Tonopah, USA	2001-2002
S&K Copper, Myanmar	1998-present

However a successful industrial scale Ni-Cu bacterial heap leaching of ore has only recently been implemented at Talvivaara in Finland (Saari and Riekkola-Vanhanen, 2011; Riekkola-Vanhanen, 2010), whilst Jinchuan Nickel company in China has also piloted Ni-Cu heap bioleaching of low-grade ore using mesophiles (Qin et al., 2009). It becomes relevant in this

study due to the prevalence of base metals (Cu, Ni, Co and Fe) as sulphide minerals in Platreef ore.

Figure 14 shows the primary mechanism of the process; it is essentially the leaching of sulphide minerals using a ferric-ferrous couple regenerated by air/oxygen and catalysed by microorganisms. In simple terms Fe^{3+} oxidises the sulphide mineral thereby releasing the target metal into solution to be recovered by the appropriate method. In so doing it is reduced to Fe^{2+} which can be oxidised back to Fe^{3+} using air/oxygen. This regenerative step is extremely slow but can be catalysed using Fe-oxidising microorganisms to the extent that it becomes commercially useful in acquiring the metals in a suitable time. Additionally, the microorganisms are also required to oxidise the sulphur completely to sulphates to avoid formation of intermediate or elemental sulphur species which bring the risk of the formation of acid rock drainage. In the case where a bioleach is followed up by a cyanide leach stage, the presence of sulphur species threatens to consume cyanide reagent by sulphur species reacting with cyanide to form thiocyanate.

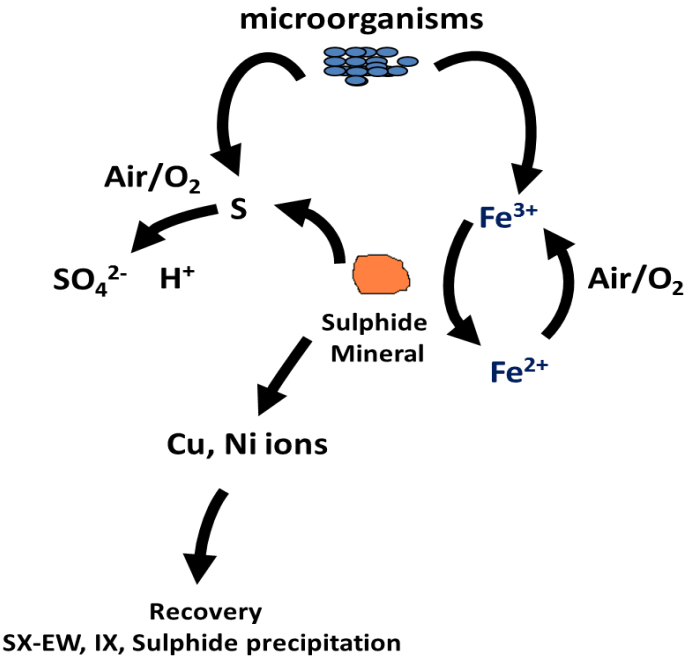

Figure 14: Mechanism of bioleaching a sulphide mineral using ferric ions catalysed by microrganisms

The process of sulphide mineral oxidation is highly exothermic and the benefit of using thermophiles (microorganisms that can survive to catalyse the process at high temperatures) at elevated temperatures of 65-85°C to speed up the reaction kinetics of sulphide mineral

bioleaching and enable the leaching of copper from chalcopyrite is well documented (Watling, 2008; Du Plessis et al., 2007; Plumb et al., 2007; Stott et al., 2003; Plump et al., 2002; Dew et al., 2000; Stott et al., 2000, Norris and Owen 1993). At moderate temperatures of say 35-45°C the leaching of chalcopyrite is widely known to be inhibited by a passivation layer. There however, is no scientific consensus on the nature of this layer with three possible causes of this layer being identified (Mpinga et al., 2015):

1. The adherent film formation of sulfur (S_0), disulfide (S_2^{2-}) and/or polysulfide (S^{2-}_n) on the mineral particle surface, which reduces the diffusion of the leaching agent to the mineral reacting surface.

2. The formation of a copper rich polysulfide layer developed on the surface as a result of solid state changes that occur in the mineral during leaching.

3. The formation of impermeable layer comprised of Fe hydroxy-oxide compounds such as jarosites, shwertmannite, ferrihydrite and other oxyhydroxysulphates. Of all these, Jarosite is the one most commonly reported by most authors. These iron precipitates are reported to cause the loss of ferric ions (for leaching) from solution, and clogging of pore spaces halting flow of solution on micro and macro-scales (Leahy and Schwarz, 2009), prevent bacterial access and restrict transfer of oxidant and leachate to the mineral surface (Stott el al., 2000). The formation of jarosite can be described by the reaction below where X can be any of a number of cations (K^+ , Mn^{2+}, Mg^{2+}, Al^{3+}, Na^+, Ca^{2+}) (Leahy and Schwarz, 2009; Ozkaya et al., 2007):

$$X^+ + 3Fe^{3+} + 2SO_4^{2-} + 6H_2O \leftrightarrow KFe_3(SO_4)_2(OH)_6 + 6H^+ \quad (2.6)$$

   In systems with chalcopyrite the above reaction is believed to be irreversible (Leahy and Schwarz, 2009).

Depending on the percentage of sulphur as sulphide minerals, the process can potentially generate enough heat to run the heap at elevated or thermophilic conditions (>50°C) (Pradhan et al., 2008; Dixon and Petersen 2003). The heat generated and resultant moisture can be conserved in the heap by manipulating the rates of solution irrigation onto the heap and air up flow in the heap (Kelly et al., 2008; Harvey et al., 2002; Dixon, 2000), and through the

appropriate use of transparent plastic sheets (Saari and Riekkola-Vanhanen, 2011). This has been successfully demonstrated in pilot operations at Newmont, Nevada (Tempel, 2003) and Kennecott, Utah (Ream and Schlitt, 1997); and a full scale industrial operation in Sarcheshmeh, Iran (Neale, 2012; Pradhan et al., 2008). This method thus, allows the leaching of ore or concentrate using the low capital and operating costs of heap leaching but with the advantage of operating at a higher temperature for faster reaction kinetics (Petersen and Dixon, 2002).

Bioleaching as a pre-treatment to cyanidation is a requirement to reduce the consumption of cyanide by the copper and nickel. These metals are easily complexed by cyanide and have the effect of consuming cyanide which is otherwise meant for precious metals especially in cases where dilute cyanide solutions are used (Marsden and House, 2006; Chamberlain & Pojar, 1984). This is especially challenging as BMs are often present in significantly larger quantities than precious metals in ore. Furthermore, base metal cyanide complexes can readily be adsorbed to carbon (Marsden and House, 2006), causing further interference in the recovery of PGMs using the widely applied adsorption to carbon process for recovery precious metals from cyanide solutions. This interference may also extend to other forms of recovery such as zinc cementation or electrowinning (Aylmore & Muir, 2001).

The use of cyanide to extract Cu and Ni has been explored (Gupta & Mukherjee, 1990; Habashi 1999). In theory, this presents the possibility of evaluating a single cyanide leach step to extract both BMs and PGMs. However, the recovery methods of BMs from cyanide solution are not well established and wide-spread on an industrial level. In contrast, several technologies, namely solvent extraction, electrowinning, sulphide precipitation and crystallisation, are well established and wide spread in recovering BMs from acidic sulphate based media.

2.4.6.3. Heap Cyanide Leaching

Cyanidation is currently the premier method of extracting gold and silver. In the case of low grade deposits, heap leaching is the choice of method for executing this process. Despite common perceptions, cyanide is the most effective and environmentally friendly reagent from a list of reagents (sodium bisulphide, thiosulphate, thiourea, hypochlorite, chloride and bromine/bromide, iodide/iodine solutions) that can be used for this application (Kappes 2002). Cyanide residues (in the form of free cyanide) on tailings will naturally degrade in the presence of air and sunlight. If copper is present, it tends to stabilize weak-associable (WAD) cyanide

to a form that is toxic to wildlife yet less amenable to natural degradation processes (Adams et al., 2008). However, to prevent this and further risk to the environment, there are several technologies to treat waste solutions and recover value cyanide waste effluents namely:

1. SART® - Sulfidization, Acidification, Recycling, and Thickening process: The process recovers copper (and other metals such as silver and zinc) as a sulfide precipitate, separates the precipitate from solution, and recovers cyanide through re-neutralization of the effluent. The neutralized solution is recycled to the leaching process (Stewart and Kappes, 2011).

2. AVR (Acidification, Volatilization, Recovery) - Influent is acidified to pH <2 in aeration tower to dissociate free, WAD, and strong cyanide complexes to metal ions and liberate gaseous HCN; HCN recovered as concentrated NaCN in adsorption tower by contact with caustic/lime; Metal ions removed as hydroxide precipitates (Stewart and Kappes, 2011).

3. Acidification, Copper Cyanide Precipitation - Influent acidified to pH < 3 to remove Cu as CuCN. CuCN filtered and collected, HCN regenerated as NaCN by adding lime or caustic (Stewart and Kappes, 2011).

4. MNR Process: Similar to the SART® process, this is a sulphide precipitation based operation. Influents are treated with acid and chemical sulphide to precipitate copper sulphide, followed by direct filtration or collection of precipitate (Stewart and Kappes, 2011).

5. Electrowinning (The DuPont process): Copper bearing solution is electrowon in a divided cell to produce copper metal and liberate free cyanide at the cathode. An ion-selective membrane prevents CN oxidation at anode (Stewart and Kappes, 2011).

6. Ion-Exchange (AuGMENT® and Vitrokele processes): WAD and free cyanides are adsorbed onto strong-base resin for pre-concentration, followed by elution and metal recovery. The AuGMENT uses commercially available resin with a combination of AVR and Electrowinning process to recover copper and cyanide while Vitrokele uses a proprietary resin in combination with AVR (Stewart and Kappes, 2011).

7. ASTER™: The Activated Sludge Tailings Effluent Remediation process can be used to treat effluent solutions containing high levels of cyanide and thiocyanate through microbial degradation in aerated reactors (van Zyl et al., 2015; van Zyl et al., 2011). To date there are two commercial ASTER™plants are in operation, one at the Barberton Mines Limited Consort plant in South Africa and the other at the Nordgold Suzdal plant in Kazakhstan. Amongst its many advantages are low operating costs, low level of operating skill required and robust technology suited for remote areas.

8. EMS® (Engineered Membrane System): Developed by H W Process Technologies, uses a thin-film membrane, to separate ions based on absolute size, shape of specific non-charged molecules, the charge, charge density and degree of hydration of charged inorganic salts or organics (Lien 2008). It can be used in the fractionation, concentration and purification of cyanide effluent streams to recover the free cyanide and remove various other cyanides (Cu, Ni, Fe, etc).

9. INCO process: In this process free cyanide and weakly or moderately bound metal cyanide complexes present in effluent streams are oxidized to the less toxic compound cyanate (OCN^-). This is achieved using sulphur dioxide and oxygen in a well-mixed and aerated reactor (Botz, 1999; Hewitt et al., n.d.) and the presence of a copper catalyst, as per the equation below.

$$SO_2 + O_2 + H_2O + CN^- \rightarrow OCN^- + SO_4^{2-} + 2H^+ \quad (2.7)$$

10. Caro's Acid Process: Caro's acid (H_2SO_5) also known as peroxymonosulfuric acid or oxone monopersulfate is a strong oxidizing agent which has found industrial application in the detoxification of cyanide waste effluents and pulps/slurrys as per the equation below.

$$H_2SO_5 + CN^- \rightarrow OCN^- + SO_4^{2-} + 2H^+ \quad (2.8)$$

It can also be used to treat thiocyanate waste but with high reagent consumption. It does not require a catalyst such as copper due to fast reaction kinetics and is especially used where the presence of copper is undesirable (Botz, 1999; Hewitt et al., n.d.).

The cyanidation process is greatly aided by the relatively low cost and efficient option to recover the precious metals from cyanide solutions through adsorption to carbon. Gold and silver heap leaching was first successfully implemented at Cortez and Smoky valley in Nevada (USA) in 1969 (Marsden and House, 2006) following the development of this process by Heinen, Lindstrom and others at the US Bureau of Mines. In the following years the process gained momentum with the development of the adsorption to carbon process to recover the gold from cyanide solution, followed by electrowinning, although some plants, past and present, still prefer to use zinc cementation as a method of recovery. Additionally aiding the spread of gold cyanide heap leaching was the development of agglomeration to treat ores with high clay content which adversely affected gold recoveries. Gold and silver heap leaching has since flourished with a reported 120 mines worldwide using the technology (Kappes, 2002) owing to developments in supporting technologies such as earth-moving equipment, liner materials and designs, stacker designs and agglomeration procedures.

A number of studies have shown that cyanide can be used to leach PGMs and in so doing open the way for studies into cyanide heap leaching of PGMs.

Chen and Huang (2006) and Huang et al. (2006) in similar studies leached Pt (90-94 %), Pd (99%) from flotation concentrates containing 80 g/t Pt+Pd, and Pt (96%), Pd (98%) and Rh (92%) from spent auto-catalysts containing 1000-2000 g/t Pt+Pd+Rh. In both cases pre-treatment in the form of acid pressure leaching for the concentrate and alkaline pressure leaching for the auto-catalysts. This was followed by two-stage cyanide pressure leaching at 160°C, 1.5 MPa O_2, solid to liquid ratio 1:4 for 1 hour. Tests were conducted using a 50 L autoclave and 5 Kg samples of material. Costa and Torres (1997) treated in ore containing 1.9 g/t Pt and 2.2 g/t Pd with a two-stage cyanidation process beginning with a room temperature leach followed by a pressure leach at 95°C and 0.3 MPa. This achieved a total recovery of 65.4% Pt and 80.9% Pd. There is no mention of what mineral forms the PGMs took in the concentrates and ores in the above studies. In their study Bruckard et al. (1992) treated samples of Coronation Hill ore in which Pt (3.6 g/t) and Pd (9.2 g/t) were in the form of Fe alloys, selenides and antimonides. Coarse 500 g samples and ground to 80% passing 74 µm were first amalgamated to remove gold and then leached with cyanide at temperatures of up to 150°C and 1 MPa overpressures of air, oxygen and nitrogen. The tests were conducted in a 4 L titanium autoclave. The best results achieved were 80% Pt and 90% Pd extraction at 100°C, pH range 9.5-10.0 for 6 hours on a finer grind sample. This study was a follow-up to one

previously conducted by McInnes et al. (1994) who used identical samples and procedures with the exception that the cyanidation was conducted at ambient pressures resulting in lower Pt extractions (30-35%). Kuczynski et al. (1992) from the US Bureau of Mines operated a 2 Kg per day batch operation to recover PGMs from automobile catalysts. The process proceeded in a two-stage autoclave leach (capacity 8.5 L) at 160°C, 0.5 MPa, solid to liquid ratio 1:2 for 1 hour. They achieved PGM extractions of between 90-95% dependent on the catalyst. Desmond et al. (1991) also from the US Bureau of Mines conducted a similar study to Kuczynski et al. (1992) using the same samples and techniques but varying certain process conditions such as sodium cyanide concentration and solid to liquid ratios but ultimately ending up with similar results of 97% extraction of PGMs.

The chemistry of the reactions between cyanide and the PGMs is reasonably understood and documented (Sibrell et al., 1994; Chen and Huang, 2006) with Pt(II) and Pd(II) reported to form the complexes $[Pt(CN)_4]^{2-}$ and $[Pd(CN)_4]^{2-}$ in a reaction similar to the Elsner equation for gold cyanidation:

$$2Pt_{(s)} + 8NaCN_{(aq)} + O_{2(g)} + 2H_20_{(l)} \rightarrow 2Na_2[Pt(CN)_4]_{(aq)} + 4NaOH_{(aq)} \quad (2.9)$$

$$2Pd_{(s)} + 8NaCN_{(aq)} + O_{2(g)} + 2H_20_{(l)} \rightarrow 2Na_2[Pd(CN)_4]_{(aq)} + 4NaOH_{(aq)} \quad (2.10)$$

The stability constants (Marsden and House, 2006; Mountain and Wood, 1987) for the PGM-cyanide complexes are high in comparison to gold showing how stable the complexes are (Table 14).

Table 14: Stability Constants for the Pt, Pd and Au at 25°C

$[Pt(CN)_4]^{2-}$	$[Pd(CN)_4]^{2-}$	$Au(CN)_2^-$	$Au(CN)_4^-$
$Log\beta_4$	$Log\beta_4$	$Log\beta_2$	$Log\beta_4$
78	63	39.3	56

It should be noted that this equation applies to all the above studies in which ambient temperature cyanidation failed to achieve high extractions of Pt in particular seemly because a high O_2 partial pressure was needed to oxidize the Pt to higher oxidation state to complex with the cyanide. With the exception of the Coronation Hill ore in which Pt was in the form of Fe-

alloys, selenides and antimonides; it seems to have been in metallic or alloy form in all the other studies. This is very different from ores in the BIC where the PGMs largely take mineral form such as sulphides, tellurides and arsenides. Therefore there is reason to investigate whether or not ambient temperature or elevated temperature (≤ 50°C) cyanide leaching can achieve successful extraction of PGMs from these ores Mwase (2009). This would be the foundation for cyanide leaching of these ores and in particular the Platreef ore.

Further, PGMs can and have been successfully recovered from cyanide leach solutions. Bruckard et al. (1992) used carbon-in-pulp to recover PGMs from solution while Chen and Huang (2006) used zinc cementation at 60-80°C, pH 9.5-10, 0.1 MPa for 2 hours to obtain precipitates with a 70-90% PGM concentration. Kuczynski et al. (1992) and Desmond et al. (1991) both used thermal hydrolysis/decomposition at 250°C for 1 hour to recover 99.8% of the PGMs from the solutions as a precipitate. Costa and Torres (1997) in their patent claimed but did not provide experimental details of recovery PGMs using carbon/resin-in-pulp/columns followed by elution and finally electrolysis, cementation and precipitation.

2.4.6.4. A Study on Heap Leaching of PGMs from UG2 concentrates

Mwase et al. (2012a) investigated the potential to heap leach PGMs on a low-grade PGM concentrate derived from Western Platinum Ltd. The results showed the potential effectiveness of a two-stage heap leaching process to extract PGMs and BMs from low-grade, high chromium, UG2 concentrates. Concentrate was used as a proxy material to demonstrate the concept, but further test work using a whole ore material (which is the subject of this thesis) was not pursued as it would take a significantly longer time. The study used laboratory scale columns to simulate heap leaching by coating the concentrate onto granite pebbles acting as support media for the concentrate. The first stage was a bioleach process operating at a temperature of 65°C with the aid of a mixed culture of thermophilic microorganisms. In a period of 4 weeks 52% Cu and 95% Ni were extracted. The residue material was washed and subjected to a cyanide leach at ambient temperature (≈23°C) for a period of 3 weeks. This resulted in extractions of 20% Pt, 87% Pd and 46% Rh with additional extractions of Cu and Ni. The study did not fully explore the potential use of elevated temperatures, nor the use of oxidants (other than air) for improving kinetics and extraction levels for the PGMs in the cyanide leach.

2.4.6.5. A Study on Heap Leaching of PGMs from Platreef concentrate

Mwase et al. (2012b) further explored the use of the two-stage heap leaching process on Platreef flotation concentrate prior to applying the process to coarse ore. The notable difference was that the cyanidation stage was conducted at an elevated temperature. Similar to Mwase et al., (2012a) concentrate was coated onto support material and packed into cylindrical columns to simulate heap leaching and treated in two stages; a bioleach followed by cyanidation. The following results were achieved and observations made.

2.4.6.5.1. Two-Stage Leaching

High levels of BMs extractions were achieved in all columns as seen from Table 15. Although the general amenability of this ore to high temperature bioleaching due to occurrence of these metals as sulphide minerals coupled with the presence of pyrite and pyrrhotite were the reasons for the high extractions, galvanic interaction (Bharathi et al., 2008) between the various sulphide mineral phases may have played a role. Galvanic leaching occurs when two mineral phases are in contact with each other and where one has a lower rest potential than the other. The mineral with the higher potential thus acts as a cathode while the one with the lower potential serves as an anode and experiences preferential leaching. Chalcopyrite in contact with pentlandite promotes faster leaching of nickel due to chalcopyrite's higher rest potential (Bharathi et al., 2008; Mason & Rice, 2002). Chalcopyrite leaching is primarily promoted by its association with pyrite (Ekmekci and Demirel, 1997).

Table 15: Extractions of BMs achieved over 88 days determined by fire assays of residual concentrate after bioleach

			Cu		Ni		Co
Column	**Temp**	**Solution Assay**	**Solid Assay**	**Solution Assay**	**Solid Assay**	**Solution Assay**	**Solid Assay**
	°C	%	%	%	%	%	%
1	65	91.1	91.1	108	98.5	83.5	92.7
2	70	65.5	84.7	104.6	96.9	86.1	100
3	75	85.4	89.4	108.3	98.0	82.7	100
4	80	56.8	69.9	97.3	93.0	76.8	100

Co-leaching of PGMs was also observed, and was comparable to the levels currently experienced in typical base metal refining in context of the typical platinum beneficiation route (Dorfling et al., 2010). However, these metals are potentially recoverable via methods such as solvent extraction, ion exchange and precipitation (Kononova et al., 2011; Bernardis et al., 2005; Seymour & O'Farrelly, 2001; Els et al., 2000).

There was considerable dissolution of the gangue elements Mg, Al and Ca. This is of importance as accumulation of these elements in the range of 10-12 g/L leads to inhibition of ferrous oxidation by bacteria (Ojumu et al., 2008). Although the concentrations of these elements were below 0.25 g/L in this test work, on an industrial scale, where the solution would typically be recycled, a bleed system would have to be built into the design to prevent the build-up of these elements over long leaching periods.

The rate and extent of Pd and gold (Au) extraction was high, reaching near complete extraction (Table 16) as compared to Pt in the same time period. From Figure 15, Mwase et al., 2012b deduced that the low Pt extraction was caused by two things. Cyanide depletion or equilibrium saturation accounted for one of these: After day 15 it was observed that in 4 days the curve would level off and then pick up on the 7^{th} day of every recycle when fresh solution was applied. This means that if the solution was changed more frequently or in a continuous flow manner, the overall rate and extent of Pt extraction may have been higher over the same period of time. However, the main cause of low Pt extraction was attributed to a mineralogical limitation. The more cyanide soluble platinum minerals were dissolved in the first 15 days, leaving the less soluble ones behind. An analysis via a mineral liberation analyser (MLA) on a sub-sample of the residual material indicated that 78 % of the remaining Pt was in the form of sperrylite ($PtAs_2$). It also indicated that at this stage the remaining PGMs were 91 % liberated, eliminating lack of contact with solution as a cause for low extraction. This confirmed that sperrylite housed a significant amount of the Pt and was slow leaching in cyanide solution compared to the other Pt minerals present.

Table 16: Precious metals extractions after 45 days of cyanide leaching

Columns	Pt	Pd	Au
	%	%	%
A	34.3	96.5	63.4
B	32.2	92.5	97.5

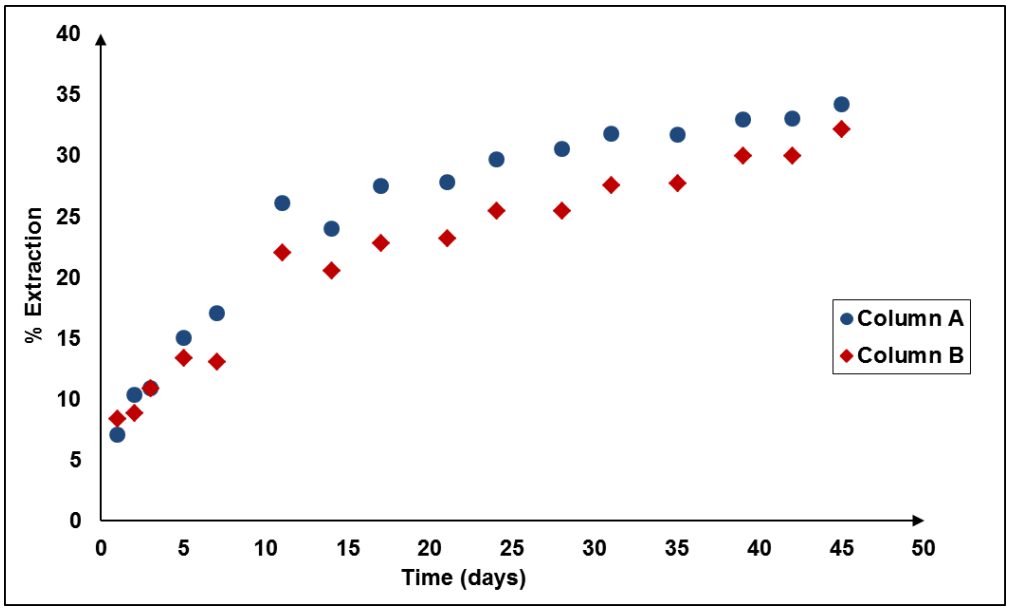

Figure 15: Platinum leach curves: Both columns leached at 50°C with 5 g/L NaCN, fed rate-1 L/day, aeration 150 mL/min (Mwase et al., 2012b).

The presence of sulphur, at a level of up to 5000 ppm, was also detected through ICP analysis of the cyanide solution in the stirred reactor experiments. High pressure liquid chromatography (HPLC) was used to confirm that the sulphur was in the form of thiocyanate. An analysis via MLA post-bioleach showed no elemental sulphur or sulphide minerals present in the concentrate, but a LECO combustion test showed that there was 44% sulphur showing incomplete sulphur oxidation during the bioleaching process. In the absence of elemental sulphur and sulphide minerals it is postulated that the sulphur was present as thiosulphate, polysulphides or polythionates, which are capable of reacting with cyanide to form thiocyanate (Luthy and Bruce, 1979) as seen in the equations below:

Polysulphides

$$S_xS^{2-} + CN^- \rightarrow S_x^{-1}S^{2-} + SCN^- \qquad (2.11)$$

Polythionates

$$S_2O_3^{2-} + CN^- \rightarrow SO_3^{2-} + SCN^- \quad (2.12)$$

Thiosulphate

$$S_xO_6^{2-} + (x\text{-}1)CN^- \rightarrow SO_4^{2-} + (x\text{-}3)SCN^- + S_2O_3^{2-} \ (x=3, 4, 5 \text{ or } 6) \quad (2.13)$$

These compounds may have crystallized out into the residual concentrate, or more likely co-precipitated with or adsorbed onto the jarosite phase and been carried over to the cyanide leach. Adsorption of PGMs onto Fe-oxyhydroxide phases has been reported (Evans, 2007) and hence BMs may also readily adsorb onto jarosites. Further test work and analysis is required to verify the source and identity of the compounds that lead to thiocyanate formation. It is also proposed that in addition to the Fe oxidizing bacteria, another culture of bacteria grown on elemental sulphur can be added to the process to complete the oxidation of the sulphur.

The amounts of BMs and gangue elements extracted in the cyanide leach (Table 17) were low considering the rather low remaining amounts of the BMs after the bioleach and the large quantities of gangue elements present. This perhaps speaks to the relative selectivity of an alkaline leach system as opposed to an acidic leach. There is the possibility that some of the more alkaline soluble gangue minerals could have been dissolved or converted in the acidic bioleach. Additionally, a number of the silicate minerals present in the concentrate are known to be unreactive in both acid and alkaline media.

Table 17: Extraction of major BMs and Gangue elements in cyanide leach

Columns	Cu	Ni	Fe	Co	Mg	Al	Si	Ca	Cr
	%	%	%	%	%	%	%	%	%
A	18.3	32.3	0.0	0.8	0.0	0.1	0.0	0.1	0.8
B	17.0	16.1	0.0	0.0	0.0	0.2	0.0	0.1	1.4

Despite some problems the two-stage heap leach process, modified to have a high temperature cyanide leach, holds promise as an alternative route to treat Platreef ore. In this regard the process has been patented (Eksteen et al., 2012) on the basis of the work on Platreef concentrate subsequently presented by Mwase et al. (2012b). The process has not, however, been tested on whole ore and this will be further investigated in the first part of this study.

2.4.6.5.2. Recovery of PGMs

In collaborative but separate test work the precious metals (Pt, Pd and Au) were shown to be efficiently recoverable from cyanide leach solutions using adsorption to carbon and subsequent elution (Mpinga et al, 2014a; Synders et al., 2013). Mpinga et al. (2014a) investigated the preferential adsorption of the precious metals (Pt, Pd and Au) over other major ions (Cu, Ni and Fe) to activated carbon in bottle roll tests. The tests used a synthetic cyanide solution made up with metal cyanide salts instead of leach liquors from the cyanide test work by Mwase et al. (2012b). The salts were added in such a manner as to have identical concentrations of Pt, Pd, Au, Cu and Ni as the leach liquors in the cyanide leach tests (Table 18).

Table 18: Concentration of target elements in bottle roll test solutions

	Pt	Pd	Au	Cu	Ni
Concentration (mg/L)	1	7	0.76	160	130

They found that the adsorption rates for the precious metals were rapid, giving more than 90% recovery in the first 60 minutes and 100% Pt, 97% Pd and 99.9% Au in 72 hours. The affinity of the ions for the carbon was found to follow the sequence:

$$Au(CN)_2^- > Pt(CN)_4^{2-} > Pd(CN)_4^{2-} > Ni(CN)_4^{2-} > Cu(CN)_3^{2-}$$

Adsorption of Ni was found to proceed at a similar rate as the precious metals and hence its concentration was found to be the most influential parameter in the process. The levels of thiocyanate and free cyanide were also found to play a small role in the adsorption of precious metals but not as important as Ni. The loading capacity for the activated carbon was found to be 0.64, 0.66 and 0.17 mg of Pt, Pd and Au per g of carbon respectively. Mpinga et al. (2014b) further found that cementation while effective for gold recovery, was not as effective in the recovery of PGMs. Test work achieved only 19% Pt and 54% Pd recoveries but as much as 91% Au. Repetition of the test with excess zinc powder resulted in 36% Pt and 48% Pd recoveries. In conjunction with Mpinga et al. (2014a), Synders et al. (2013) investigated the elution of precious metals from loaded carbon using an analogue of the Anglo American Research Laboratory (AARL) elution process. The process was found to be effective eluting 100% of the Pt and Pd at 80°C but only 64% of the Au. Schoeman et al. (2012) investigated

the use of resins to recovery PGMs from cyanide solution through ion exchange and subsequent elution. Promising results for recovery and elution were achieved, but the low loading capacity and expensive cost of resins compared to activated carbon disqualifies this route for immediate use.

On top of the current technology available to recover BMs from acidic sulphate solutions, collaborative but separate test work has shown that the BMs can be recovered from bioleach solutions by ion exchange resins and subsequent elution (Liebenberg et al., 2013).

2.4.6.5.3. Energy Management and Conservation

This section deals with how the high temperature cyanide leach can be achieved in a full scale operation. Unlike the heap bioleach which is exothermic, the cyanide heap leach is roughly energy neutral. However, high temperatures would enhance the extraction of precious metals as initially established by Mwase (2009) and it is proposed that this be achieved by heating of cyanide solution via means of solar energy (or other available natural sources such as geothermal heat). A collaborative study with De Lange and Reinecke (2012) showed that it was technically feasible to build a solar system to warm up solution prior to irrigating the heap and incorporating sufficient insulation of solution ponds and piping/tubing to maintain temperatures. This study used data about heap operations from literature, mainly provided by Mwase et al. (2012a) and Mwase (2009), and was deemed to be financially beneficial in terms of the value gained from increased Pt extraction (comparing extractions achieved in Mwase et al., 2012a with 2012b) at higher temperatures when taking into account the capital and operating costs of this solar heating system verses other forms of energy to warm the solution. South Africa has some of the best conditions for solar energy in the world and on average receives between 2100-2200kWh/m^2 (GHI- global horizontal irradiance) per year. By comparison, Spain which is currently one of the world leaders in solar technologies, receives between 1700-1800 kWh/m^2 (GHI) per year (Lange and Reinecke 2012).

It is also proposed that the water used to wash the ore in between heap leaching stages also be heated by the same energy sources. This will aid in conserving some of the heat from the bioleach process and thus, the ore will not have to be re-heated for the cyanide leach stage. Figure 16 is a graphical representation of this system.

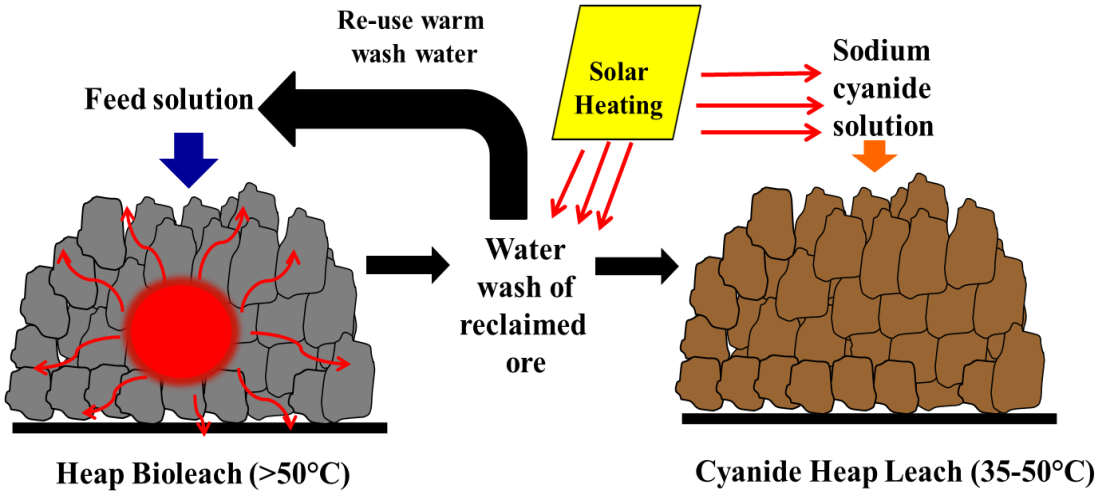

Figure 16: Energy management and conservation system for the patented two-stage process.

This collaborative work on processing the Platreef ore has resulted in the conceptualization of the flowsheet (Figure 17) as an alternative means to process the ore.

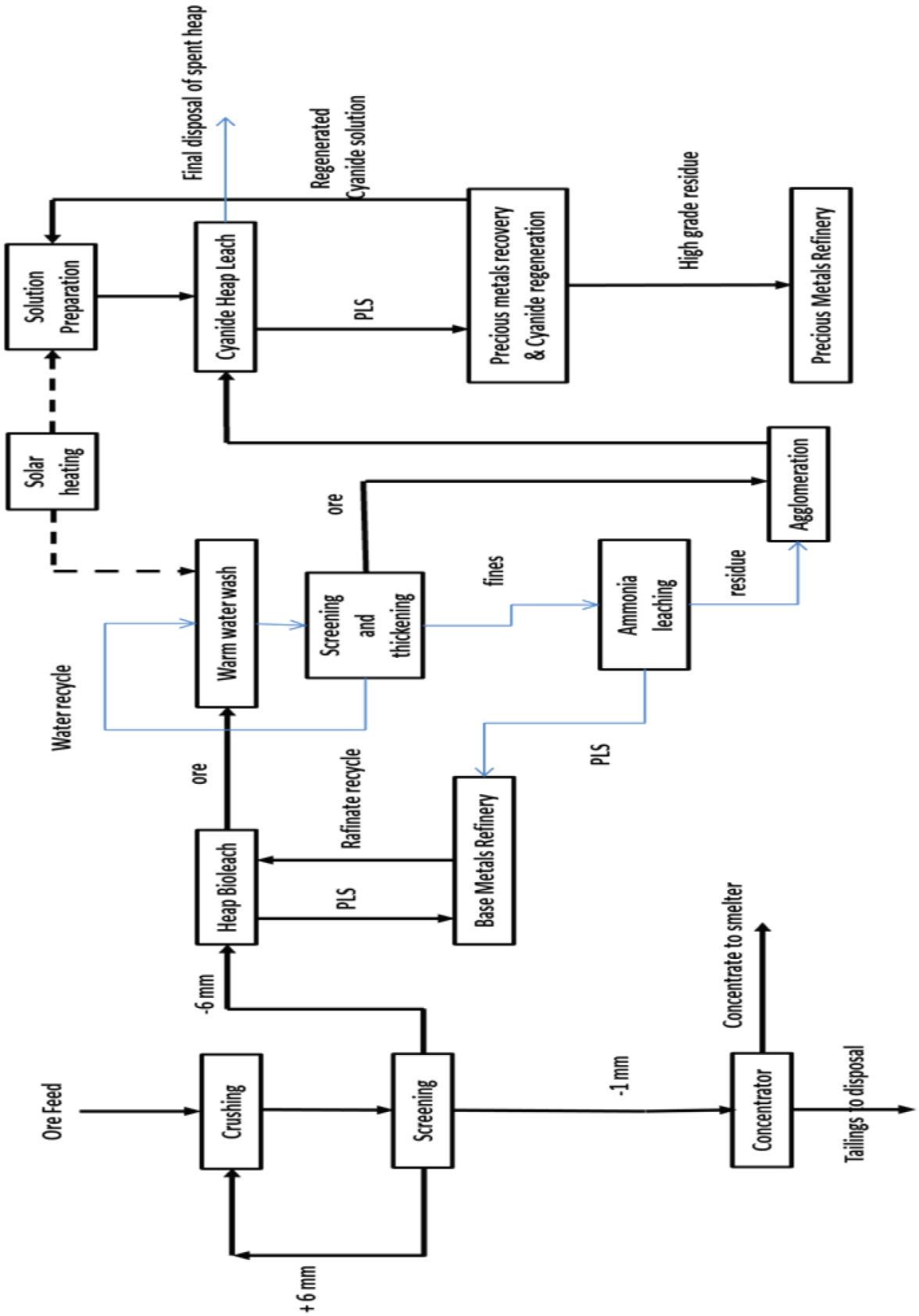

Figure 17: Two-stage heap leaching process for Platreef ore (PGMs)

2.4.7. Investigating the Cyanide Leaching of Sperrylite

The occurrence of a significant portion of the Pt as sperrylite ($PtAs_2$) in the Platreef concentrate has prevented the successful high temperature cyanide leaching of the Pt from this material as seen in section 2.4.6.5.1. Only 34% of Pt was extracted as compared to over 90% of Pd and Au in the same leach test. The second part of this study will thus investigate why sperrylite leaches slowly in cyanide. Presented in the following is a brief literature review of sperrylite chemistry.

2.4.7.1. Leaching Chemistry of Sperrylite in Cyanide

There is virtually no literature on the chemistry of sperrylite in cyanide or any common leach solution, as prior to the studies by the author Mwase (2009) and Mwase et al. (2012a and 2012b) which proposed heap leaching and non-aggressive approaches; PGMs have been recovered using the conventional route, and the alternatives investigated have also been aggressive methods guaranteed to dissolve everything in a concentrate even unwanted gangue minerals. Sperrylite is a chemically stable compound that does not readily decompose or weather through normal weathering processes such as those that affect BM minerals like chalcopyrite. Laboratory test work has shown that if calcined at temperatures of up to 800°C in the presence of air, it becomes soluble in cyanide (Snyders et al., 2013). The most suitable proxy for this mineral is gold arsenides which are even rarer, with no known significant deposits and processing operations (Habashi, 2011, pers. comm.; Nicol, 2011, pers. comm.; Lotz, 2011, pers. comm.). However, it has been suggested that exploratory work at laboratory level has achieved successful leaching of gold from arsenides using chlorine (Habashi, 2011, pers. comm.). These two separate studies suggest the need for oxidation in the successful leaching of an arsenide. There is no information that outright states the oxidation states of Pt or As in sperrylite in literature. Pt in the mineral could be in the more prevalent +2 or +4 states (Seymour and O'Farrelly, 2001; Giandomenico, 2000) or perhaps the extremely rare +6 oxidation state (Seymour and O'Farrelly, 2001; Giandomenico, 2000); all of which easily complex with cyanide. The most common valence states of As are -3, 0, +3 and +5 (Marinov and Brebbia, 2010; Henke and Hutchison, 2009). Therefore the most likely state of As should be -3, but this would make Pt be in the unlikely state of +6. Henke and Hutchison (2009) report that like sulphide in pyrite, As in arsenic-rich (arsenian) pyrite and many arsenide and arsenosulpide minerals has a valence of -1 or 0. Marinov and Brebbia (2010) have also acknowledged the possibility of the rare -1 or -2 oxidation states of As. These oxidation states

are a result of the As or S being present in multiple/mixed oxidation states in the mineral. An oxidation state of -1 for As would mean that Pt is therefore in the most common and likely state of +2. Therefore from the literature alone it is impossible to conclusively state the oxidation states of Pt and As in sperrylite. Whatever the case, this would mean that As or a part of the As is definitely in a lower oxidation state. In these lower oxidation states arsenic (in a compound) is reported to be least soluble (Anderson, 2010; Vladmir and Moran, 2006). Hence it is suggested that successful leaching of sperrylite requires the oxidation of As (or the part of the As that is in the lower oxidation state) to a higher more soluble oxidation state thus breaking the chemical bond with Pt and releasing it into solution. Therefore the part of the As in the sperrylite that is in the lower oxidation form, is oxidised to a higher state either +3 or +5 as per one of the equations below:

$$As^{3-} \rightarrow As^{3+} + 6e \quad (2.14)$$

$$As^{3-} \rightarrow As^{5+} + 8e \quad (2.15)$$

$$As^{2-} \rightarrow As^{3+} + 5e \quad (2.16)$$

$$As^{2-} \rightarrow As^{5+} + 7e \quad (2.17)$$

$$As^{-} \rightarrow As^{3+} + 4e \quad (2.18)$$

$$As^{-} \rightarrow As^{5+} + 6e \quad (2.19)$$

Depending on its state or states one or more of these equations could be the anodic reaction in an oxidative dissolution process.

Arsenic dissolved in natural waters occurs mostly as +3 and +5. In both states it usually bonds with oxygen to form arsenite (As^{3+}) and arsenate (As^{5+}). Depending on pH As^{3+} usually exists in low-oxygen (reducing) groundwaters and hydrothermal waters, and further can be found as $H_3AsO_3^0$, $H_2AsO_3^-$, $HAsO_3^{2-}$, and/or AsO_3^{2-} (See Figure 18 which shows the dissociated forms for some of the anions). As^{5+} on the other hand is more prevalent in oxidizing groundwaters and surface waters typically as $H_3AsO_4^0$, $H_2AsO_4^-$, $HAsO_4^{2-}$, and/or AsO_4^{3-} dependant on pH (). More detailed chemistry of these forms of As can be found in Henke and Hutchison (2009).

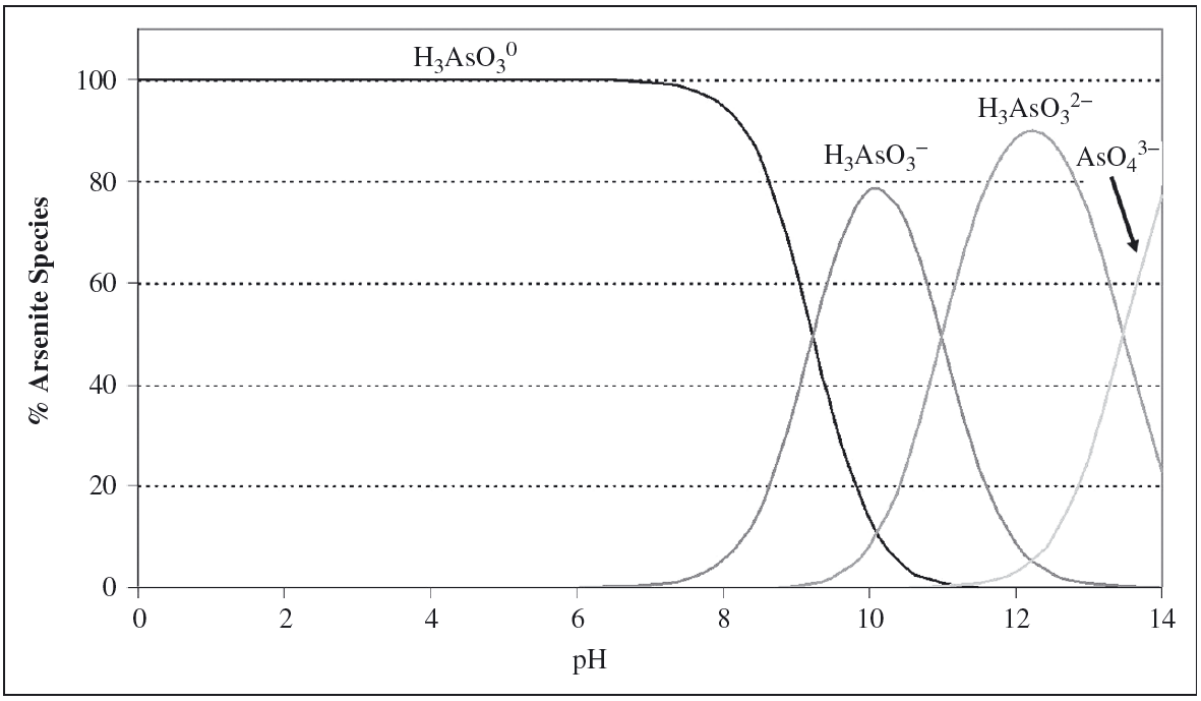

Figure 18: Speciation of arsenious acid with pH, taken from Henke and Hutchison (2009)

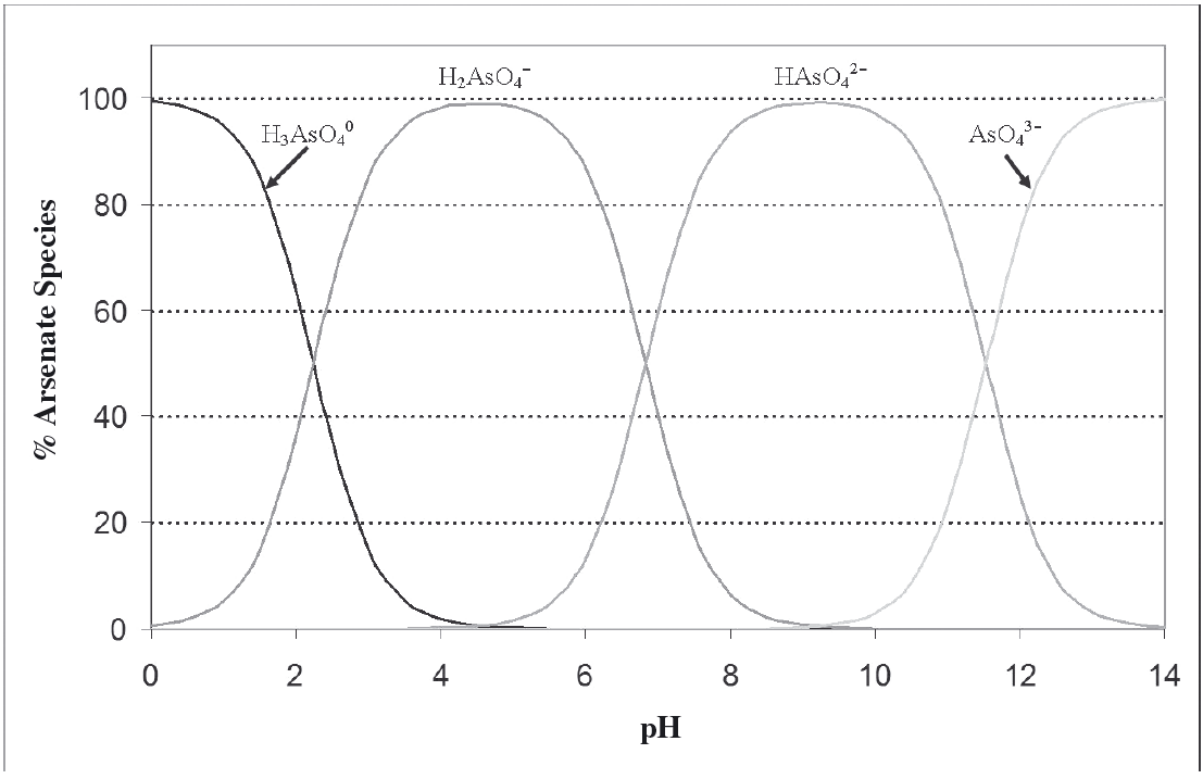

Figure 19: Speciation of arsenic acid with pH, taken from Henke and Hutchison (2009)

During test work on concentrate (Mwase et al., 2012b), at the point where the rate of extraction was at its lowest and mostly sperrylite was left, a sample of concentrate was leached in 1 M

NaCN solution at 75°C in a stirred tank reactor (as compared to 0.1 M and 50°C in the columns) for 21 days. There was an insignificant increase in the rate of leaching. This suggests that the reaction was not influenced significantly by temperature or reagent concentration, but is most likely a diffusion controlled reaction. It is postulated that some form of passivation may occur at the surface of the mineral. It is proposed that a small quantity of Pt leaching out leaves behind an As layer which passivates the surface of the mineral. This means that there is partial oxidation of the As from a lower state to 0 state or a transitional state as per the equations below:

$$As^{3-} \rightarrow As^{0} + 3e \quad (2.20)$$

$$As^{2-} \rightarrow As^{0} + 2e \quad (2.21)$$

$$As^{-} \rightarrow As^{0} + e \quad (2.22)$$

The columns were aerated during cyanide leaching, which provided a small amount of oxygen possibly supporting the slow leaching of sperrylite, and this may explain why the leaching did not stop completely. In the cyanide leaching of Au, where the pH is similarly alkaline and the solution aerated, the equation below represents the cathodic reaction (Marsden and House, 2006). These would also possibly be the cathodic reaction in the cyanide leaching of PGMs:

$$O_2 + 2H_2O + 4e \rightarrow 4OH^{-} \quad (2.23)$$

This would imply that if more oxygen was available in solution, then the As could be fully oxidized allowing a higher rate of Pt extraction. But, oxygen has a low solubility in solution and this decreases with temperature, hence other suitable oxidizing agents must also be considered for practical application. Ferricyanide has been investigated as a supplement oxidant (Xie and Dreisinger, 2009; Xie et al., 2008) to oxygen in the cyanide leaching of certain gold and silver sulphides which are similarly slow leaching in cyanide. The reduction potential for ferricyanide is slightly lower than oxygen in alkaline aqueous solutions (Greenwood and Earnshaw, 1997; Xie and Dreisinger, 2007; Song and Zhang, n.d), as seen in the equations below.

$$Fe(CN)_6^{3-} + e \rightarrow Fe(CN)_6^{4-} \quad E= 0.36V \text{ (SHE)} \quad (2.24)$$

$O_2 + 2H_2O + 4e \rightarrow 4OH^-$ E= 0.4V (SHE) (2.25)

However, the oxidation capability of ferricyanide can be maintained at a relatively high level due to high solubility in cyanide solution as ferricyanide and ferrocyanide are stable over a wide pH range (Figure 20) and will not react with cyanide (Xie and Dreisinger, 2007).

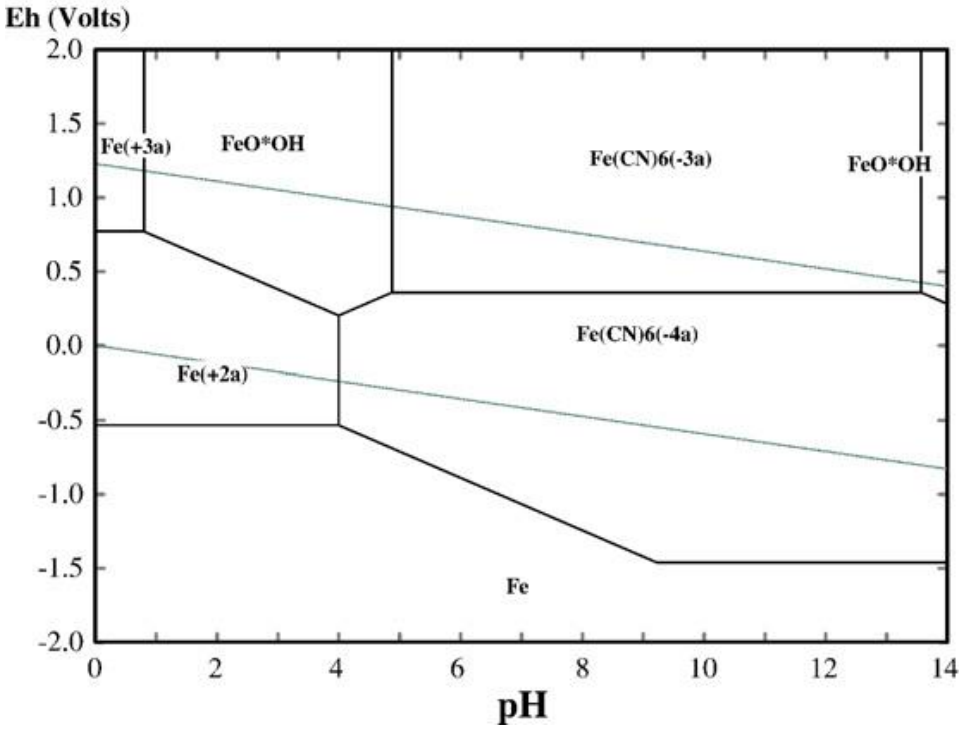

Figure 20: Eh-pH diagram of Fe-CN-H2O system at 25°C ([Fe]=10^{-2} M, [CN]=1 M) (Xie and Dreisinger, 2007)

Reagents of the per-oxygen (hydrogen peroxide and calcium peroxide) and per-manganate (potassium permanganate) species have all been studied as potential supplementary oxidants to oxygen in cyanide leaching of slow leaching gold and silver minerals (Xie and Dreisinger, 2009; Xie et al., 2008). However none have been successfully applied in practice due to high cost and their tendency to react preferentially with free cyanide at the high concentrations required to make them effective.

2.5. Hypotheses

Bench scale test work on UG2 and Platreef flotation concentrate have shown the potential for the development of PGM heap leaching which is currently not practiced in industry. The results from these studies are motivation enough to further explore this option by conducting test work on whole ore Platreef material. For Platreef concentrate the extractions for BMs (up to 91.1% Cu, 98.5% Ni and 100% Co) and precious metals (96.5% Pd and 97.5% Au) have been encouraging, with the exception of Pt (34.3%). In the case of the Platreef ore this has been linked to the occurrence of Pt in the form of sperrylite. In this form it has shown to be resistant to leaching with cyanide under the typical conditions of heap leaching-atmospheric pressure, less aggressive reagents, low-moderate temperatures. Further scrutiny of the structure of sperrylite shows that the As (or part of the As) is in a lower oxidation state which is the most insoluble form for the element and hence likely contributes to the stability of the arsenides. Pt on the other hand is likely to be in the higher oxidation states where it complexes easily with cyanide. In the absence of enough of a suitable oxidant it is hypothesized that:

1. Sperrylite leaches slowly in cyanide due to some form of passivation at the surface of the mineral. Based on the discussion above it is postulated that this passivation occurs as As transitions from a lower to a higher oxidation state. The transition is incomplete leaving As in a 0 oxidation state, preventing it from entering solution and instead it builds-up at the surface.

2. Increasing the amount of oxygen (or other oxidants) in solution will increase the rate of sperrylite leaching by fully oxidizing the arsenic to a higher more soluble state and preventing the formation of the passivation layer.

The objectives of this study are therefore to:

1. Explore the use of a two-stage heap leaching process, combining bioleaching to extract BMs followed by high temperature cyanide leaching to extract precious metals, on coarse ore material and thus further evaluate the potential of PGM heap leaching first explored using flotation concentrates as test material.

2. Explain and verify the nature of the passivation layer at the surface of the sperrylite and the mechanism by which it is formed, and thus account for the slow leaching of sperrylite in cyanide.

3. Explain the influence of oxygen and other oxidants on preventing the formation of the passivation layer, thus increasing the rate of sperrylite leaching in cyanide.

2.6. Novelty of this Study

PGMs are traditionally obtained hydrometallurgically from metallic sources, specifically alloys which tend to form during the smelter process on the conventional PGM route (Crudwell et al. 2011; Merkle and McKenzie, 2002). To a much smaller but not insignificant, extent they are also obtained from spent catalysts (Kuczynski et al., 1992, Desmond et al., 1991; Huang et al., 2006; Chen and Huang, 2006) where they are also in metallic form. In this form the PGMs need to be brought to higher oxidation states to be able to go into solution and complex with the available agent. This often requires high temperatures (excess of 120°C) and pressures (excess of 6 bar) and must be conducted in autoclaves on high grade materials (50-65% PGMs) and at relatively low volumes of materials (a few hundred kg at a time). The current conventional route and other proposed alternatives use aggressive chloride systems (Crudwell et al., 2011; Adams et al., 2011; Green et al., 2004; Fleming, 2002; Cabri, 2002; Seymour and O'Farrelly, 2001; Rapson 1997). In contrast, this study will investigate hydrometallurgical extraction of PGEs directly from minerals, where they are already in higher oxidation states, and from lower grade (4-70 g/t) and high volume (hundreds of thousands of tons at a time) sources such as crushed whole ore. Whereas there is data on the mechanisms, products and kinetics of PGM dissolution from metallics/alloys in chloride systems, the study aims to produce some fundamental knowledge with regards to PGM dissolution from minerals, specifically sperrylite, in the less aggressive cyanide system which is more conducive to heap leaching.

3. Chapter 3: Coarse Ore leaching

Using identical methods and equipment as Mwase et al. (2012a and 2012b), a two-stage heap leaching process will be applied to coarse ore from the Platreef in this first part of the study to evaluate the potential for this method to be used over the conventional process.

3.1. Sample Preparation

The samples for this study were drill core ore samples obtained from Lonmin Plc as part of their Akanani project to develop a site in the Northern Limb of the BIC (Platreef) specifically the Mokopane area. The samples were initially prepared by Mintek where they were crushed using high pressure grinding rolls (HPGR) at a pressure of 2.5 N/mm^2 resulting in a particle size range from 25 mm right down to fines in the micron range. The product was delivered to UCT where two samples were prepared from the bulk by splitting with a 2-way riffle splitter and screening to remove particles below 1 mm. One sample had a size distribution of -25 mm +1 mm (Sample 1) and the second was screened to a size range of -6 mm +1 mm (Sample 2). Each of the samples was prepared to weigh 4 kg. Due to a lack of sample only two columns were run hence experiments could not be conducted in triplicate. The head grades (Table 19 and Table 20) were determined by further crushing and pulverzing a sample, followed by splitting to generate sub-samples. This was follwed by fire assay consisting of acid digestion and analysis via inductively coupled plasma atomic emission spectroscopy (ICP-AES) for the precious metals, while the BMs in addition to the procedure described above required sodium peroxide fusion and further acid dissolution and analysis by ICP-AES. The bulk mineralogy (Table 21) and PGM mineralogy were determined by MLA analysis. All the analysis to determine head grades and bulk mineralogy was conducted by ALS Chemex, South Africa. The PGMs consisted mostly of tellurides, namely moncheite [$PtPd(BiTe)_2$] and $PtTe_2$, merenskyite [$PdPt(BiTe)_2$] and $PdTe_2$, maslovite (PtBiTe) and kotulskite [Pd(Te,Bi)] followed by arsenides (mostly sperrylite-$PtAs_2$) (Figure 21) with a small amount of sulphides (mostly cooperite-PtS), sulpharsenides and PtFe alloys. The silicates were the most common host minerals for PGMs, and where PGMs were associated with sulphide minerals; pentlandite and pyrrhotite were the most common hosts with chalcopyrite to a lesser extent. The total sulphur content was determined using the sulphur LECO test also conducted by ALS Chemex, South Africa.

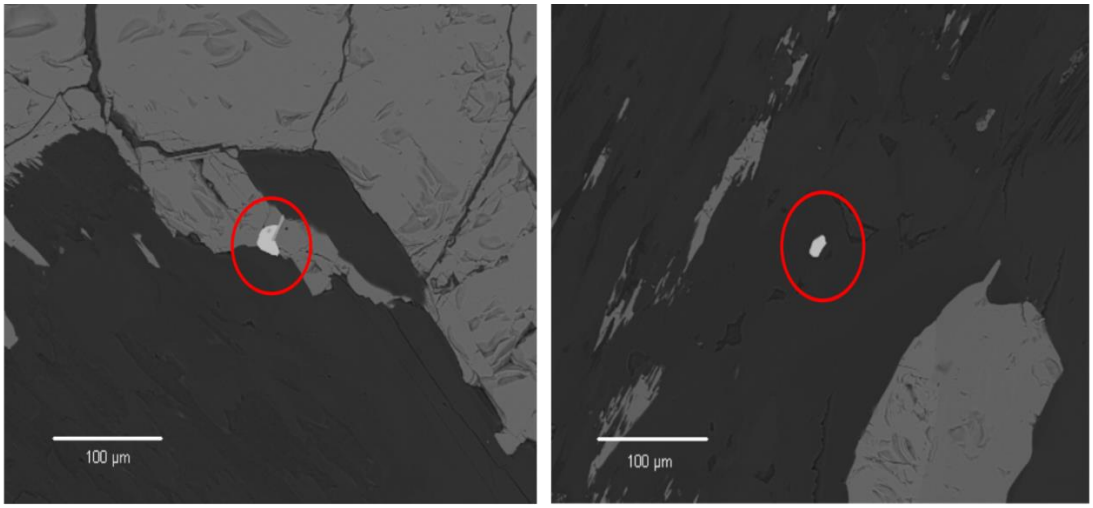

PdBiTe at grain boundary of pentlandite/silicate

$PtAs_2$ in silicate mineral

Figure 21: MLA images showing the PGM mineralogy of Platreef ore

Table 19: Head grade of target elements in coarse ore

	Pt	Pd	Au	Cu	Ni	Co	Fe	S
	g/t	g/t	g/t	%	%	g/t	%	%
Sample 1	1.6	2.0	0.3	0.13	0.35	130.0	8.6	0.8
Sample 2	1.6	2.0	0.3	0.12	0.35	129.0	8.6	0.8

Table 20: Major gangue and trace elements in coarse ore

	Mg	Al	Ca	Cr	Si	Mn	Ti	Pb	V	Zn	As	Se	Te	Bi
	%	%	%	%	%	%	%	g/t	g/t	g/t	g/t	g/t	g/t	g/t
Sample 1	14.1	2.5	4.2	0.3	23.3	0.2	0.1	19.5	93.0	33.0	3.3	1.8	4.3	0.1
Sample 2	14.9	2.5	4.1	0.3	22.3	0.2	0.1	13.3	93.0	24.0	5.0	2.1	4.4	0.1

Table 21: Bulk mineralogy of coarse ore

Mineral	Weight %	Mineral	Weight %
Pyrrhotite	1.8	Chlorite	3.2
Pentlandite	1.7	Talc	5.7
Chalcopyrite	0.8	Clinopyroxene	13.0
Pyrite	0.1	Magnetite	6.6
Olivine & Orthopyroxene	36.0	Chromite	0.8
Serpentine	22.7	Chlorite	3.2

3.2. Experimental Methods

3.2.1. High Temperature Bioleach on Coarse Ore

The two samples of whole ore were leached using the same equipment and similar procedure used for the bioleach on concentrate (Mwase et al., 2012b). Figure 22 shows a schematic diagram of the columns used while Figure 23 is a photograph of the actual experimental set-up and the experiment in progress. The samples were each packed in a separate column by placing them between two layers of glass marbles which acted as distributors of feed solution from the top and air fed through the bottom of the columns (Figure 22). The columns were heated up to and operated at a temperature of 65°C using an external heating coil wrapped around the columns and aerated with compressed air at a rate of 130 mL/min (equivalent to a superficial column area of 0.34 L/m^{2}s). Then the samples were initially leached with a 30 g/L H_2SO_4 solution which was pumped into the columns from the top at a rate of 1 L/day (equivalent to the standard industrial flow rate of 5-7 L/m^2/h) and the effluent was collected at the bottom of the columns. The samples were treated for 44 days in order to dissolve as much of the acid soluble BM minerals as possible. Thereafter the acid solution was replaced with the main feed solution containing 0.5 g/L Fe (as ferrous sulphate) and 10 g/L H_2SO_4, which was fed into the column at an identical rate and in the same manner to the 30 g/L H_2SO_4 solution.

From this point the columns were inoculated with a culture of thermophilic microorganisms (capable of oxidising Fe at temperatures greater than 35°C) to initiate the bioleach process. Quantitative real time polymerase chain reaction (qRT PCR) identified the culture as essentially being an almost pure culture of *Metallosphaera hakonensis*. *M. hakonensis* was readily available in the laboratory and had proven to be robust and effective at oxidising Fe at elevated temperatures of up to 80°C, specifically in bioleaching experiments on sulphide ores (Searby, 2006). This particular culture had been grown on pure pyrite at 65°C. The inoculation was done at a temperature of 65°C by mixing the culture with a small amount of feed solution (50 mL) and pumping into the columns in the same manner as the feed solution.

Samples of solution were collected from the effluent every day during the first 7 days of the acid wash and then every fourth and seventh day for the rest of the acid wash and the bioleach. The quantities of BMs and gangue elements present in solution were determined via inductively coupled plasma optical emission spectrometry (ICP-OES) to subsequently calculate the

amounts of metals leached. Each time a sample was taken the pH and redox potential were also measured and recorded using a standard pH meter and Ag/AgCl-Pt combination redox probe, respectively. On the onset of inoculation the increase in redox potential was taken as an indication of healthy microbial activity and hence successful inoculation. These samples were also inspected under a microscope, to monitor the wellbeing of the microorganisms. The experiment was allowed to run for a total of 304 days including the 44 days of acid wash. The extractions achieved were determined from the solution assays via inductively coupled plasma optical emission spectrometry (ICP-OES) and by fire assay (same procedure that was used in the sample preparation) of sub-samples from the residual ore samples. None of the samples, solution or solid residue, were collected in duplicate or triplicate. However all ICP analyses (in the case of solid residues the solution from digesting the sample) automatically involves running the sample three times and if an RSD less than 5% is detected then it is reported as an error. All the data used in this chapter and chapter 4 had an RSD less than 5%.

On completion of the experiment, the samples were collected from the columns and dried. Sub-samples were obtained for fire assays and quantitative evaluation of minerals by scanning electron microscopy (QEMSCAN) analysis. The image data from the QEMSCAN was processed and analysed using iDiscover™ software. The remaining bulk of the samples were then subjected to the main experiment, which is cyanide leaching to extract the precious metals. The bioleaching although recovering BMs can be considered as a form of pre-treatment to facilitate cyanide leaching of precious metals.

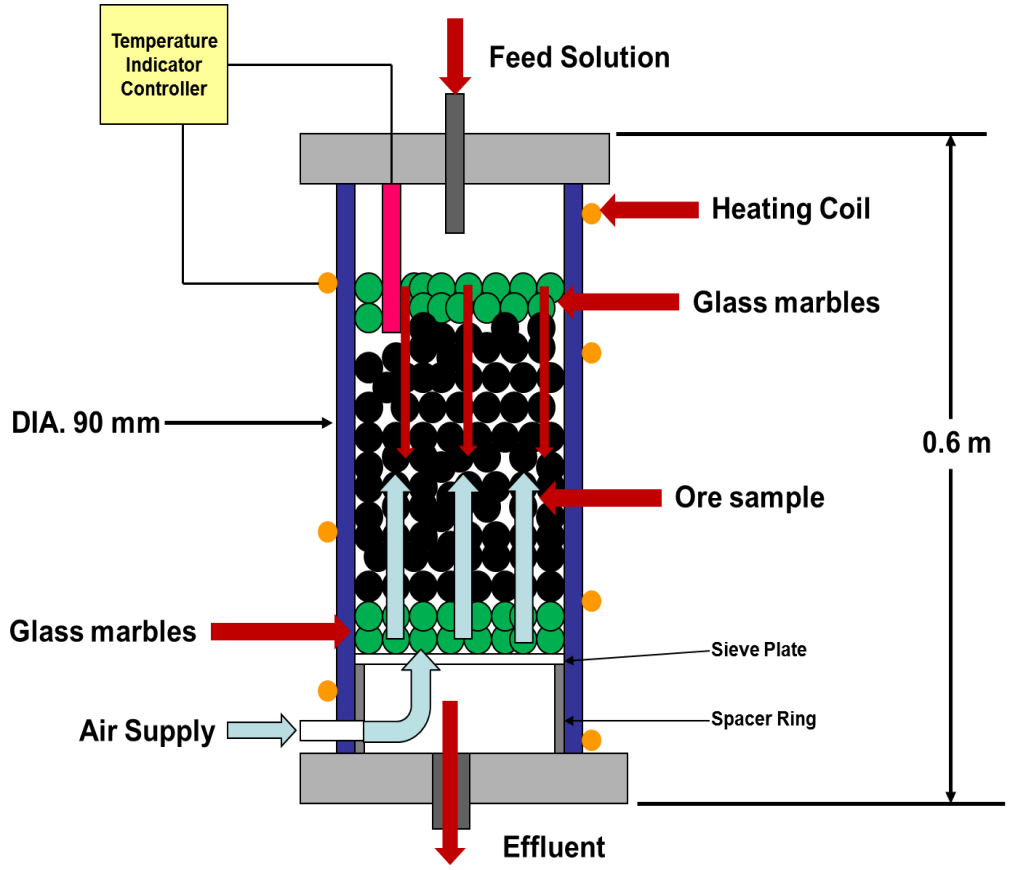

Figure 22: Schematic drawing of columns used in experiment

Figure 23: Actual columns used for bioleaching Platreef coarse ore. Column 1: -25 +1 mm, Column 2: -6 +1 mm; both columns leached at 5 L/m^2/hr with 0.5 g/L Fe (as ferrous) and 10 g/L H_2SO_4 solution; 65°C; aeration rate: 130 mL/min.

3.2.2. High Temperature Cyanide Leaching on Coarse Ore

Although motivated by the promising results achieved on cyanide leaching of bioleached concentrate (Mwase et al., 2012b), the cyanide leaching in this study was operated as a continuous solution fed reactor system in contrast to the batch-recycle system used by Mwase et al. (2012b). This was done with the aim of improving the output of Pt specifically, which was seen to be hindered by saturation constraints.

Coming off the bioleach process, the two samples contained a greater amount of fines than before due to the acidity of the bioleach. Hence they were agglomerated by adding Portland cement (5 g/kg ore) and water (8 wt %) to the samples in buckets, and thoroughly mixed by tilting and continuously turning for ten minutes. The samples were leached using separate but identical columns and a similar procedure to the ones used in the bioleach experiment. Figure 24 shows how they were set up in a walk-in fume cupboard as a safety measure for working with cyanide. The samples were packed in the columns and left for 24 hours at a temperature of 50°C to cure and form agglomerates. Thereafter a solution of 5 g/L sodium cyanide was fed into the columns at a rate of 1 L/day with no recycle using a peristaltic pump. The solution was buffered using a combination of 1.01 g/L sodium bicarbonate and 9.32 g/L sodium carbonate to keep the pH above 9.6. The columns were operated at a temperature of 50°C and aerated at a rate of 130 mL/min. Samples were taken from the effluent solution collected at the bottom of the columns every fourth and seventh day. The samples were analysed via inductively coupled plasma mass spectrometry (ICP-MS) for precious metals and ICP-AES for BMs and gangue elements. The leachate samples were also analysed for thiocyanate via HPLC and for free cyanide using the Cynoprobe® instrument developed by Mintek. The Cynoprobe® accurately measures the amount of sodium cyanide in solution based on amperometry (Mintek, n.d.). The sodium cyanide consumption calculated from the readings from this instrument is defined as the amount consumed in complexing all elements that react with cyanide forming weak and strong complexes, volitalization (however Sibrell et al. (1994) reports that volatilization only poses a problem at temperatures higher than 100°C), conversion to thiocyanate and oxidation either naturally or by reaction with a component of the ore. At the end of the experiment the columns were emptied and the contents washed, dried and sampled, and the sub-samples underwent fire assays and MLA analysis.

Figure 24: Experimental set up for cyanide leaching on coarse ore. Column 1: -25 +1 mm, Column 2: -6 +1 mm; both columns leached at 5 L/m^2/hr with 5 g/L NaCN solution; 50°C; pH 10.4-10.7; aeration rate: 130 mL/min.

3.3. Results and Discussion: Coarse Ore leaching

3.3.1. High Temperature Bioleach

The bioleach experiment achieved high extractions of BMs (Table 22) as expected, showing that it is a promising route to further explore for pre-treating the Platreef ore prior to precious metal leaching. Further test work needs to be conducted on larger samples (ideally a pilot heap) to determine whether this process has promise to operate at a full-scale similar to the Talvivaara Ni-Cu heap leach operation in Eastern Finland (Saari and Riekkola-Vanhanen, 2011) which has similar grades of Cu and Ni, and operates profitably. Apart from the level of extractions that can be achieved, there are two other important aspects that would have to be evaluated in piloting this process. The first being how high of an elevated temperature can be achieved by the sulphur oxidation in this ore. Secondly, although the test work artificially provided heating to immediately inoculate the thermophile organisms, in an actual heap operation the process would be different. It would require inoculation with a mixed culture containing mesophiles and moderate thermophiles, in an ideal situation these would be indigenous to the mine site. The mesophiles would operate at the lower temperature range (ambient to 35°C) and hence

initiate sulphur oxidation and heating of the heap. They would die off at higher temperatures to be succeeded by the moderate thermophiles, in a process termed as succession (Dew et al., 2011).

Table 22: Extractions achieved through bioleaching after 304 days

	Cu		Ni		Co		Fe	
	Solution Assay %	**Solid Assay** %	**Solution Assay** %	**Solid Assay** %	**Solution Assay** %	**Solid Assay** %	**Solution Assay** %	**Solid Assay** %
Column 1	96.5	66.9	56.6	77.4	35.8	45.7	30.6	13.5
Column 2	101.9	84.2	66.3	83.4	45.3	61.2	47.9	18.1

Figure 25 and Figure 26 show that Column 2 (-6 mm +1mm) performed better than Column 1 (-25 mm +1 mm) in all cases. This is not surprising as the smaller size fraction particles likely had better liberation of minerals. Some discrepancies between the results for Cu and Ni, obtained by solution assay of leach samples and those obtained by solid residue assay of ore samples were observed (Table 22). In all cases the difference between the two is larger than the normally accepted level of 10%, and although the solution assay shows that extraction of Cu was higher than Ni, the solid residue assay indicates it was the other way around. It is speculated that the source of this discrepancy might have been with the sub-sampling of the residual ore. The sub-samples were too small and thus may have been unrepresentative in an effort to conserve a sufficient size sample for the subsequent cyanide experiment. Therefore, although the solid assay analyses may have been accurate, they were performed on what were possibly unrepresentative samples. In the case of coarse ore as opposed to concentrate, it is difficult to obtain small representative samples. Further, a small set of samples, representing less than 10% of the total solution samples taken over the entire experiment, were duplicated and analysed by an independent laboratory to verify the accuracy of the ICP analysis used for all the samples and the results tallied within 2% of both sets of results. However, because only a small sample was used, overall the actual source of the discrepancy between solid and solution assay could not be determined conclusively. However the values for both assays are an indication of the potential to heap leach the Platreef ore. The extractions are typical of what is achieved in full-scale operations (Ghorbani et al., 2015; Saari and Riekkola-Vanhanen, 2011; Scheffel, 2002) and thus this ore can be further considered for heap leaching.

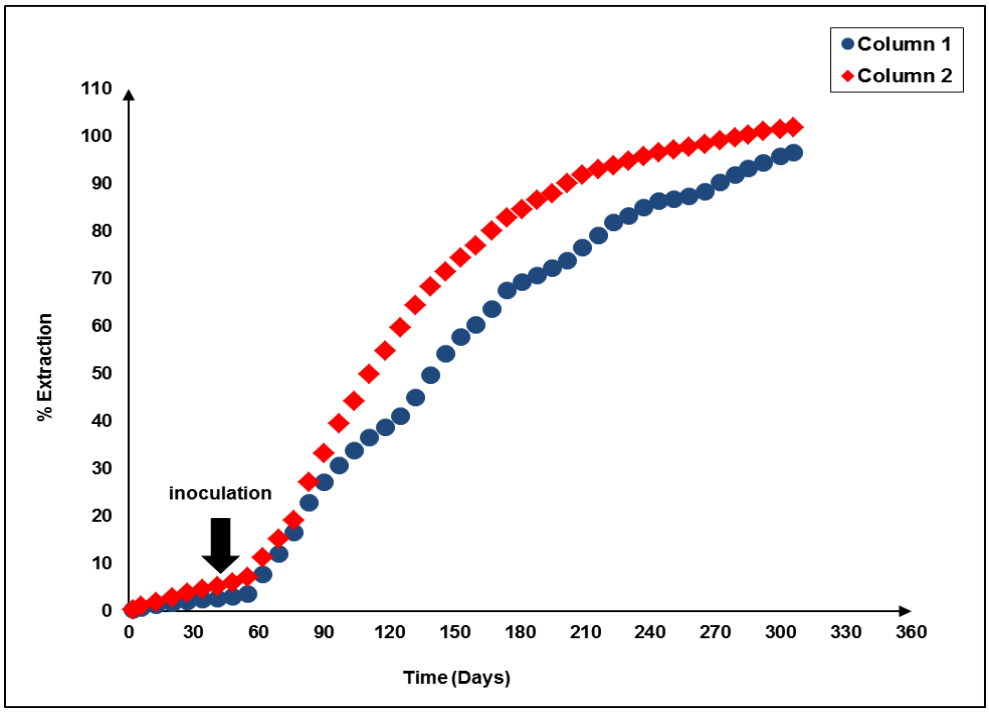

Figure 25: Cu leach curves. Column 1: -25 +1 mm, Column 2: -6 +1 mm; both columns leached at 5 L/m^2/hr with 0.5 g/L Fe (as ferrous) and 10 g/L H_2SO_4 solution; 65°C; aeration rate: 130 mL/min.

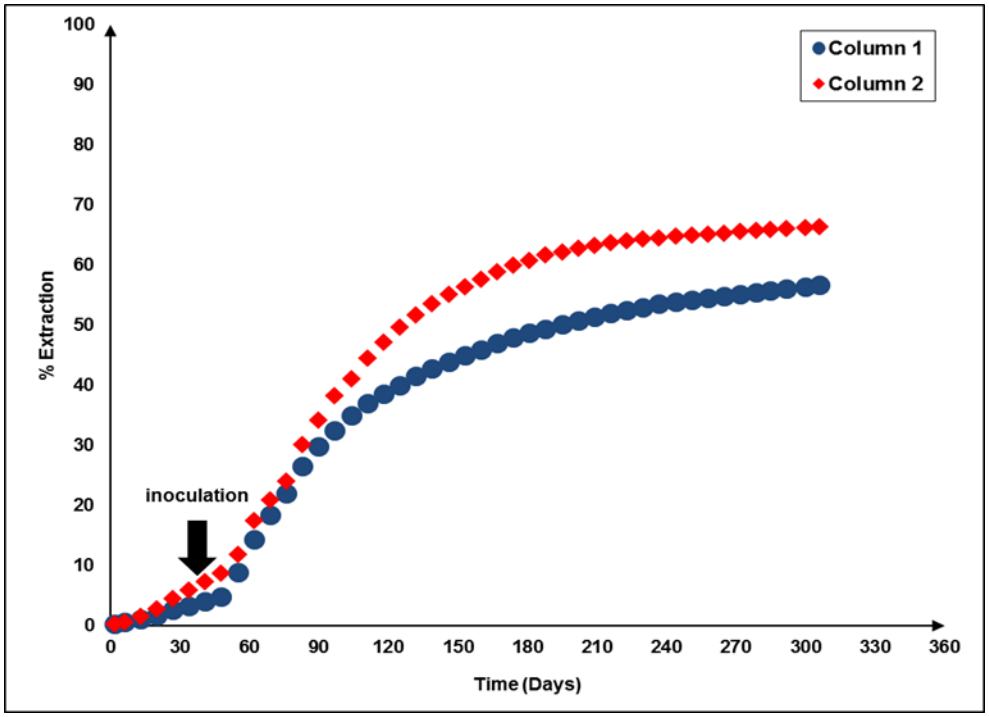

Figure 26: Ni leach curves. Column 1: -25 +1 mm, Column 2: -6 +1 mm; both columns leached at 5 L/m^2/hr with 0.5 g/L Fe (as ferrous) and 10 g/L H_2SO_4 solution; 65°C; aeration rate: 130 mL/min.

Table 22, Figure 25 and Figure 26 show that the extraction of Ni was not as high as Cu which is in contrast to what was observed in the study by Mwase et al. (2012b) on Platreef concentrate material in which the extent and rate of extraction Ni was higher than Cu. In that study it was suggested that galvanic leaching facilitated almost complete extraction of Ni and faster leaching than Cu. This was partially due to the intergrowth of pentlandite, and chalcopyrite mineral grains, and mostly due to physical contact between these mineral grains because the sample had been finely milled and mixed into a slurry. However QEMSCAN analysis (Figure 27) of selected ore particles from the whole ore bioleach experiment shows little or no contact between pentlandite (purple) and chalcopyrite (orange) mineral grains. Therefore galvanic leaching of Ni in preference to Cu could not take place.

Figure 27: QEMSCAN image of a selected particle from the bioleached ore from Column 1, -25 +1 mm, leached at 5 L/m^2/hr with 0.5 g/L Fe (as ferrous) and 10 g/L H_2SO_4 solution; 65°C; aeration rate: 130 mL/min.

Unlike the flotation concentrate used in the concentrate leaching (Mwase et al., 2012b) the Ni in the ore was perhaps not largely pentlandite but some of it was in other non-sulphide mineral forms such as the silicates. This would render it unrecoverable via bioleaching. This is in line with flotation test work conducted by Schay (2009) and Mogoseti (2006) on identical ore

samples which achieved only up to 75% recovery of Ni. However, QEMSCAN analysis of both samples indicated that the remaining Ni was almost entirely in the form of pentlandite and copper was entirely in the form of chalcopyrite. But this may have been a limitation with the QEMSCAN database of minerals and thus, a failure to recognize the Ni in lesser known forms, resulting in assigning of those minerals to pentlandite as a default. It was additionally observed from the QEMSCAN images that a number of particles had cracks between chalcopyrite and pentlandite mineral grains, and the bulk silicate mineral grains. It is postulated that these cracks are a result of the HPGR processing and not solution erosion, otherwise the minerals would have leached out. This would suggest that the solution flow pattern or hydrodynamics play a critical role in the leaching of the minerals; the minerals may be liberated through the cracks, but they will not leach if no solution is in contact with the mineral grains.

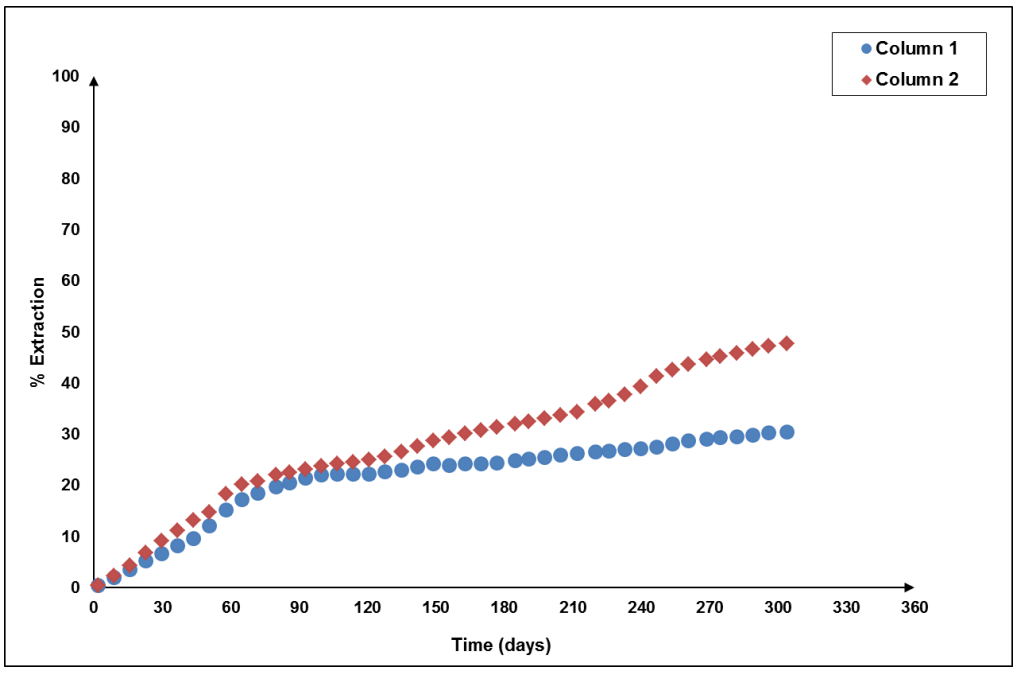

Figure 28: Fe leach curves. Column 1: -25 +1 mm, Column 2: -6 +1 mm; both columns leached at 5 L/m^2/hr with 0.5 g/L Fe (as ferrous) and 10 g/L H_2SO_4 solution; 65°C; aeration rate: 130 mL/min.

Figure 28 shows the Fe leaching curves. The percentage extraction calculated took into account the 0.5 g/L Fe present in the feed solution and this amount was subtracted to obtain the figures calculated in the curves. As with the other target elements there is a big discrepancy between the percentage extraction from the solution assays (used to plot the leach curves) and the fire assays of the solid residues. Like the previous elements this may be attributed to the sub-samples for the fire assay not being representative. Without a post-bioleach MLA it is not possible to give an accurate account of the source of the Fe in solution. But using the study by

Mwase et al. (2012b) as an approximation, it is suspected that the Fe came from the sulphides and the silicate minerals Hornblende [(Ca, Na)(MgFeAl)$Si_6O_{22}(OH)_2$] and Chlorite [(Mg_3, Fe_2)$Al(AlSi_3)O_{10}(OH)_8$]. While the Fe that was not leached is associated with Bronzite [(Mg, Fe, Ca)SiO_3] and Actinolite [Ca_2(Mg, Fe)$Si_8O_{22}(OH)_2$].

The pH patterns in Figure 29 show that the dissolution of gangue minerals was quite high initially and reduced almost mid-way through the leaching period. As stated in the method the columns were initially rinsed abiotically with 30g/L sulphuric acid for 44 days and pH and ORP values were consequently low. From day 44, when the columns were inoculated and the bioleach process began, the pH of the feed solution was 1.3 before it was pumped into the columns, but up until day 180 it is seen to be higher than 1.3, increasing to higher values of up to 2.0. This strongly indicates acid consumption by the gangue minerals which are largely silicates or acid consumption by the bio-oxidation process. After day 180, the pH starts to drop showing that the acid consuming portion of the gangue is mostly depleted. This also indicates that the acid fed into the columns and the acid produced from oxidation of sulphur is no longer consumed by the acid-consuming gangue minerals. In a full-scale heap operation, careful consideration must be paid to the influence of gangue elements on acid consumption, possible inhibition of microbial activity, on the viscosity and other properties of recycled leachate solution and the environmental impact of having large quantities of sulphates in the effluent for disposal. Sulphate removal by neutralization and gypsum precipitation offers a possible solution but the lime/limestone requirements may be high. The redox potential patterns in Figure 30 correspond with the leaching pattern in that when the potential is low it is an indication of a high rate of leaching as the ferric is being converted to ferrous. Hence, by the Nernst equation the ratio [ferric/ferrous] produces a low number as there is more ferrous than ferric. When the leaching rate reduces there is more ferric in solution than ferrous as it is not being reduced to ferrous as much, and the microorganisms are oxidizing ferrous to ferric, therefore that ratio is greater and the potential is at its highest.

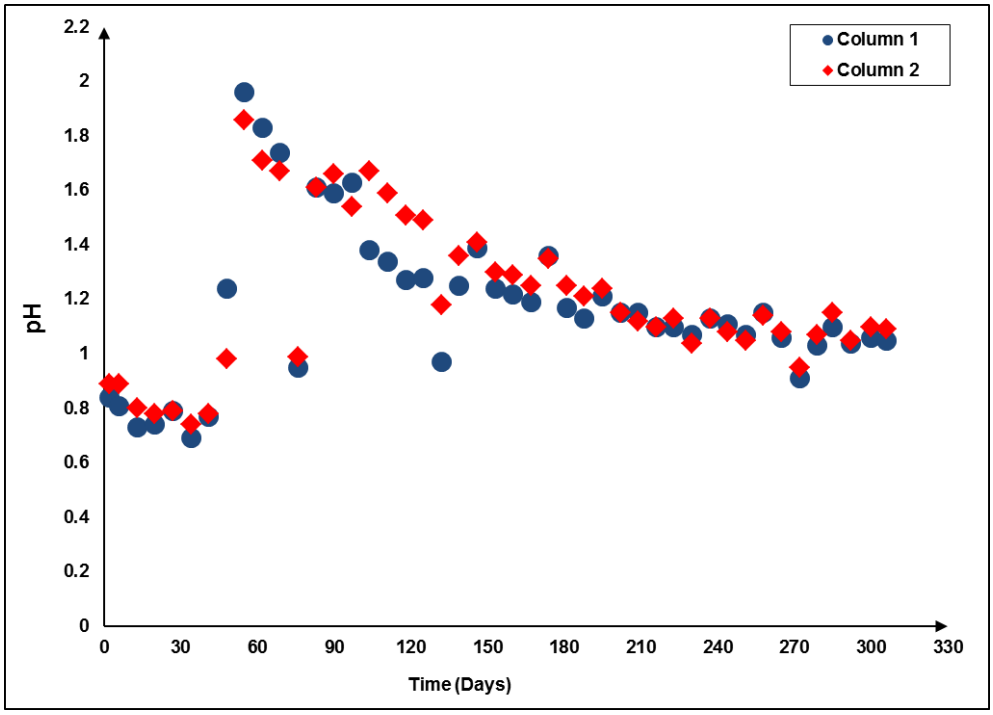

Figure 29: pH profiles from bioleach experiments. Column 1: -25 +1 mm, Column 2: -6 +1 mm; both columns leached at 5 L/m^2/hr with 0.5 g/L Fe (as ferrous) and 10 g/L H_2SO_4 solution; 65°C; aeration rate: 130 mL/min.

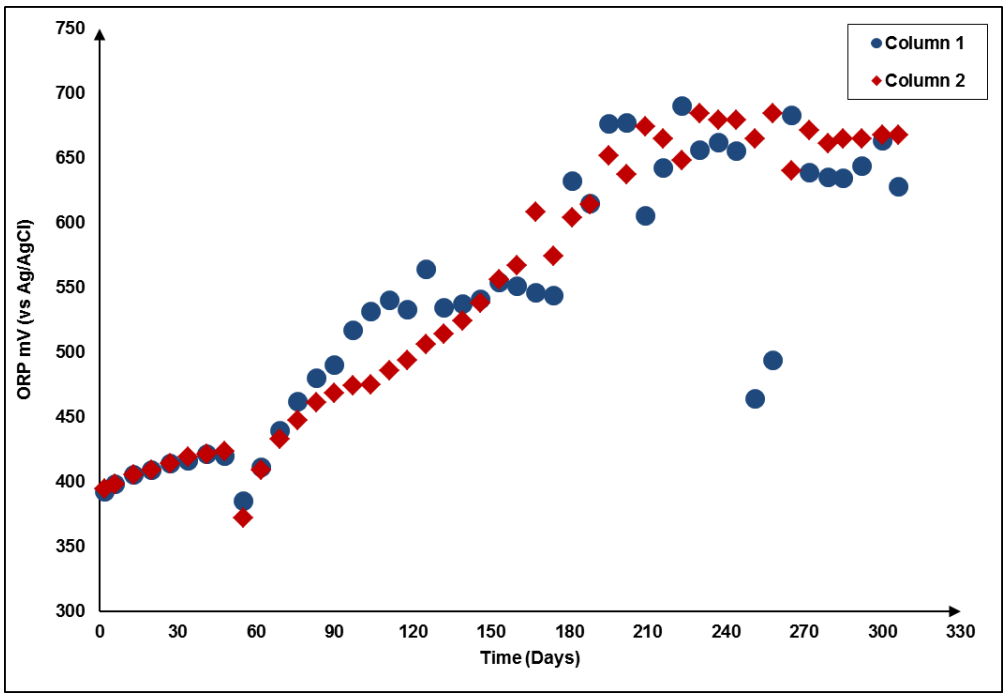

Figure 30: Redox profiles from bioleach experiments. Column 1: -25 +1 mm, Column 2: -6 +1 mm; both columns leached at 5 L/m^2/hr with 0.5 g/L Fe (as ferrous) and 10 g/L H_2SO_4 solution; 65°C; aeration rate: 130 mL/min.

3.3.2. High Temperature Cyanide Leach

3.3.2.1. Leaching of Precious Metals

Table 23: Grade of target metals and sulphur in ore going into cyanide leach post bioleach

	Pt g/t	Pd g/t	Au g/t	Cu %	Ni %	Fe %	S %
Column 1 (-25 mm)	2.3	2.3	0.3	0.04	0.08	7.5	0.3
Column 2 (-6 mm)	2.3	2.5	0.4	0.02	0.06	7.1	0.2

The grade of the ore with regards to the precious metals, base metals and total sulphur, going into the cyanide column leach is detailed in Table 23. The bulk of the ore (50-60%) was mainly silicate minerals with silicon as an element accounting for 27% of both ore samples by mass.

Table 24: Extractions achieved through cyanide leaching after 60 days

	Pt		Pd		Au	
	Solution Assay %	Solid Assay %	Solution Assay %	Solid Assay %	Solution Assay %	Solid Assay %
Column 1	41.0	58.3	79.3	81.4	80.6	85.5
Column 2	55.9	59.8	105.3	94.3	88.4	92.3

Table 25: Concentration of Pt in solution from Figure 31

	4 days µg/L	Next 28 days µg/L	Last 28 days µg/L
Column 1 (-25 mm)	340	60	5-10
Column 2 (-6 mm)	490	60	5-10

A comparison of extractions of precious metals achieved based on data from solution assays and from fire-assays of ore samples before and after the leaching experiment, can be seen in Table 24. The results between solution and solid assay tally much better than those in Table 22 for the bioleach experiment with the exception of Pd in Column 1. This is attributed to the fact that the solid assays were conducted on much larger and thus more representative sub-samples

than those obtained after the bioleach experiment. The use of a continuous feed system resulted in considerably improved rates and extent of precious metals extraction compared to the results achieved on concentrate material which used a batch-recycle system, given the similar mineralogy of the two materials. Particular focus is paid to the 53% Pt extraction achieved with the -6mm+1mm size fraction in 32 days, as compared to the 35% achieved on concentrate in 45 days (Mwase et al., 2012b). Pd and Au in both columns leached out rapidly (Figure 32 and Figure 33), but Pt was observed to leach out at a much slower rate and through a distinct pattern (Figure 31). Almost half the Pt (about 30%) is rapidly leached in the first 4 days, followed by another 23% over the next 28 days, but at a slower rate, and the remaining 47% leaches at a significantly slower rate than the first 53%. Table 25 sheds more light on this pattern by showing the actual concentrations of Pt in solution over the three sections of the leach curves in Figure 31. It basically emphasizes the difference in leaching rates over the different sections/periods.

Typically the presence of silver interferes with gold leaching since the dissolution of silver is faster (Marsden and House, 2006; Chamberlain and Pojar, 1984). The rapid leaching of the Au which was mostly electrum (AuAg) can perhaps be attributed to the high concentration of cyanide used which may have off-set the faster reaction with silver. Additionally the quantity of electrum in the ore was very low, hence it did not take long to leach. Literature only states that electrum leaching by cyanide may pose problems but there are no detailed studies to compare the kinetics with the cyanide leaching of other gold minerals. Therefore a more in-depth explanation cannot be provided.

The lack of scatter for the Pd and Au leach curves, Figure 32 and Figure 33 respectively, is due to the unexpected rapid leaching of Pd and Au. As stated earlier this test work is a follow-up from test work conducted on concentrate, where such rapid leaching of the precious metals did not occur. Furthermore, the sampling intervals took into account that coarse ore was being used and thus was not expected to proceed at such rapid leaching rates.

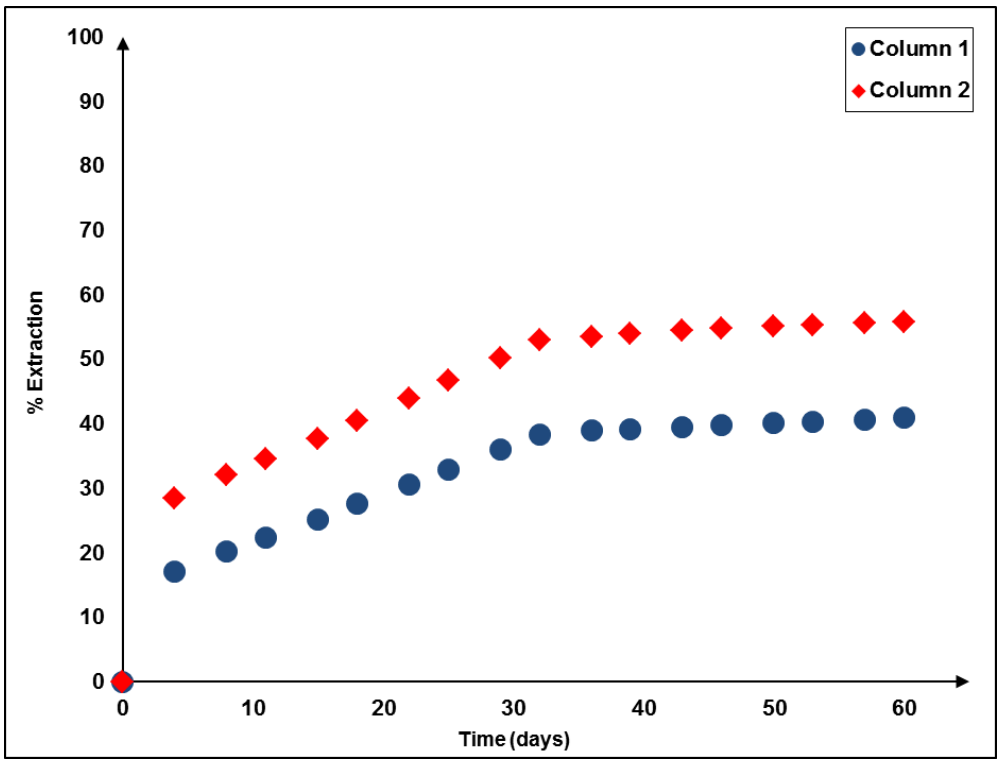

Figure 31: Pt leach curves from cyanide experiments. Column 1: -25 +1 mm, Column 2: -6 +1 mm; both columns leached at 5 L/m^2/hr with 5 g/L NaCN solution; 50°C; pH 10.4-10.7; aeration rate: 130 mL/min.

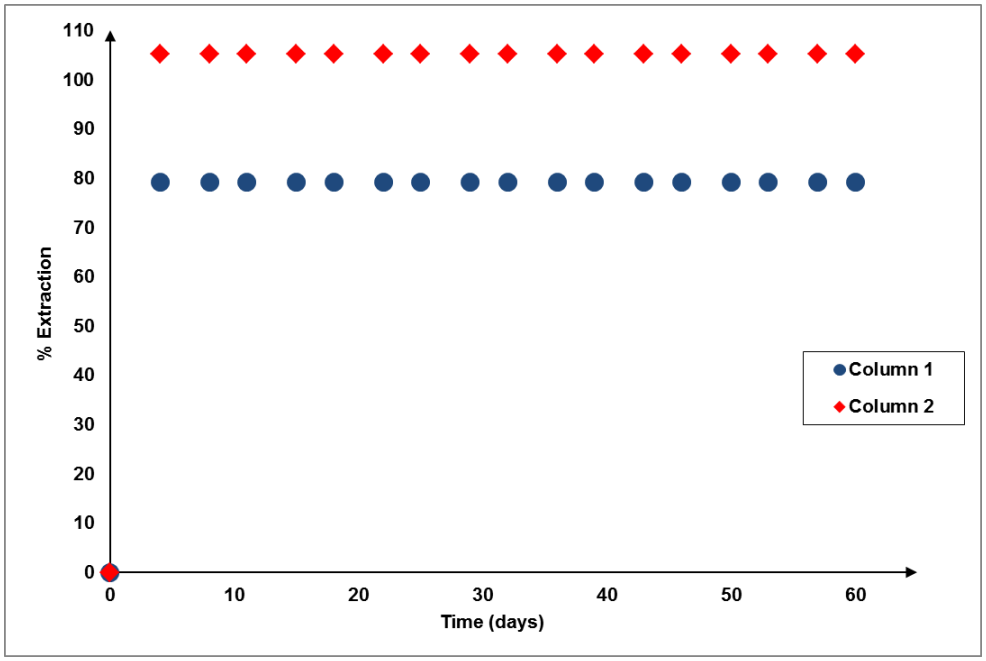

Figure 32: Pd leach curves from cyanide experiments. Column 1: -25 +1 mm, Column 2: -6 +1 mm; both columns leached at 5 L/m^2/hr with 5 g/L NaCN solution; 50°C; pH 10.4-10.7; aeration rate: 130 mL/min.

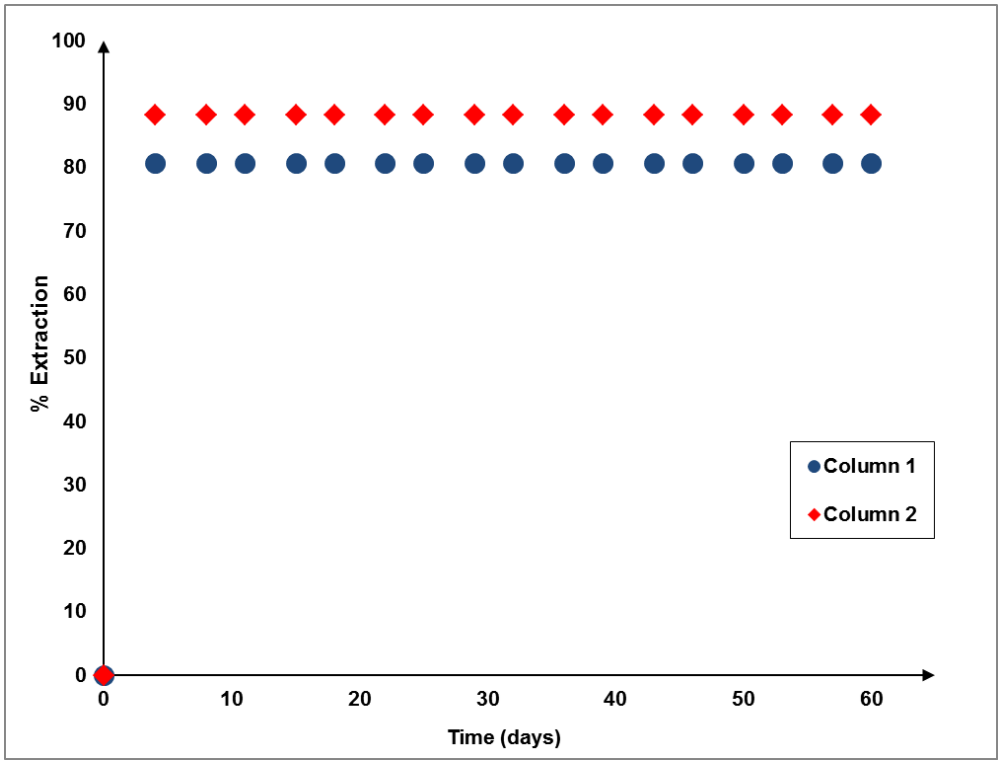

Figure 33: Au leach curves from cyanide experiments. Column 1: -25 +1 mm, Column 2: -6 +1 mm; both columns leached at 5 L/m^2/hr with 5 g/L NaCN solution; 50°C; pH 10.4-10.7; aeration rate: 130 mL/min.

Table 26 shows the PGM mineralogy of the ore residue sub-sample from column 2 and was obtained using an MLA. Of the remaining Pt and Pd minerals, 80% were arsenides, with sperrylite ($PtAs_2$) accounting for 76% of the total PGM content and palarstanide ($Pd_8Sn_{1.5}As_{1.5}$) accounting for 3%. The remaining platinum group minerals were in the form of tellurides (8%), sulpharsenides (6%), alloys (4%) and sulphides (2%) with trace amounts of gold and silver entirely from electrum. The remaining minerals of note were maslovite (PtBiTe) and platarsite [(Pt, Rh, Ru)AsS] both accounting for 6% each. All the remaining precious metals minerals were overall not well liberated. The sulpharsenides were the most liberated with an exposed surface area of 26%, followed by the sulphides, tellurides and arsenides with partial liberation in the range of 2-7%. The remaining electrum and alloys were 100% locked and were thus not in contact with solution to facilitate leaching. However, for the other minerals it is most likely a mineralogical limitation that prevented their leaching. Leaching, unlike flotation, requires only partial liberation. The partial liberation of the Pt sulpharsenides, tellurides and arsenides suggests that they are resistant to cyanide leaching under the prevailing conditions. This observation in combination with the leach curves from Figure 31 and data in Table 25 strongly suggest that the Pt minerals leach out at the same time but at different rates. Therefore it is concluded that the distinct pattern in Figure 31 comes about because in each individual section

the rate of Pt leaching is controlled by the fastest leaching mineral. Once that mineral is depleted, the rate drops and is controlled by the remaining next fastest leaching mineral, until sperrylite was left as the slowest leaching mineral (Table 25).

The results from this analysis via MLA confirm what was established by the study on the concentrate material (Mwase et al., 2012b) as the present results are almost identical to those obtained for concentrate. The remaining PGMs were largely in the form of sperrylite and accounted for 76-78% of the remaining total PGMs. It is therefore clear that the key to making the PGM heap leach process of Platreef ore viable rests with understanding why sperrylite leaches slowly in cyanide and finding a method to leach the sperrylite at a faster rate in a heap under the prevailing conditions. The lower extraction of Pt, relative to Pd and Au, can be additionally explained by the high deportment of Pt to sperrylite and to a lesser extent maslovite and platarsite. The higher extraction of Pd as compared to Pt can also be explained by the high deportment of Pd to the tellurides which appear to be more cyanide soluble, than the arsenides and sulpharsenides which are resistant to cyanide leaching. Comparing these MLA results to the pre-bioleach MLA analysis, it appears that Pt and Pd were mostly leached from the minerals moncheite and merenskyite. Although MLA anaylsis was not conducted on the whole ore samples post-bioleach, in Mwase et al. (2012b) a post-bioleach MLA analysis was conducted and showed that the process conditions of the bioleach had no significant influence on the PGM mineralogy of the Platreef ore concentrate. In particular the bioleach did not affect the major mineral groups namely the arsenides, tellurides, sulphides, sulpharsenides. Given that the concentrate is derived from the ore and has a strong similarity in terms of mineralogy, it is reasonable to assume this holds true for the bioleach whole ore residues and thus the PGM mineralogy remained mostly unaltered through the bioleaching process from fresh samples.

Table 26: MLA analysis-PGM minerals in residue from column 2

Groups	Mineral	Formula	% Area
Arsenides	Sperrylite	$PtAs_2$	76.0
	Arsenopalladinite	$Pd_8(As,Sb)_3$	0.7
	PtPdAs	(Pt,Pd)As	0.1
	Palarstanide	$Pd_8Sn_{1.5}\ As_{1.5}$	3.4
Sulpharsenides	Platarsite	(Pt,Rh,Ru)AsS	6.4
	PtPdSulpharsenide	(Pt,Pd)AsS	0.1
Tellurides	Maslovite	PtBiTe	6.0
	Moncheite	$(Pt,Pd)(Te,Bi)_2$	<0.1
	Kotulskite	Pd(Te,Bi)	2.1
Alloys	Ferroplatinum	PtFe	2.6
	Atokite	$(Pd,Pt)_3Sn$	0.2
	Sudburyite	PdSb	0.6
	Stumpflite	Pt(Sb,Bi)	<0.1
	Sobolevskite	PdBi	<0.1
	PtPdRhSe	PtPdRhSe	0.2
Sulphides	Cooperite	PtS	1.6
	Braggite	PtPdS	0.1
Electrum	Electrum	AuAg	<0.1
	PtElectrum_HiAg	PtAgAu	0.1

3.3.2.2. Leaching of Major BMs and Gangue Elements

The impact that BM and gangue elements leaching would have on the process was assessed. The concentrations of the elements that were present in solution over various sampling periods are detailed in Table 27. The data was reported as concentrations rather than percentage extractions, as this would more accurately reflect the prevailing situation. With the BMs, the percentage extraction figures seemed high, but only because they were calculated against residual amounts that remained after the bioleach. Similarly but opposite, for the gangue elements they seemed extremely low only because the bulk of the ore was composed of gangue

elements. Table 27 shows only data from the first 32 days, as this is the period when the process is most feasible in terms of precious metals extraction.

The levels of dissolution, although high relative to the precious metals concentrations (which were in the ppb levels), did not appear to interfere with the extraction of the precious metals. Si had the highest presence, but there is no literature indicating the existence of Si-CN complexes, and therefore it is postulated that it is most likely colloidal or sodium silicates that may have been detected. The primary concern is with the influence that Cu, Ni and Fe have on the downstream processing of pregnant liquor solution to recover the precious metals. Separate test work has shown that the presence of these elements at concentrations of 50 ppm and higher, increase the amount of carbon and resins required to recover the precious metals (Schoeman et al., 2012; Synders et al., 2013). They do this by occupying spaces on the resins and carbon and thus reducing the amount of precious metals that can be adsorbed and thus increasing the amount of carbon and resin that has to be used. However, there is no literature on the influence of the observed levels of Si on the adsorption process. At industrial scale, where a solution recycle system is used, these levels of Cu, Ni and Fe could build up to the 200-300 mg/L range, and thus become problematic to the recovery of precious metals. Section 2.4.6.3 discusses the various methods that can be considered to pre-treat the solution, containing high levels of BMs, before precious metals recovery. These methods essentially involve separating the metal cyanide complexes from the pregnant solution selectively and without interfering with the precious metals; recovering Cu and Ni as saleable sulphide products or a higher purity product such as cathode and potentially recovering cyanide as K, Ca or Na cyanide salts that can be returned to the heap.

Table 27: Cu, Ni, Fe and Si concentration over a 32 day leaching period

		First 4 days mg/L	Next 28 days mg/L
Cu	Column 1	40	6-20
	Column 2	30	3-8
Ni	Column 1	22	4-10
	Column 2	36	1-5
Fe	Column 1	33	16-28
	Column 2	28	10-20
Si	Column 1	200	500-700
	Column 2	180	500-700

3.3.2.3. Assessing the Consumption of Sodium Cyanide

The amount of sodium cyanide used was calculated and determined with the aid of the Cynoprobe® instrument. This instrument was used to analyse the concentration of sodium cyanide in solution before it was fed into the columns and after it exited the columns. The amount of sodium cyanide used was expressed as a percentage of the original amount fed into the column at a particular sampling point. On average only half the cyanide in solution was consumed (Figure 34) suggesting that the process could still proceed successfully using a solution concentration of 2.5 g/L. Gold heap leach operations typically operate in the range of 0.1-2.5 g/L (Kappes, 2002; Chamberlain and Pojar, 1984). This rather wide range of solution concentration is likely due to varying grades of ores and other factors such as the presence of copper, iron, organic materials and silver which can make the ore refractory to cyanide leaching. After 32 days the cyanide consumptions in columns 1 and 2 have been determined to be 16.5 and 27.5 kg/t respectively, as compared to typical gold heap leaching operations for run-of-mine and crushed ore (excluding refractory ores) which are reported to consume only 0.1-2.5 kg/t (Roxburgh, 2011; Marsden and House, 2006; Kappes, 2002). On the other hand, a comparison should be made with a similar process being cyanide tank leaching operations on concentrate residues of bacterial oxidation. These processes are reported to experience cyanide consumptions of 15-28 kg/t (Aswegen et al., 2007; Miller and Brown, 2005) and in the range of 2-122 kg/t in various test work projects (Miller and Brown, 2005). However, Roxburgh (2011) reports that actual gold heap leaching operations use only 40-65% of the cyanide used

in column test work. Stewart and Kappes (2011) report that certain gold minerals have exhibited a higher affinity for cyanide in environments with high Cu and sulphur content, resulting in preferential leaching of the gold over undesirables. In these cases much lower concentrations of cyanide solution are used and no treatment prior to recovery is required. Additionally, Pt, Pd and Au form significantly stronger complexes with cyanide than elements like Cu, Ni, Fe and Co (van Rensburg and Lotz, 2010; Marsden and House, 2006); hence even when lower cyanide concentration solutions are used there may be preferential leaching of precious metals. The bioleached residues of Platreef ore are yet to be tested with lower sodium cyanide concentrations to determine if the minerals in Platreef also exhibit similar behaviour. The only foreseen trade-off is that leaching may not occur as rapidly as it has occurred in the test work, if lower solution concentrations are used.

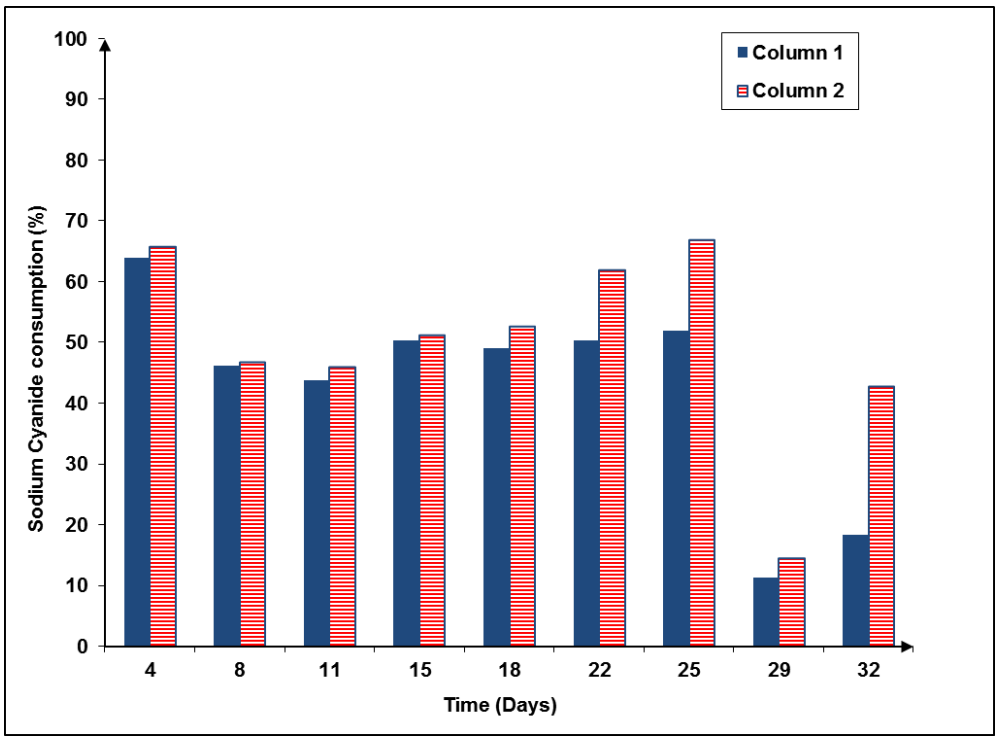

Figure 34: Cyanide consumed as a percentage of cyanide put in at that point. Column 1: -25 +1 mm, Column 2: -6 +1 mm; both columns leached at 5 L/m^2/hr with 5 g/L NaCN solution; 50°C; pH 10.4-10.7; aeration rate: 130 mL/min.

A further analysis and comparison with gold heap leach operations is conducted using sodium cyanide consumed per ounce of precious metals leached (kg/oz.). This was considered a useful form of analysis, considering that the process leaches multiple precious metals at the same time. Typical heap operations process gold ores with grades in the range of <0.1-1.8 g/t and consume sodium cyanide in the range of 0.1-2.5 kg/t in actual operations and laboratory test

work prior to actual operations (Roxburgh, 2011; Kappes, 2002; van Zyl et al., 1990; Chamberlain and Pojar, 1984). These same literature sources associate the lower cyanide consumptions with lower grade ores and high consumptions with higher grade ores. Therefore, in making this comparison it is assumed that ore with a grade of <0.1 g/t has a 0.1 kg/t consumption of sodium cyanide, and ore with a 1.8 g/t ore has a sodium cyanide consumption of 2.5 kg/t for 80% recovery of Au. From this the calculated consumption range for gold operations is hence 39-54 kg/oz. Identical calculations were conducted for the cyanide column test on Platreef ore using the actual amount of cyanide consumed from Figure 34 and the recoveries of Pt, Pd and Au up to the 32nd day. Considering column 2 only as it had the highest extractions, Table 28 shows that in the first 4 days the consumption is comparable to those of typical gold heap leaches. One contributing factor to this is the use of an elevated temperature for leaching, which results in a rapid rate of extraction (especially for Pd and Au) and most likely reduced the consumption of cyanide to a lower amount than would have been required at ambient temperature. The higher than usual concentration of cyanide reagent used for leaching may also have provided excess reagent to be consumed by undesirables and thus not interfere with the precious metals leaching. After 4 days the consumption increases significantly, and Pt remains the only metal being extracted and it is leaching out at a much slower rate. From this point on the process becomes uneconomical, as the Pt extracted would barely cover the cost of cyanide alone without considering other operational costs. However, as stated earlier, there is still precedence to evaluate the use of lower sodium cyanide concentrations for this part of the leach and in fact throughout the whole operation.

Table 28: Sodium cyanide consumed per oz. of precious metals leached

	NaCN used in kg $\times 10^{-3}$	**Pt leached in oz.** $\times 10^{-5}$	**Pd leached in oz.** $\times 10^{-4}$	**Au leached in oz.** $\times 10^{-5}$	**First 4 days (kg/oz.)**
Column1 (-25 mm)	9.5	3.5	1.6	2.4	**44.5**
Column 2 (-6 mm)	9.7	5.0	1.9	2.5	**36.0**
	NaCN used in kg $\times 10^{-3}$	**Pt leached in oz.** $\times 10^{-5}$	**Pd leached in oz.** $\times 10^{-4}$	**Au leached in oz.** $\times 10^{-5}$	**Next 28 days (kg/oz.)**
Column1 (-25 mm)	41.7	4.3	-	-	**959.3**
Column 2 (-6 mm)	58.5	4.3	-	-	**1360.5**

3.3.2.4. Investigating the Conversion of Sodium Cyanide to Thiocyanate

The presence of thiocyanate is of concern in this process as high levels of this compound in the effluent solution indicate a high amount of sodium cyanide being consumed for purposes other than precious metals leaching and poses an environmental risk. Whereas Cu and Ni cyanide complexes can be processed to obtain saleable products, and the process effluent which can be treated to regenerate cyanide, the cyanide converted to thiocyanate cannot be converted back to re-usable cyanide salts or reagent. Furthermore, if thiocyanate (as various complexes) is present in leachate solution, it can be adsorbed to either the resins or carbon used for precious metals recovery. At concentrations greater than 100 ppm it has been shown to reduce elution of Pt, Pd and Au from the resins and carbon (Snyders et al., 2013) presumably by occupying and thus reducing the adsorption sites for the precious metal-cyanide complexes. Figure 35 indicates that the presence of thiocyanate may have a negative effect on the recovery of the precious metals in this process. The initial conversion to thiocyanate is high; it gradually decreases over the 32 day period and the final total conversions for columns 1 and 2 are 12.7% and 6.5% respectively (Figure 36). These percentages are not excessive and may not necessarily be a hindrance to commercial operation, but if more diluted solutions of cyanide are used, the effect may be different. The patterns in Figure 35 and Figure 36 are an indication of the presence of reduced sulphur compounds which readily react with cyanide to form thiocyanate. After a rapid initial reaction, a gradual decrease occurs indicating the depletion of these compounds. QEMSCAN analysis confirmed the presence of sulphide minerals such as pentlandite, chalcopyrite, pyrrhotite, pyrite and molybdenite as the main sulphide compounds in the ore residues after bioleaching, with molybdenite accounting for most of the residual sulphur. These sulphides are known to react with cyanide but at a relatively slower rate as compared to reduced sulphur compounds (polysulphides and polythionates) which are reported to react rapidly (Luthy and Bruce, 1979). Although not detectable by QEMSCAN it is therefore suspected that polysulphides and polythionates, resulting from incomplete biooxidation of sulphur, are the main group of sulphur species that are responsible for the initial high levels of thiocyanate in the effluent.

Even though the percentage conversion is low, the levels of thiocyanate in mg/L are still high and exceed the acceptable limits for discharge to municipal sewers or drinking water supply (Nsimba, 2009; Stander et al., 1970). Therefore the levels in the effluent (Figure 35) need to be lowered. It should be noted that in the coarse ore leach the amount of sulphur oxidised was

75% of the starting total as compared to 44% in the concentrate study. Further still in order to make a fair comparison, the total sulphur before leaching in both cases was quantified and found to be similar (32-35g per sample). This proves that the longer leaching time in the coarse ore leach results in higher sulphur oxidation. However this is still not sufficient for the present application. The use of microorganisms that oxidise only sulphur in addition to the current species of *Metallosphaera hakonensis* in the bioleach stage maybe a potential route to explore. This may help to oxidise more of the remaining sulphur species in the ore further minimising sulphur compounds that are migrating to the cyanide leach. This has proven successful in tank leaching of gold concentrates containing high levels of sulphide minerals (Aswegen et al., 2007). Chemical treatments such as HCL, HNO_3, NaOH or SO_3^{2-} at temperatures of 50-95°C are most likely to be effective in completely oxidising the sulphur, but are not economically, technically and environmentally viable for the scale of size at which a whole ore heap leach operates.

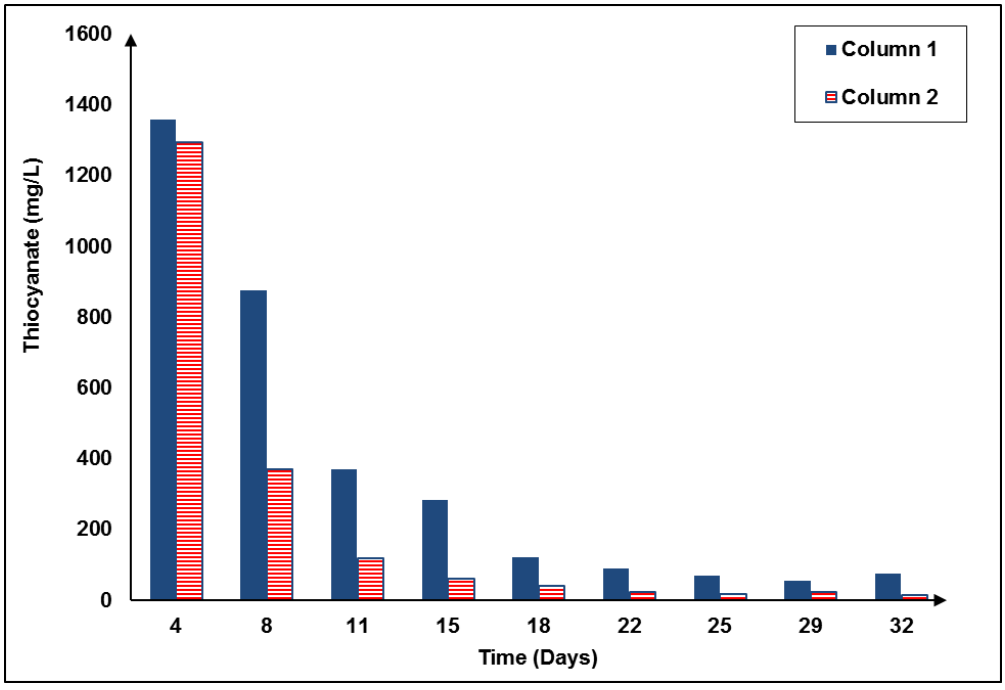

Figure 35: Thiocyanate in cyanide effluent solution. Column 1: -25 +1 mm, Column 2: -6 +1 mm; both columns leached at 5 L/m^2/hr with 5 g/L NaCN solution; 50°C; pH 10.4-10.7; aeration rate: 130 mL/min

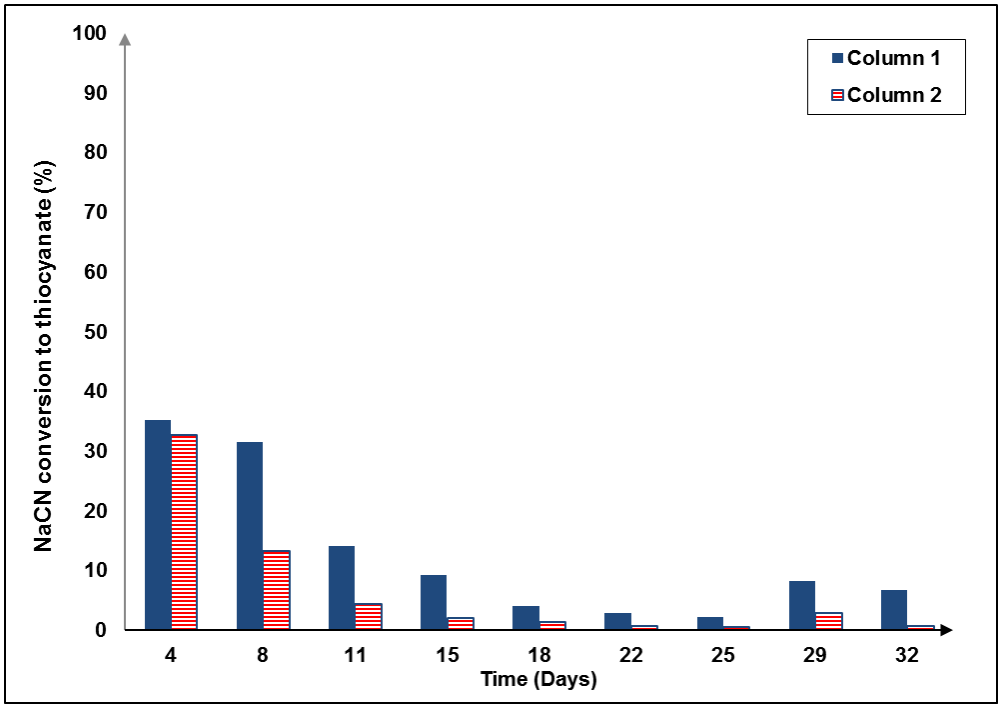

Figure 36: Percentage conversion of NaCN to thiocyanate. Column 1: -25 +1 mm, Column 2: -6 +1 mm; both columns leached at 5 L/m^2/hr with 5 g/L NaCN solution; 50°C; pH 10.4-10.7; aeration rate: 130 mL/min

3.4. Conclusion: Coarse Ore Heap Leaching of Platreef Ore

The heap leaching of PGMs from Platreef ore directly, by circumventing the energy intensive steps of milling, floating, smelting and pressure leaching, presents a promising alternative to the conventional process. The test work on coarse ore showed that pre-treatment via bioleaching can result in high extractions of BMs in the ranges of 96.5-66.9% Cu, 83.4-56.6% Ni and 61.2-35.8% Co for the bioleach. While in the main process, a cyanide leach achieves extractions of 59.8-41.0% Pt, 94.3-79.3% Pd and 92.3-80.6% Au. Extractions are dependent on the size range of the crushed ore. While the extractions for the rest of the target metals are encouraging, the lower extractions of Pt which is the most valuable metal amongst them all, creates a hindrance to further developing the process. A significant portion of the Pt has been identified as sperrylite which appears to be slow-leaching in cyanide, especially in comparison to the Au and Pd minerals. However, the extraction levels achieved thus far for the precious metals may be economically viable considering that a coarse ore heap leach would offer substantial savings in capital and operating costs by eliminating the conventional process steps.

While reducing the cyanide consumption levels and the levels of thiocyanate in the effluent from the cyanide heap leach is also a priority, section 3.3.2.4. has detailed sufficient methods in which the gold industry has dealt with this challenge via treating the material with a combination of both Fe and S oxidising microorganisms prior to cyanidation.

3.5. Additional Applications of Two-Stage PGM Heap Leaching Process

Although currently focused on Platreef ore, PGM heap leaching can potentially find applications outside Platreef ore:

The results from test work conducted on Platreef ore strongly suggest that ore bodies where sperrylite is less prevalent, may produce higher extractions of platinum. This may be the case for Merensky and UG2 ores and concentrates. This presents an opportunity for current platinum producers in the face of rising production costs and possible participation in the PGM industry by smaller organisations that do not have the capital for the standard route. Although very effective on Merensky and UG2 ore, the conventional process is not 100% efficient. The process produces tailings and intermediate/secondary concentrates that represent 70% of the total input of material and 5% of the PGMs (Mwase et al., 2012a; Mwase 2009). This figure may not seem large but when the accumulation of these materials, and consequentially the PGMs is calculated annually; it can be seen that these PGMs represent a considerable amount of value that is lost. Due to the nature of these materials, low PGM grade and high through-put, conventional methods cannot be used. However some value may still be recovered through heap leaching, specifically by coating these materials onto support rock and heap leaching. Heap leaching can also be considered for weathered and oxidised PGM ore bodies. These ores typically report poor PGM recoveries via flotation (Becker et al., 2014; Ramonotsi, 2011; Becker et al., 2011) as the sulphides have been converted to oxides and the tellurides and arsenide have been passivated with an oxide layer. However such deposits can still be economically important as they eliminate the cost of deep shaft mining. These ores can potentially be exploited by direct cyanide heap leaching.

Whereas the copper and gold industry that have widely applied, with huge success, various percolation leaching technologies (heap, dump and vat leaching) to treat ores that cannot be processed by conventional methods, no such application can be currently seen in the PGM industry. As a result a number of opportunities for further development in the industry are left

unexploited. Although South Africa holds the majority of the worlds' PGM reserves, there are only 13 PGM producers, of which only 4 have smelter capacity (Department: Minerals and Energy). This is because the current processing methods ore are capital intensive, restricting entry by smaller organisations. Heap leaching may be the means to allow more participants in the PGM industry and extend processing operations to remote locations without easy access to smelters.

4. Chapter 4: Sperrylite Leaching

Having identified that the extraction of Pt in Platreef ore is limited due to its occurrence as the mineral sperrylite, which in turn has proven resistant to cyanide leaching, the second part of the study will be a more in-depth investigation of this phenomenon. This part of the study employs various techniques to explain the slow leaching of Pt in cyanide with a view to finding a solution that can be applied to the heap leaching of Platreef ore.

4.1. Sample Preparation

A sample of pure sperrylite mineral was obtained from the Wallbridge Mining Company of Canada courtesy of Lonmin Plc. The sample originated from the nickel ore deposit of the Sudbury Basin in Ontario Canada. Originally, the sample was in what appeared to be crystalline form of various sizes from 2 mm down to fines in the micron range. For the experiments sub-samples of 3.5 g (capacity of the micronizer) were micronized to minus 5 µm. Analysis using XRD showed the samples was 100% sperrylite while energy dispersive x-ray spectroscopy (EDS) showed a few impurities of Cu, Si and S but ultimately the weight and atomic ratios of Pt to As were similar to the literature (Henke and Hutchison, 2009; Sperrylite, n.d.) values of sperrylite. (Figure 37) shows a microscopic image generated using scanning electron microscopy (SEM) (Nova NanoSEM) of the sample.

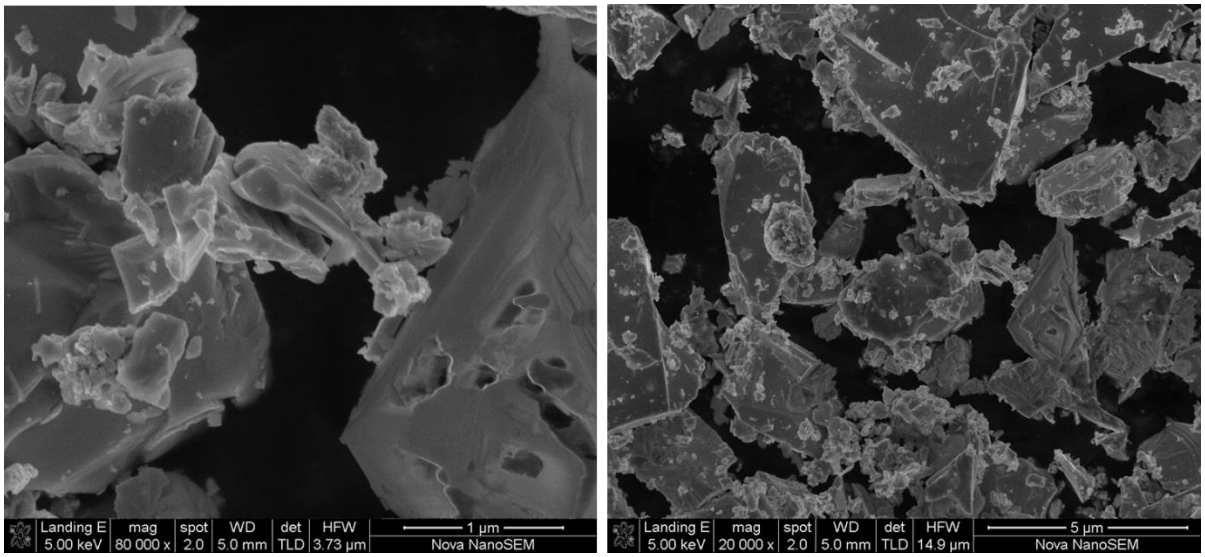

Figure 37: SEM image of sperrylite sample after being micronized to 5 um

Solid state nuclear magnetic resonance (NMR) analysis was conducted on a micronized sample of sperrylite by the NMR and CD Unit at Stellenbosch University. The results although inconclusive, strongly suggested that the oxidation state of Pt was most likely a lower state specifically +2. This was concluded from the apparent tight overlap of a number of peaks in the sample (Figure 38) in comparison to the more distinct of a sample of $(NH4)_2[PtCl_6]$ crystal (Figure 39), where the oxidation state of Pt was known to be +4.

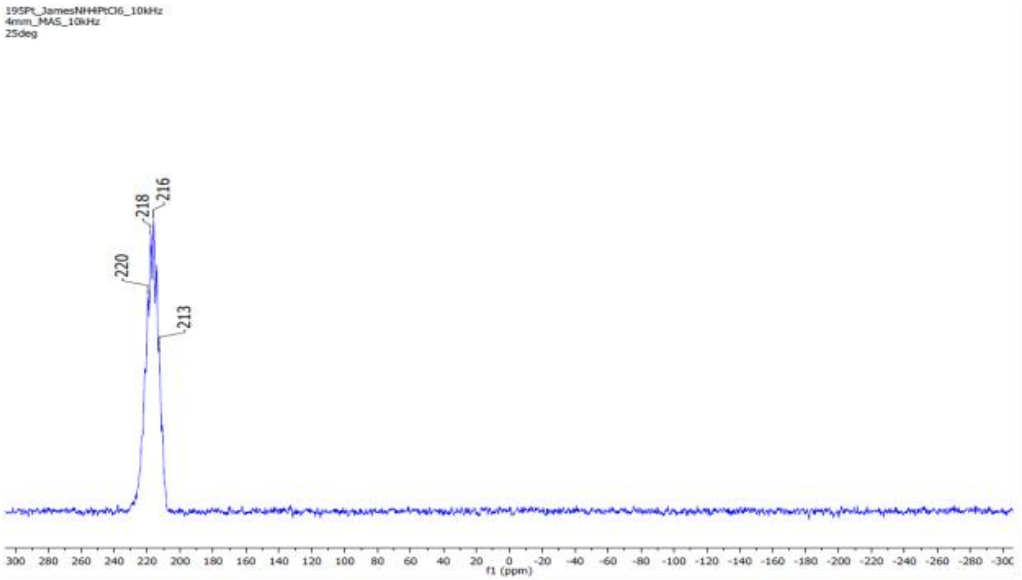

Figure 38: NMR spectra of sperrylite sample

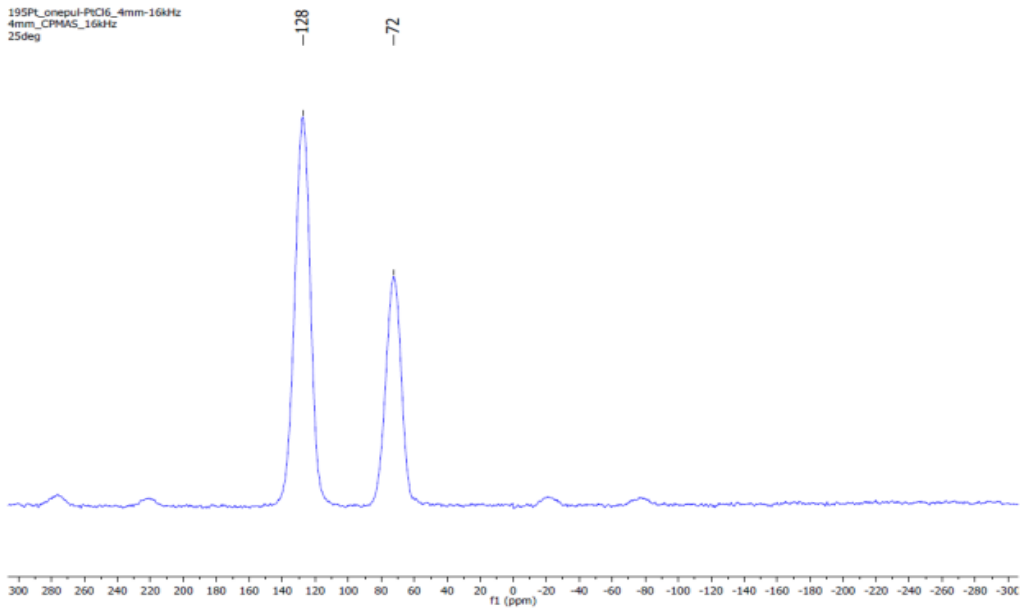

Figure 39: NMR spectra of $(NH_4)_2[PtCl_6]$ crystal

4.2. Experimental Methods

4.2.1. Batch-Stirred Tank Reactor (BSTR) Leaching

The leaching tests were conducted using the following method with variations in sample quantity, temperature, reagent concentration, type of oxidising method/agent (Table 29). A sample of sperrylite was leached in a 500 mL jacketed glass reactor with 500 mL of reagent. The mixture was agitated using a magnetic stirrer and temperature was set and maintained using a water bath. To test the hypotheses, compressed air or pure oxygen or nitrogen were sparged into the mixture. In some cases no sparging was done (but because the vessel was not air-tight, some atmospheric air would enter the reactor and solution) to approximate the conditions in the earlier column tests where the columns were aerated at a low rate. This was termed as passive aeration. The temperature was monitored using a thermometer at various intervals over the duration of the experiment. Samples of solution were withdrawn using a syringe during various intervals and vacuum filtered for analysis via ICP-OES to determine the amount of Pt and As in solution. Additionally, the pH of the samples was measured using a standard pH meter. On completion of the experiments, the solid residual samples of sperrylite were recovered using vacuum filtration and dried in a desiccator for XPS and SEM analysis. Figure 40 shows the general set up of the leaching tests.

The cyanide solution was prepared using pure sodium cyanide supplied by Merck, South Africa and a combination of 1.01 g/L of sodium bicarbonate and 9.32 g/L sodium carbonate was used to keep the pH sufficiently alkaline, specifically above 9.6. Ferricyanide was added using high grade potassium ferricyanide purchased from Sigma-Aldrich, South Africa.

The influence of different oxidants was determined by conducting a variety of experiments as per the general conditions, equipment and procedures above. All experiments were conducted at 50°C for a period of 30 hours. Samples were withdrawn at various intervals for analysis via ICP-OES to measure the levels of Pt and As in solution. For selected experiments the influence of time was investigated by allowing the experiment to proceed to 5 days. Due to the exploratory nature of the work, the focus of the experiments was discovery by varying as many parameters as possible to learn as much as possible rather than choosing a few parameters and conducting tests in repeats or triplicate.

Figure 40: General set up of leaching tests

Table 29: Leaching tests to determine the influence of oxidants

Experiments	Range of Concentrations
Cyanide no/passive aeration	5 g/L NaCN
Cyanide compressed air	0.5-50 g/L NaCN
Cyanide pure oxygen	5 g/L NaCN
Cyanide/ferricyanide no/passive aeration	5 g/L NaCN and 5 g/L $K_3[Fe(CN)_6]$
Cyanide/ferricyanide compressed air	5 g/L NaCN and 0.5-50 g/L $K_3[Fe(CN)_6]$
Cyanide/ferricyanide pure oxygen	5 g/L NaCN and 5 g/L $K_3[Fe(CN)_6]$
Ferricyanide no/passive aeration	5 g/L $K_3[Fe(CN)_6]$
Cyanide/ferricyanide nitrogen	5 g/L NaCN and 5 g/L $K_3[Fe(CN)_6]$

4.2.2. X-ray Photoelectron Spectroscopy (XPS) analysis

4.2.2.1. Theory of XPS

Having postulated that the slow leaching of sperrylite in cyanide is due to the occurrence of a change at the surface of the mineral during leaching, it is appropriate that a suitable surface analysis technique be identified to investigate this. X-ray photoelectron spectroscopy (XPS) also referred to as Electron Spectroscopy for Chemical Analysis (ESCA) is a well-established method for surface-sensitive quantitative spectroscopic analysis of various materials ranging from mineral samples, alloys to organic tissue and human bone. Amongst its many capabilities and uses, the ones relevant to this study include its ability to identify elements and quantities of those elements present within the top 1-10 nm of a sample surface; the oxidation states of the elements present; the empirical formula of the sample material at the surface and through depth profiling measure the uniformity of the elemental composition as a function of depth. There are several studies in which this tool has been successfully used to characterize the surface changes of varying mineral samples after they have been subjected to treatment such as oxidation, sulphate leaching and bioleaching (Sasaki et al., 2010; Parker et al., 2003; Klauber et al., 2001; Yuzer et al., 2000; Hackl et al., 1995; Mycroft et al., 1995; Pratt et al., 1994).

The process works by irradiating a surface (sample) with X-rays (commonly Al Kα or Mg Kα) in vacuum. The x-ray photons hit and transfer energy to the core level electrons causing them to be excited and emitted with a kinetic energy dependent on the binding energy of the atomic orbitals from which they originated (Figure 41). The energy and intensity of the emitted photoelectrons are analysed to identify and determine the concentrations of the elements present. These photoelectrons originate from a depth of 0 -10 nm, therefore the information obtained is from within this depth. Essentially the kinetic energy of the released photoelectrons is measured and subtracted from the x-ray photons energy (1486 eV from a monochromatic/constant source) to calculate the binding energy, which in turn is used to identify elements which all have unique binding energies with the exception of H and He which tend to overlap.

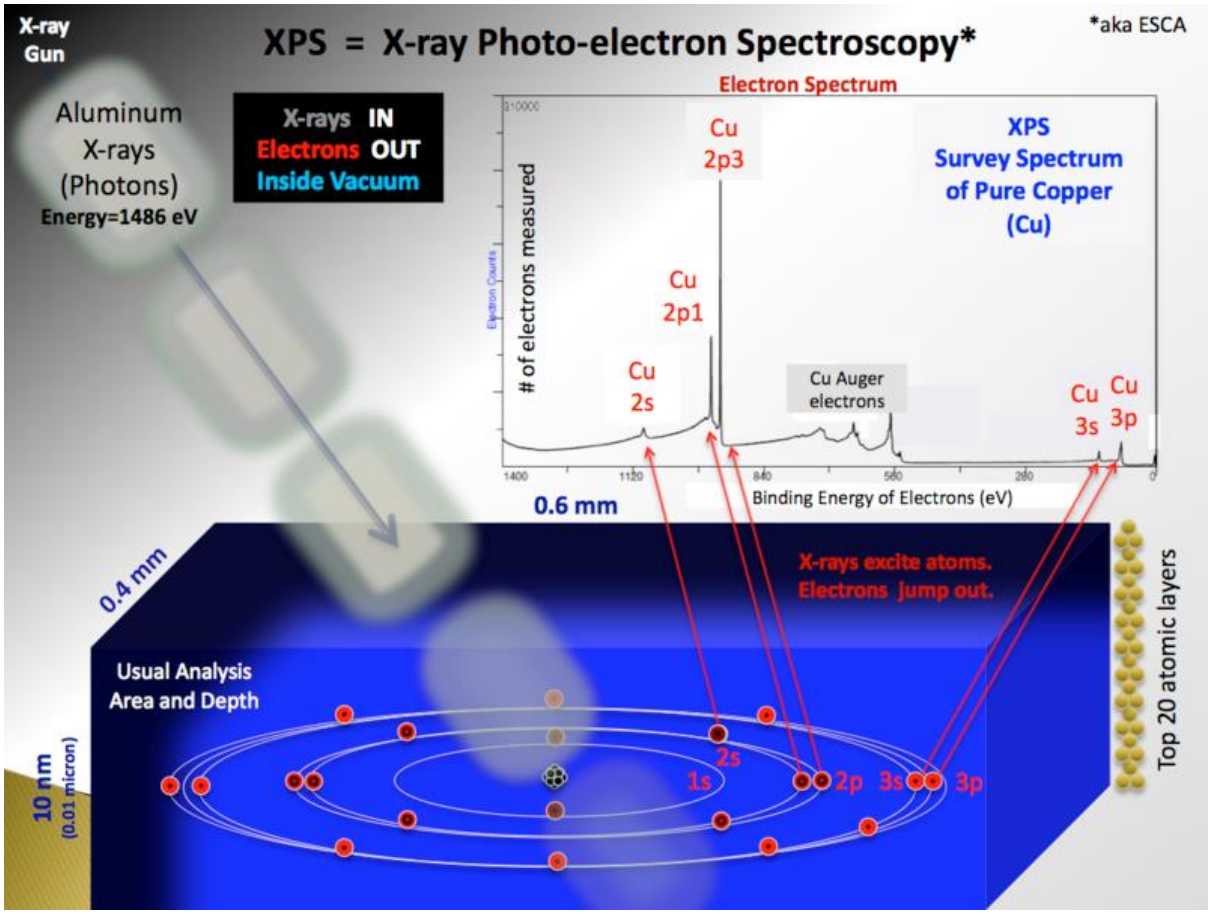

Figure 41: A schematic of the XPS process taken from https://en.wikipedia.org/wiki/X-ray_photoelectron_spectroscopy

It should be noted that x-ray absorption near edge structure (XANES) can also be used to determine the oxidation states of Pt and As in the sperrylite. It has been used in similar studies to this to determine the chemical structure of passivating layers at the surface of minerals that have been leached (Yang et al., 2013; Chang-Li et al., 2011; Xia et al., 2010; Oblonsky et al., 2000). However, this method was not available to this study.

4.2.2.2. Equipment and Procedures

XPS equipment used was the PHI 5000 Scanning ESCA Microprobe located at the Department of Physics at the University of the Free State, Bloemfontein, South Africa.

The PHI VersaProbe is driven by a patented high flux X-ray source providing a focused monochromatic X-ray beam that can be scanned upon the sample surface. The X-ray source utilizes a focused electron beam scanned upon an Al anode for X-ray generation and a quartz

crystal monochromator that focuses and scans the generated X-ray beam upon the sample surface. The monochromator is based on a 200 mm Rowland circle with quartz (100) crystals on an ellipsoidal substrate to generate micro focused X-ray beam. The X-ray energy dispersion eliminates the Kα3,4, Kα5,6, and Kβ X-ray lines and the Al Bremsstrahlung radiation background and narrows the Al Kα1,2 line to approximately 0.26 eV FWHM (full width at half maximum). This narrow line allows core and valence band spectra to be acquired with high energy resolution of the photoemission peaks and without X-ray satellite-induced photoemission peak overlaps. This is illustrated in Figure 42.

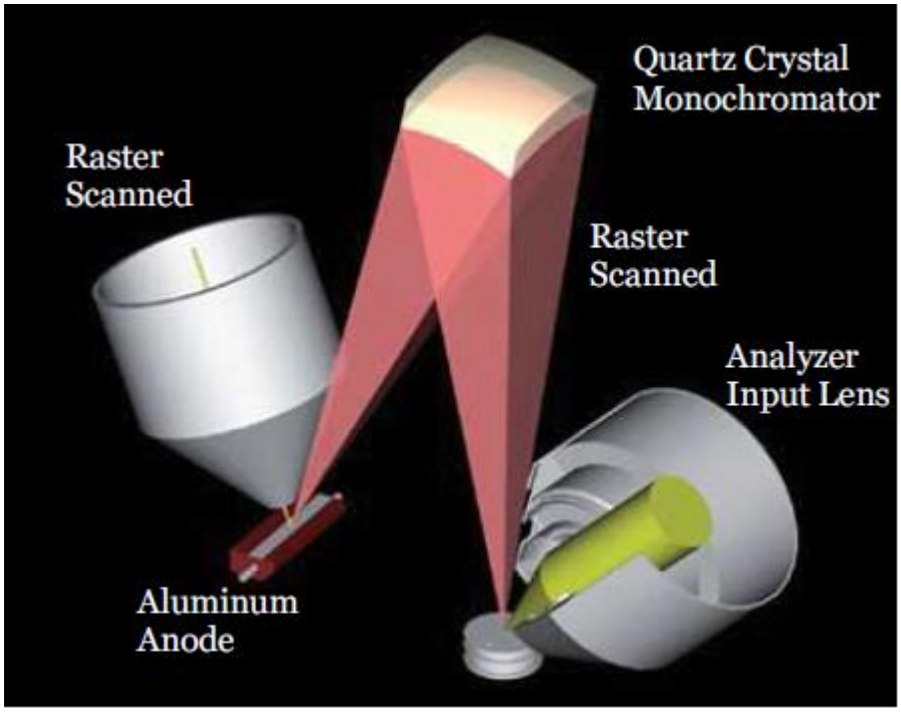

Figure 42: Inner working of the PHI VersaProbe (Coetsee-Hugo, 2015)

The removal of X-ray and Bremsstrahlung satellite radiation coupled with a narrow principal excitation line width results in significantly higher signal-to-background ratio data. The narrower X-ray line width also allows an electron energy analyzer to be observed with higher transmission, thereby reducing the observed damaged rate in monochromator-excited XPS spectra of X-ray sensitive sample. With the proper geometry configuration of X-ray source, crystal substrate and analysis target, the reflection beam yields a highly focused, monochromatic source of X-rays.

A 100 μm diameter monochromatic Al Kα x-ray beam (hν = 1486.6 eV) generated by a 25 W, 15 kV electron beam is used to analyse the different binding energy peaks. If the pass energy is set to 11 eV it gives an analyser resolution ≤ 0.5 eV. Multipack version 9 software is utilized to analyse the spectra to identify the chemical compounds and their electronic states using Gaussian–Lorentz fits.

A low energy Ar+ ion gun and low energy neutralizer electron gun is used to minimize charging on the surface.

Samples of sperrylite, untreated and after specific leach tests were mounted onto a small holder cup of area 3 mm^2. The initial analysis was conducted on the surface of the sample to identify elements present and quantities prior to depth profiling. The depth profiling involved an identical analysis first for two minutes resulting in a more penetrative scan (36 nm from the surface).

4.2.3. Electrochemistry Study of the Leaching of Sperrylite in Cyanide Systems

4.2.3.1. Theory of Electrochemistry

Having identified that the leaching of sperrylite is most likely a redox reaction, electrochemical techniques have been applied to have some understanding of the process. The leaching process, analogous to the corrosion process, can be studied in terms of the principles of electrochemistry. The solid material (electrode) in contact with the solution (electrolyte) provides a solid/liquid interface for electron transfer (and hence leaching) to take place. The critical parameters can be related by Faraday's law (Mogase, 2012):

$$i.t = \frac{n.F.w}{M} \qquad (3.1)$$

Where:

i = current (amps)
t = time (seconds)
n = number of electrons transferred per molecule

F = Faraday's constant (96 500 C/mol)
w = mass of leached material (grams)
M = molecular mass of the metal (grams/mol)

If the leaching system (vessel, solution and mineral) is considered as a cell, the cell potential can be calculated under non-standard conditions using the Nernst equation:

$$E = E° - \frac{R.T}{n.F} lnQ \quad (3.2)$$

Where:

E = cell potential at temperature of interest
E° = standard cell potential
R = universal gas constant (8.314 J/K mol)
T = absolute temperature (K)
n = number of electrons transferred
F = Faraday's constant (96 500 C/mol)
Q = the reaction quotient which is a function of the activities or concentrations a_{ox}/a_{red}

The Butler-Volmer equation is one of the fundamental relationships in electrochemistry. It relates the current density to the overpotential (Mogase, 2012) or in simpler terms, it shows how the electrical current on an electrode is dependent on the electrode potential if both the cathodic and anodic reactions occur at the same electrode. Given Faraday's Law in turn links current to the rate of leaching, the Butler-Volmer equation is effectively a rate law for electrochemical reactions. This becomes relevant in a leaching system where this typically happens at the solid-liquid interface. The equation is expressed as follows:

$$i = i_o . \{ e^{\frac{\alpha_a nF\eta}{RT}} - e^{\frac{\alpha_c nF\eta}{RT}} \} \quad (3.3)$$

i = electrode current density (A/m^2)
i_o = exchange current density (A/m^2)
α_a = anodic charge transfer coefficient (dimensionless)
α_c = cathodic charge transfer coefficient (dimensionless)

NB: $\alpha_a + \alpha_c = 1$

n = number of electrons transfer from electrode

F = Faraday's constant

R = universal gas constant (8.314 J/K mol)

T = absolute temperature (K)

η = overpotential ($E - E_{eq}$)

The overpotential is the difference between the mixed potential (reaction potential) and the equilibrium potential. The mixed potential will occur when the current densities of the cathodic and anodic reactions are equal but opposite (Free, 2013).

The relationship between the rate of an electrochemical reaction and the overpotential is expressed using the Tafel equation. From the Butler-Volmer equation; if the term for the anodic reaction (which is or promotes metal dissolution/leaching) is isolated we get:

$$i_a = i_o . \{e^{\frac{\alpha_a nF\eta}{RT}}\} \quad (3.4)$$

Rearranging the terms and taking the log of both sides, the above equation becomes:

$$\eta_a = \beta_a \log(\frac{i_a}{i_o}) \quad (3.5)$$

β_a is the Tafel coefficient and is given by:

$$\beta_a = \frac{2.303RT}{\alpha_a nF} \quad (3.6)$$

The Tafel coefficient can be obtained graphically from by plotting η_a vs log i_a. The intercept of the plot gives the value for i_o. Similarly the cathodic reaction, which will have a negative slope, can be represented by the equation:

$$\beta_c = \frac{2.303RT}{\alpha_c nF} \quad (3.7)$$

4.2.3.2. Equipment and Procedures

The equipment used in these experiments consisted of a glass reactor to hold the solution (cyanide and cyanide-ferricyanide). A mineral electrode (working electrode) constructed from a sperrylite crystal embedded in epoxy resin block with one face of the crystal exposed. Using a high resolution image from a microscope and ImageJ software, the surface area of the exposed face of the crystal was calculated to be 1.3 x 10^{-6} m^2. This block was permanently connected to a brass rod with the other end threaded to screw into an overhead stirrer (Figure 43). The other two electrodes to complete the arrangement were a reference electrode (saturated calomel electrode-SCE) and counter electrode (platinum wire). All three electrodes were dipped into the solution in the reactor vessel (Figure 44).

Sperrylite crystal in epoxy resin block | Sperrylite crystal in epoxy resin block permanently attached to rod | Threaded end of mineral electrode

Figure 43: Details of the mineral (working) electrode

The mineral electrode was attached to an over-head stirrer to rotate the electrode for controlled mass transfer effects and agitation. Additionally this was preferred to a magnetic stirrer bar which would result in interference with the readings. The electrodes were connected to a potentiostat with Gamry™ software, imbedded in a regular desktop computer. The reactor was jacketed and ran at a maximum temperature of 40°C (beyond that temperature the epoxy coating holding the crystal would crack) using a water bath. For safety the entire rig was placed in a bench top fume hood to create a physical barrier between other laboratory users and the cyanide experiment (Figure 45). The experiments involved taking measurements and observing trends through:

1. Open circuit potential measurements (OCP): measuring the change in mineral potential with time in the different solution systems.

2. Cyclic voltammetry (CV): measuring the resultant current when potentials in excess of those measured in the OCP experiments are applied.

3. Chronoamperometry (CA): measuring the current as a function of time when a fixed potential is applied to the mineral electrode.

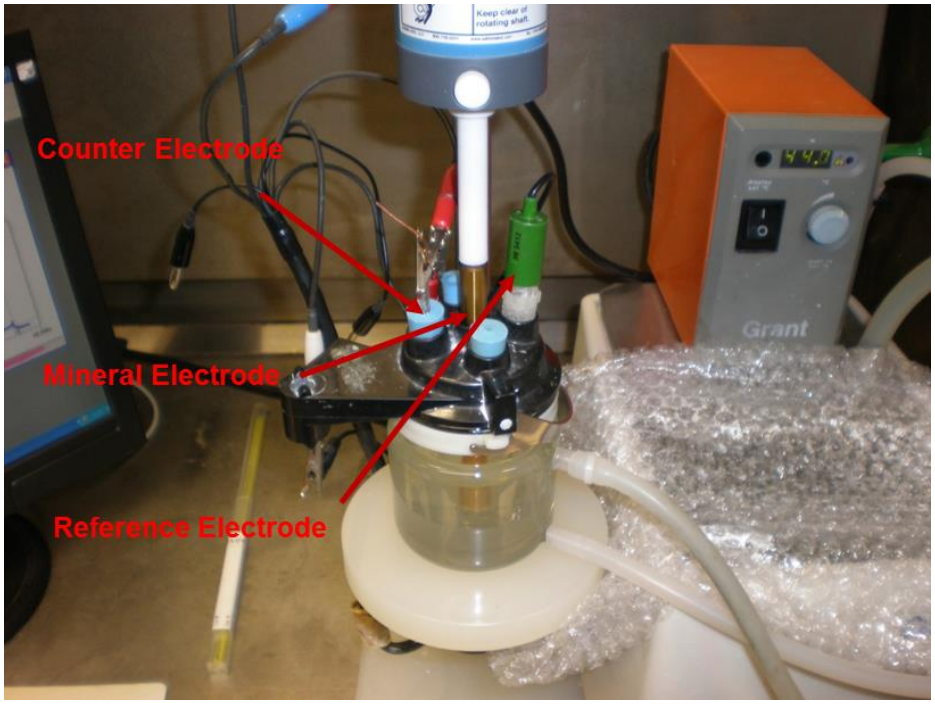

Figure 44: Various electrodes in the electrochemical experimental set-up

Figure 45: Entire electrochemical set-up in fume hood

4.2.4. Leaching in mini-column (continuously fed system)

This was achieved by fixing a 500 mg bed of micronized sperrylite sample between 2 beds of fine quartz in a thin glass tube with a diameter of 5 mm and length of 20 cm (Figure 46). The quartz material was washed in a dilute solution of HCl (15 %) and dried prior to use. Glass wool was placed at the ends of each tube to act as a filter, preventing loss of particles at the entrance and exit. The whole arrangement was held horizontally using a clamp and retort stand placed above a water bath to run the experiment at 50°C (Figure 47). A section of the silicon tubing was coiled prior to entry in the mini-column to act as a heat exchanger and allow heating of the solution before contacting with the sperrylite. This was set up in a walk in fume hood for safety. A combination of 5 g/L sodium cyanide and 5 g/L potassium ferricyanide solution, buffered with 1.01 g/L of sodium bicarbonate and 9.32 g/L sodium carbonate, was fed through the tube at a rate of 2 L per day using a peristaltic pump. Initially solution was fed to the column until it reached the entrance and then the flow was stopped before it made contact with the sperrylite. Then the column was completely immersed in water and the bath heated to 50°C. After about 20 minutes, giving the system time to reach 50°C, the flow of solution was resumed and the effluent collected in clean 5 L plastic containers. Samples were collected after 1, 4 and 8 hours and thereafter every 24 hours for analysis of Pt and As using ICP-OES. The pH of each

sample was also measured using a standard pH meter. Figure 48 shows an image of the experiment in full progress.

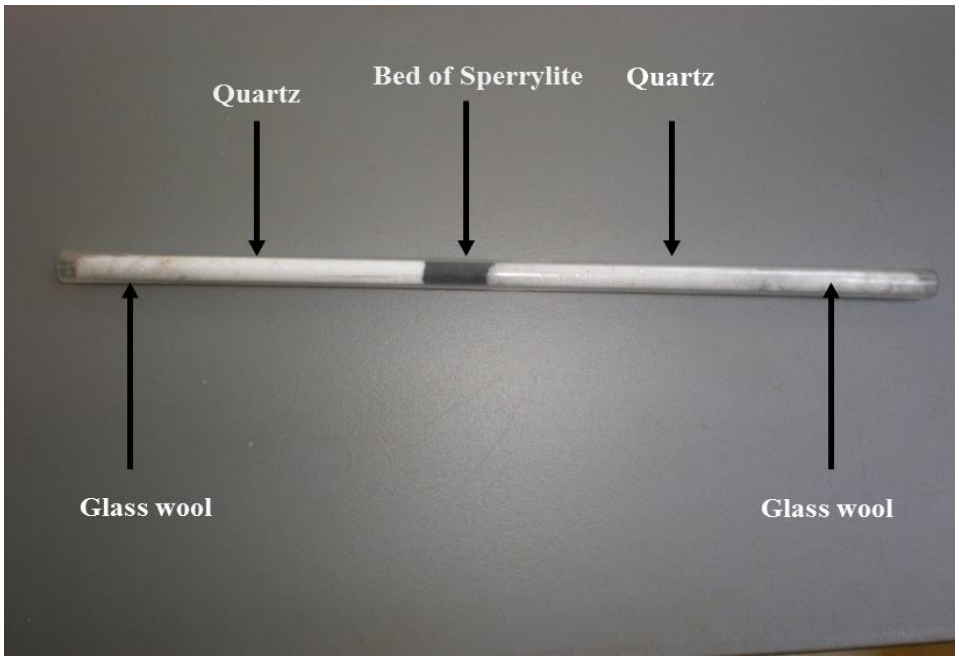

Figure 46: Mini-column with bed of sperrylite

Figure 47: Mini-column immersed in water bath

Figure 48: Mini-column experiment in full progress

4.3. Results and Discussion: Sperrylite Leaching

4.3.1. Leaching Tests in BSTRs

Curves for the experiments were plotted as concentration in solution (mg/L) versus time. The percentage extractions were very low, in the range ≤6 %. Figure 49 shows that the best oxidant is ferricyanide, with the best results being achieved when ferricyanide is combined with cyanide regardless of whether oxygen, compressed air or nitrogen was sparged into the solution. The Pt levels extracted in the cyanide-ferricyanide systems are in the order of 12-16 times more than what is extracted by the cyanide-only systems. Data Set 2 (ferricyanide alone) is only slightly lower in Pt dissolution than Data Set 4 and 6 (compressed air and pure oxygen), but a significant improvement over the plain cyanide extractions (Data Sets 1, 3 and 5). Data Sets 1, 3 and 5 show that the use of oxygen, either pure or as compressed air makes no difference to the amount of Pt dissolved in the cyanide-only systems. From Figure 49 it can also be seen that ferricyanide on its own is ineffective (this experiment ran for only 18 hours). As hypothesized, the ferricyanide acts as an oxidant with cyanide acting as the complexing agent for Pt. Considering Figure 49 and Figure 50 together, the curves for Pt and As have nearly

identical shapes and the quantities in solution are similar. The graphs from Figure 49 and Figure 50 all suggest that after some time the leaching levels off.

Further, the molar ratios of Pt to As leached at the various sampling points corresponding to the points in the all the leach curves in Figure 49 and Figure 50 (Table 30) were considered. The increase in the molar ratio with each sampling point, corresponding to the points on the curves, show that the increase in Pt extracted was more than the increase in As over time. These observations provide some credibility to one of the hypotheses in that the leaching of Pt may be dependent on the solubilisation of the As which requires an effective oxidant. In the case of the cyanide-only experiments this supports the theory that Pt leaches out leaving an As enriched surface which is the gradual onset of passivation. In the case of the cyanide-ferricyanide systems the molar ratio is much higher than the cyanide only systems, showing that the Pt is coming out much faster with a molar ratio of 0.5 in solution which is the molar ratio of Pt to As in sperrylite. This also shows that the mineral sperrylite is leaching consistently in the cyanide-ferricyanide systems i.e. all the As molecules bonded to a Pt molecule are oxidised and solubilised hence the molar ratio of 0.5 in solution.

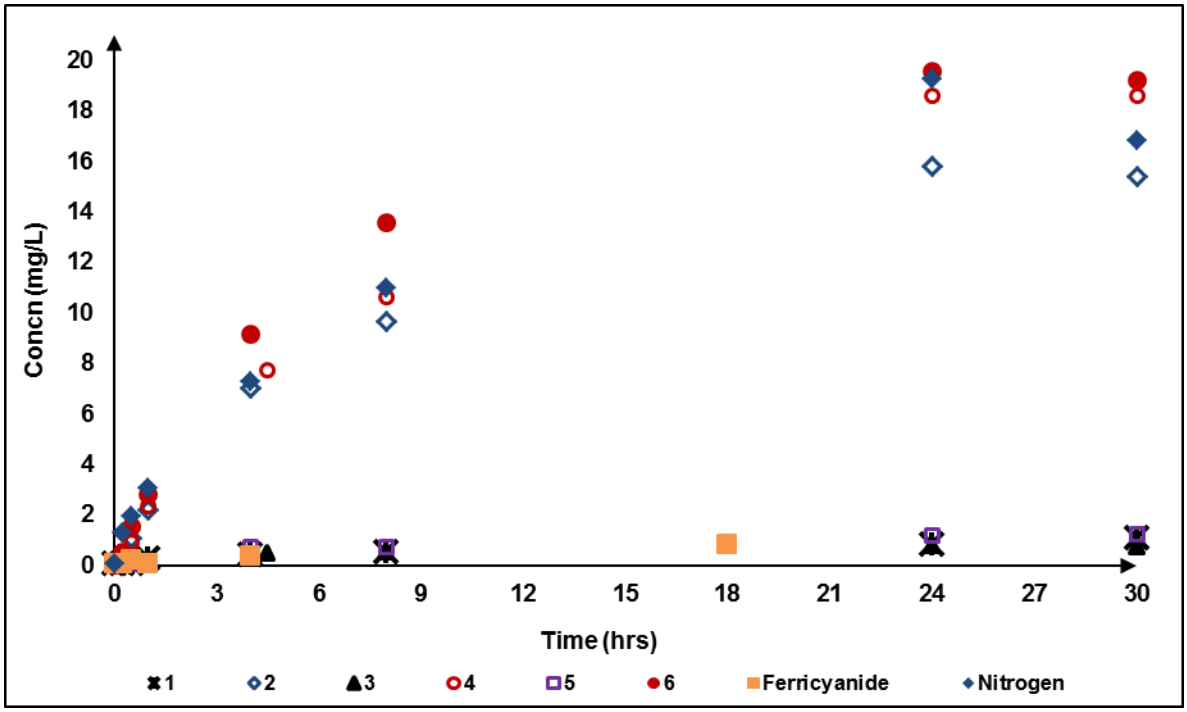

Figure 49: Platinum leach curves for various oxidants at 50°C, 500 mL solution, 250 mg sperrylite, 5 g/L NaCN and 5 g/L $K_3[Fe(CN)_6]$. 1. Cyanide no aeration; 2. Cyanide-ferricyanide no aeration; 3. Cyanide compressed air; 4. Cyanide-ferricyanide compressed air; 5. Cyanide pure O_2; 6. Cyanide-ferricyanide O_2

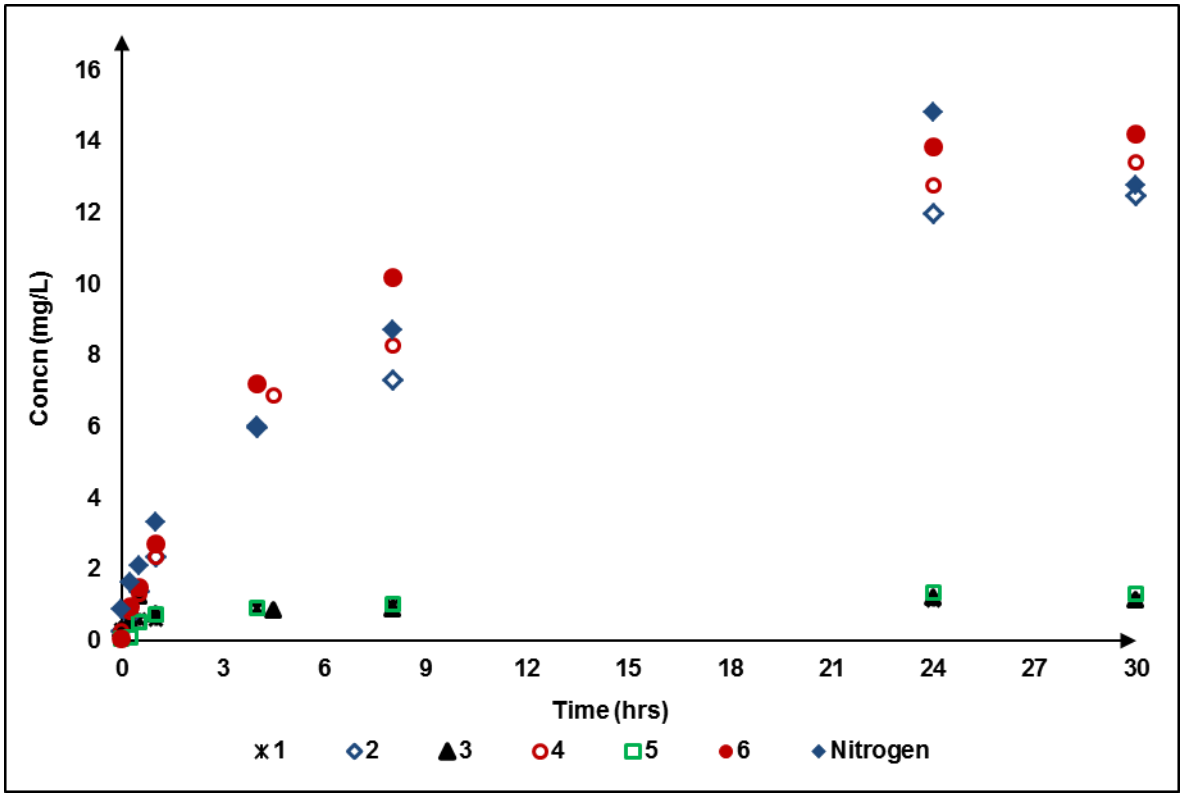

Figure 50: Arsenic leach curves for various oxidants at 50°C, 500 mL solution, 250 mg sperrylite, 5 g/L NaCN and 5 g/L $K_3[Fe(CN)_6]$. 1. Cyanide no aeration; 2. Cyanide-ferricyanide no aeration; 3. Cyanide compressed air; 4. Cyanide-ferricyanide compressed air; 5. Cyanide pure O_2; 6. Cyanide-ferricyanide O_2

Table 30: Molar ratios of Pt to As leached

Time (hrs)	1	2	3	4	5	6
0	0.05	0.09	0.04	0.04	0	0
0.25	0.05	0.21	0.05	0.21	0.21	0.27
0.5	0.06	0.30	0.04	0.28	0.05	0.40
1	0.19	0.36	0.14	0.39	0.04	0.40
4	0.18	0.45	0.21	0.43	0.30	0.49
8	0.20	0.51	0.22	0.50	0.28	0.51
24	0.284	0.51	0.25	0.56	0.34	0.54
30	0.37	0.47	0.24	0.53	0.36	0.52

1. Cyanide no aeration; 2. Cyanide-ferricyanide no aeration; 3. Cyanide compressed air; 4. Cyanide-ferricyanide compressed air; 5. Cyanide pure O_2; 6. Cyanide-ferricyanide O_2

Having identified the cyanide-ferricyanide system as a superior alternative to the cyanide-only system, the influence of reagent concentration in each system was evaluated. In Figure 51 there is no clear discernible pattern of extraction with the varying concentration of NaCN. After 30

hours the highest amount of Pt dissolved was with 25 g/L NaCN leaching more than the 50 g/L. The lowest amount of Pt dissolved was from the 5 g/L NaCN which leached less than the lower concentration tests. It is also seen from Figure 51 that the curves for the 2.5 and 5 g/L NaCN show increasingly higher Pt leaching than the rest of the curves which only attain the same levels between days 8 and 22. However, given the relatively small amounts dissolved by all concentrations, in the range of 0.71 – 1.81 mg/L it can be concluded that the concentration of NaCN under those conditions has very little influence on the leaching of Pt from the sperrylite.

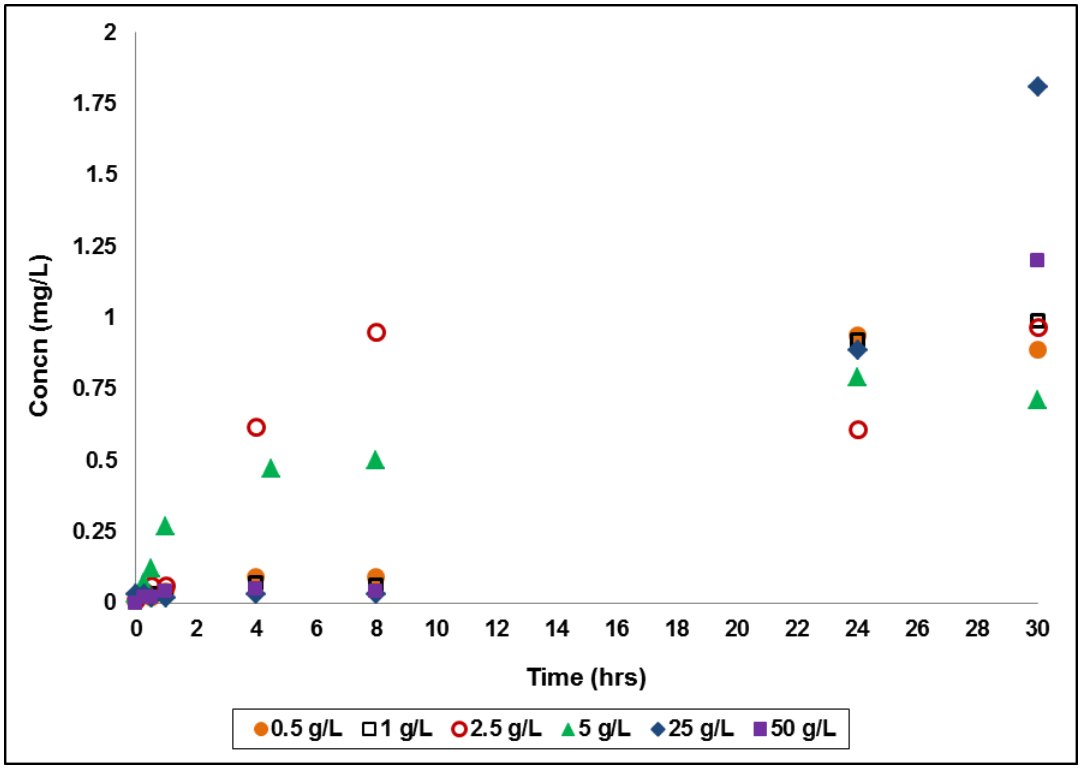

Figure 51: Pt leach curves for cyanide leaching experiments at 50°C, 500 mL solution, 250 mg sperrylite, sparging with compressed air and varying concentrations of NaCN

For the cyanide-ferricyanide system, Figure 52 shows that if the lower concentrations (0.5, 1, 2.5 and 5 g/L of $K_3[Fe(CN)_6]$) are compared with the higher concentrations (25 and 50 g/L of $K_3[Fe(CN)_6]$), then it can be generally observed that overall the lower the concentration of $K_3[Fe(CN)_6]$ the higher the amount of Pt leached from sperrylite. Compared to Figure 51, the cyanide-only tests, the lower concentration tests once again achieved much higher Pt extractions in the order of 10-20 times more. However a closer look at Figure 52 shows no clear pattern with 5 g/L being the highest followed by 1 g/L, then 2.5 g/L then 0.5 g/L. As the concentration of $K_3[Fe(CN)_6]$ increases to very high values, however, the amount of Pt leached

reduces, with 50 g/L being the lowest. The systems with the lower amounts of $K_3[Fe(CN)_6]$ all have an identical trend for the Pt leach curves and the amounts being comparable. The system initially leaches at a high rate and then levels off or drops after 24 hours. In contrast the two systems with the highest amount of $K_3[Fe(CN)_6]$ don't have as high a rate of leaching throughout and level off from 9 hours into the leach. Of particular note is the test with 50 g/L $K_3[Fe(CN)_6]$ which does not even take off until after 8 hours and even then has a comparably low extraction level compared to the other systems. Overall it is observed that the best Pt extractions were produced with a concentration of between 1 and 5 g/L $K_3[Fe(CN)_6]$, while a concentration of less than 1 and more than 5 results in lower Pt extractions.

In all the above experiments it is seen that after 30 hours the leach curves seem to level off. Further test work conducted to determine whether it was a solubility constraint or passivation involved leaching for a longer period and in another set, leaching for longer periods then recovering the residual material and re-leaching with fresh solution. This was done for both systems; cyanide alone and cyanide-ferricyanide.

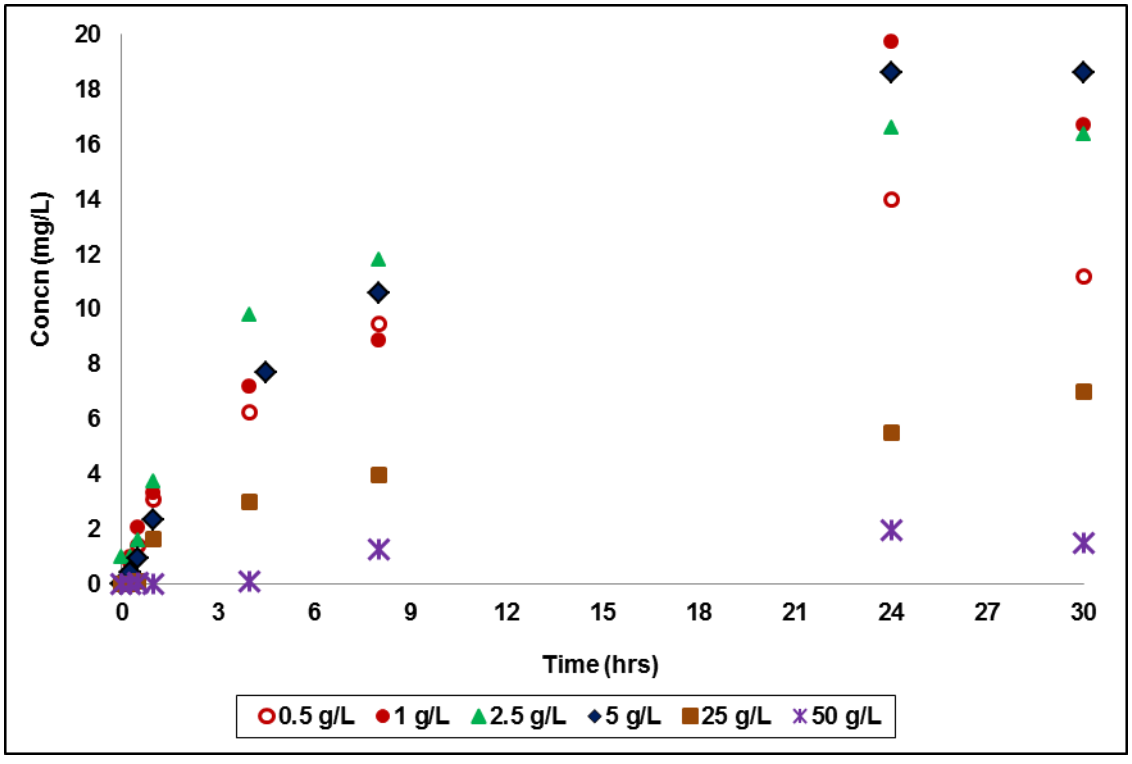

Figure 52: Pt leach curves for cyanide leaching experiments at 50°C, 5 g/L NaCN, 500 mL solution, 250 mg sperrylite, sparging with compressed air and varying concentrations of $K_3[Fe(CN)_6]$

In all cases the results of the extended leaching tests (Figure 53, Figure 54, Figure 55 and Figure 56) for both systems show almost identical patterns, in which after 30 hours the leaching, which appeared to be levelling off suddenly spikes to a higher (peak level) then drops and levels off again. In the cyanide-only experiment it is observed that the As is seen to initially leach out more rapidly than the Pt (compare Figure 53 and Figure 54). The experiments were conducted in duplicates, side-by-side. A slight deviation can be seen with reactor 2 of the cyanide-only experiment where the peak came much later than the other reactors. But the data point after that seems to drop, suggesting a similar pattern thereafter. Although patterns were identical the same observations as before were made, i.e. the cyanide-ferricyanide experiments performed much better than the cyanide-only experiments and the Pt and As leach curves followed identical patterns.

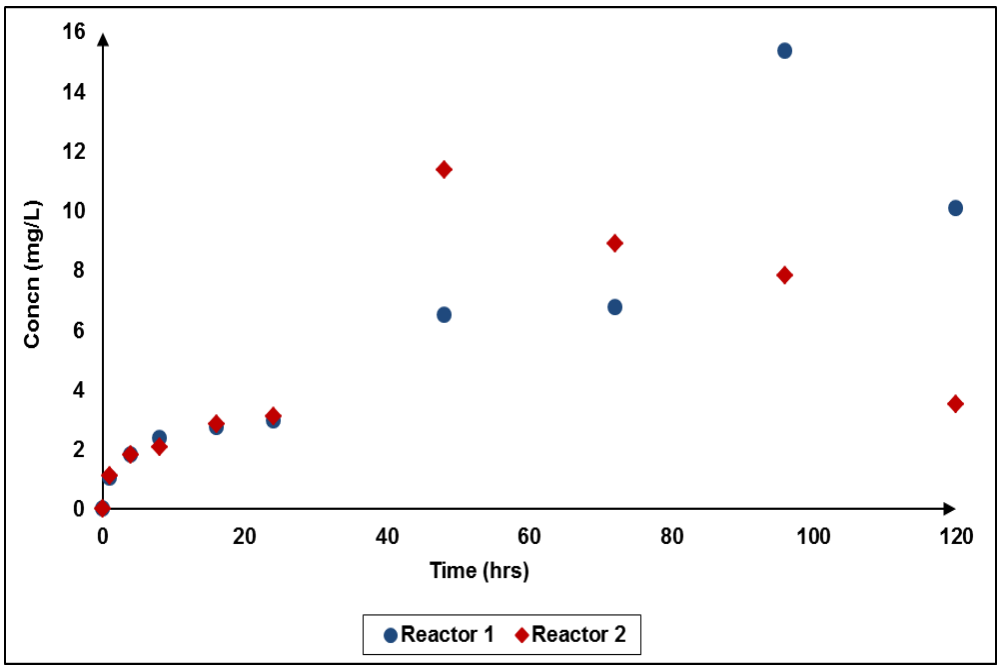

Figure 53: Pt leach curves extended leaching experiments using 5 g/L NaCN and 1 g sperrylite at 50°C, using 500 mL of solution

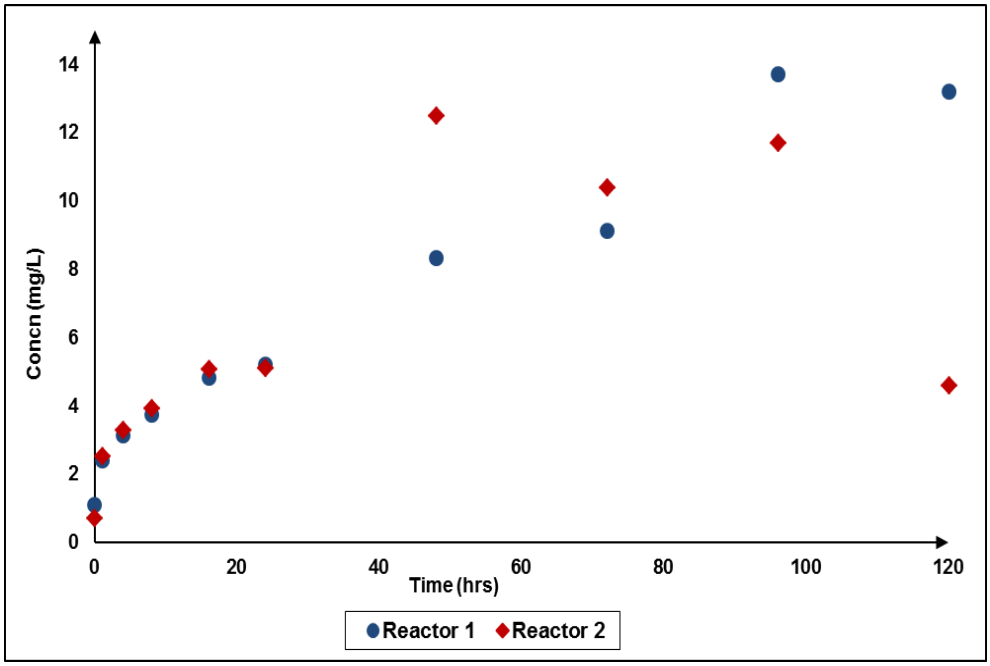

Figure 54: As leach curves extended leaching experiments using 5 g/L NaCN and 1 g sperrylite at 50°C, using 500 mL of solution

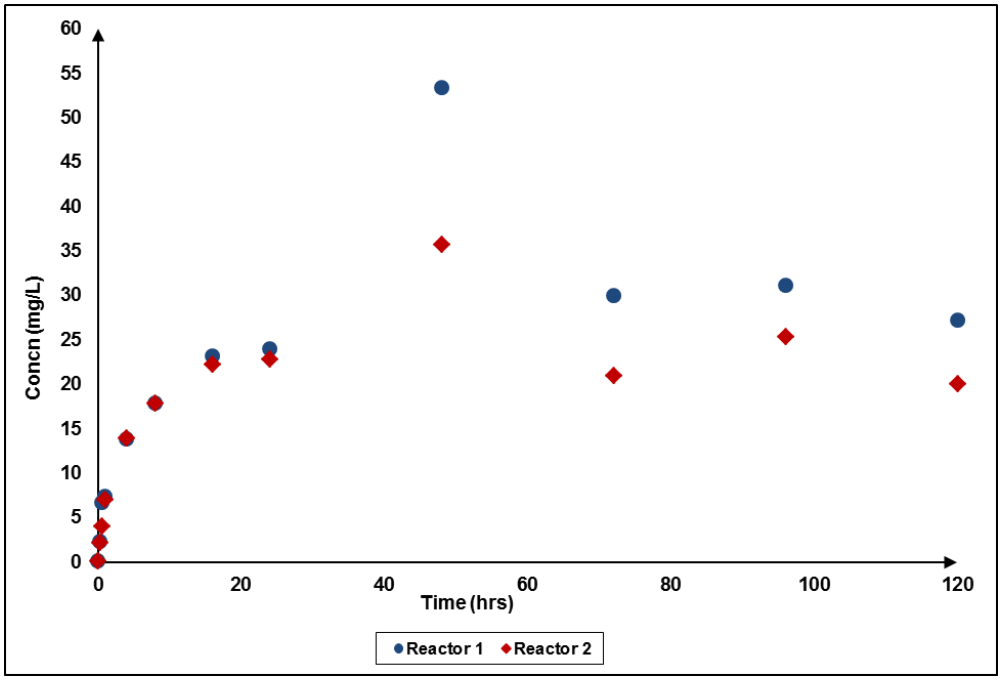

Figure 55: Pt leach curves extended leaching experiments using 5 g/L NaCN, 5 g/L $K_3[Fe(CN)_6]$ and 1 g sperrylite at 50°C, using 500 mL of solution

To determine whether the eventual levelling off was a solubility constraint or passivation, the residual material from all experiments was recovered by vacuum filtration, dried in a desiccator overnight at room temperature (23°C) and leached under identical conditions with fresh solution for each system for an equal length of time. This was done for two additional "runs"

in each case. Prior to re-leaching the recovered sample, a small sub-sample was taken out for analysis via SEM and XPS. All experiments were done in duplicate.

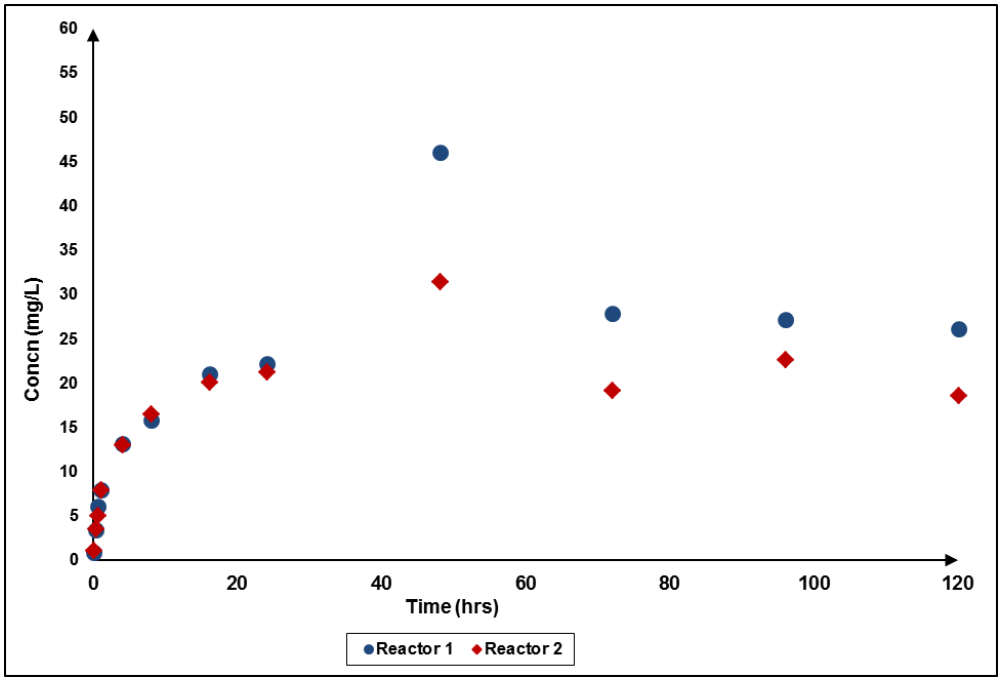

Figure 56: As leach curves extended leaching experiments using 5 g/L NaCN, 5 g/L $K_3[Fe(CN)_6]$ and 1 g sperrylite at 50°C, using 500 mL of solution

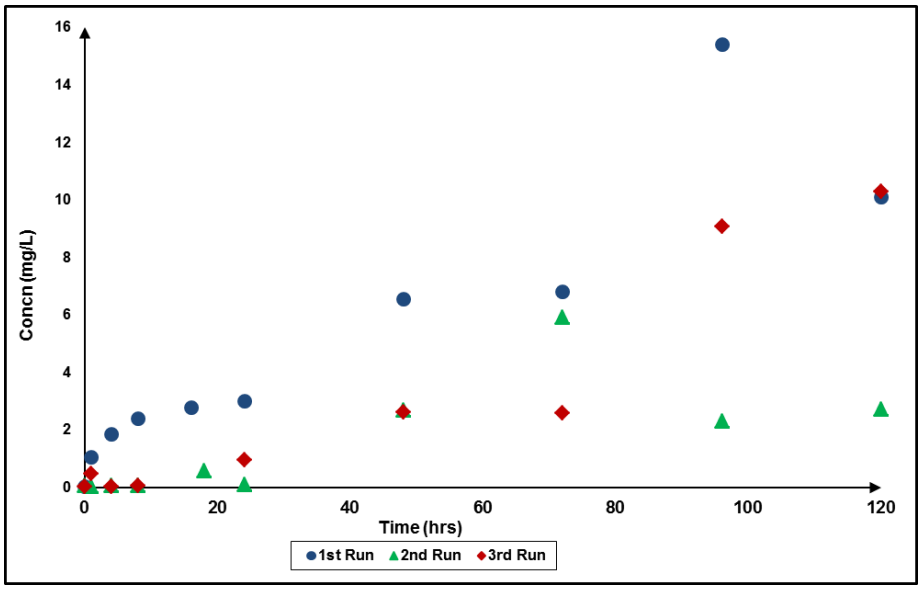

Figure 57: Reactor 1-Pt leach curves for repeated run leaching experiments using 5 g/L NaCN and residual sperrylite from each run before, at 50°C, using 500 mL of solution

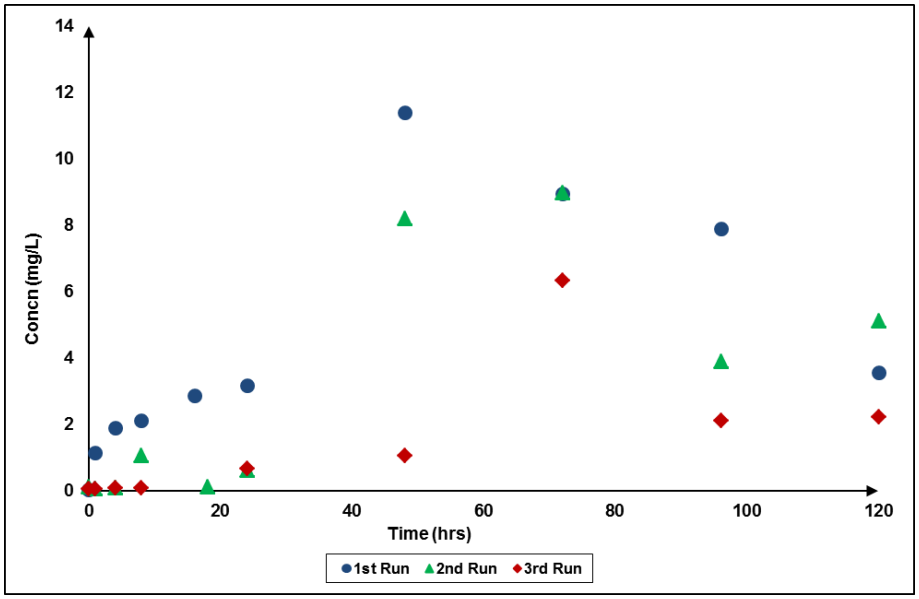

Figure 58: Reactor 2-Pt leach curves for repeated run leaching experiments using 5 g/L NaCN and residual sperrylite from each run before, at 50°C, using 500 mL of solution

From Figure 57 and Figure 58 a clear pattern is not discernible from the two reactors. In reactor 1 after the first run, the subsequent runs dissolve less Pt with the third run dissolving more than the second at the end of the experiment. In the case of reactor 2, again the subsequent runs dissolve less than the first run but this time the second run dissolves more than the third run and the final data point for this run exceeds the final point for the first run. In both reactors it was also observed that the 2nd and 3rd runs seemed to suffer a 24 hour lag in leaching before finally taking off to higher levels comparable to the 1st run. Overall, from this data it can be seen that even with fresh solution a certain amount of Pt dissolved is not exceeded. In fact it can be argued that with subsequent runs less Pt is leached because the 2nd and 3rd run curves never exceed the 1st run curves. This observation becomes more relevant when compared to the experiments in which ferricyanide was introduced as seen below. This observation points more towards passivation than solubility constraint as with the latter, there would be some similarity in the amounts of Pt leached and the leach curves among the 3 runs in each reactor. Further, the molar ratios of Pt to As in solution were analysed for the cyanide only systems (Table 31). The points correspond with the leaching points from the leach curves (Figure 57 and Figure 58). As concluded earlier the increase in the ratio is an indication of the increase in Pt over As in solution once again adding credibility to the theory that small amounts of Pt leach out and some of the As which is not sufficiently oxidised, remains behind gradually passivating the mineral surface resulting in low Pt extractions.

Table 31: Molar ratio of Pt to As in solution for repeated leaching experiments for cyanide-only system

	Reactor 1			Reactor 2		
Time (hrs)	1st Run	2nd Run	3rd Run	1st Run	2nd Run	3rd Run
0	0.0	0.4	0.3	0.0	0.0	0.5
1	0.2	0.2	2.8	0.2	0.2	0.0
4	0.2	0.3	0.2	0.2	0.0	0.3
8	0.2	0.4	0.2	0.2	5.8	0.5
16	0.2	0.4		0.2	0.1	
24	0.2	0.1	0.2	0.2	0.3	0.4
48	0.3	3.0	0.3	0.4	4.1	0.6
72	0.3	4.3	0.4	0.3	0.4	0.8
96	0.4	0.3	0.5	0.3	0.3	0.4
120	0.3	0.4	0.5	0.3	0.7	0.6

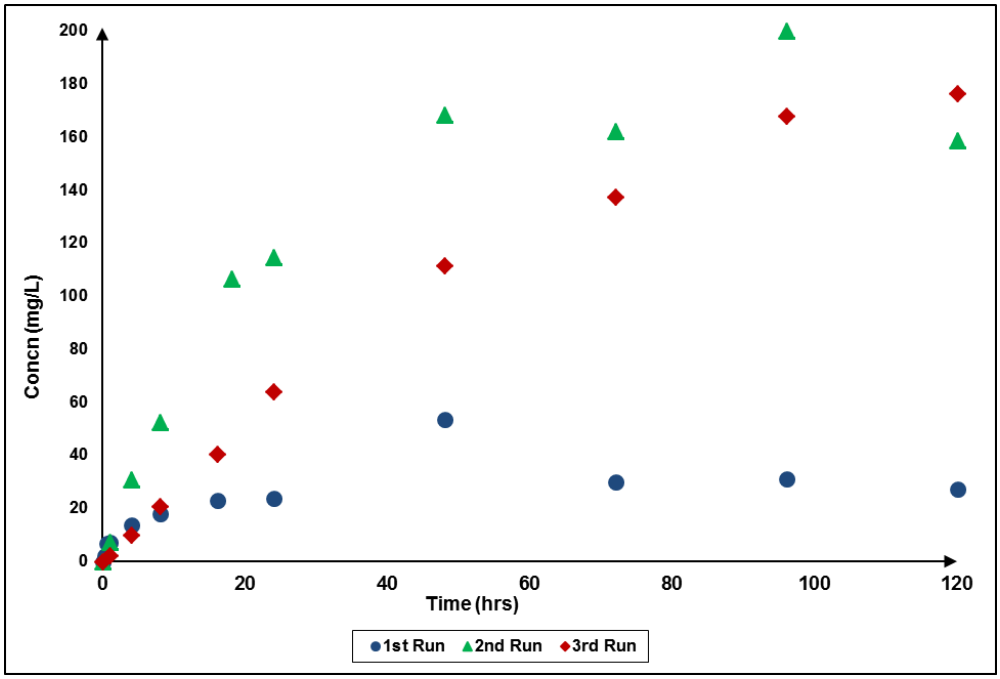

Figure 59: Reactor 1-Pt leach curves for repeated run leaching experiments using 5 g/L NaCN, 5 g/L $K_3[Fe(CN)_6]$ and residual sperrylite from each run before, at 50°C, using 500 mL of solution

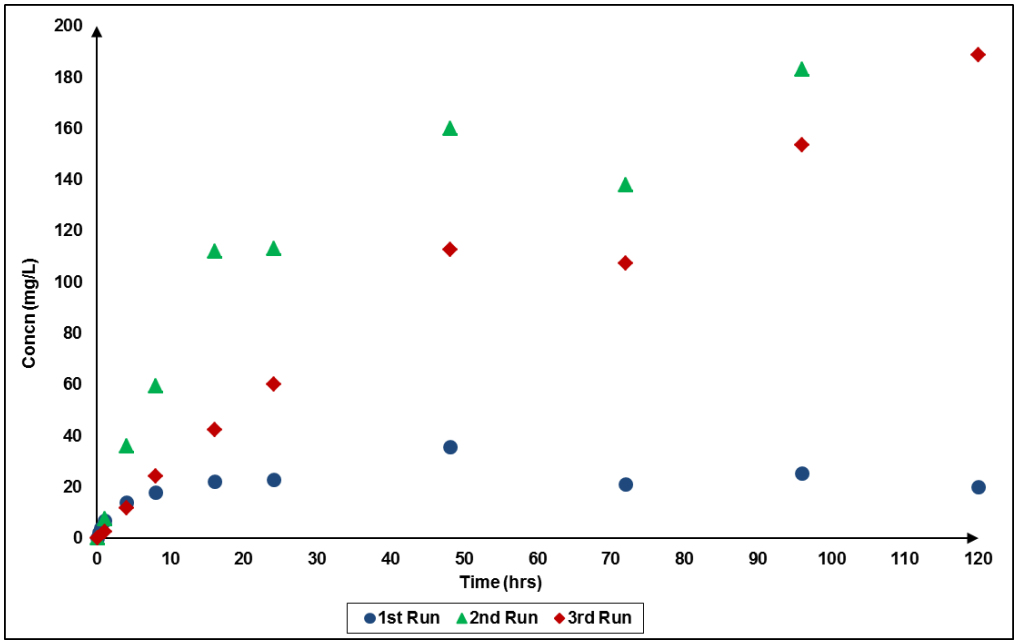

Figure 60: Reactor 2-Pt leach curves for repeated run leaching experiments using 5 g/L NaCN, 5 g/L $K_3[Fe(CN)_6]$ and residual sperrylite from each run before, at 50°C, using 500 mL of solution

From the graphs (Figure 59 and Figure 60), for the cyanide-ferricyanide system almost identical leaching patterns are observed in the duplicate reactors. After the first run levels off, more Pt is extracted in subsequent runs (as compared to the experiments with only cyanide) ruling out a solubility constraint in this system but rather indicates a more complex interaction at the surface of the mineral particles which is yet to be explained. It appears that the use of the ferricyanide has a significant effect on changing the surface structure of the mineral particles over a period of time, in the 1st run, resulting in much improved extraction levels of the Pt in the 2nd and 3rd runs. However, the levelling off still seems imminent in these runs but at or after 5 days, unlike in the 1st run where it occurred after 18 hours. It is proposed that perhaps in the cyanide-ferricyanide system the complete oxidation of As is gradual and the transition to the higher state goes through an intermediate state (possibly As^0) which passivates the mineral surface initially. Over time and with fresh solution the full oxidation of As occurs and leaching is resumed. In the case of the cyanide-only system the lack of oxidant results in the surface remaining and increasingly becoming passivated. It is also possible that the introduction of ferricyanide salt in the cyanide system results in the formation of some unknown reaction products that deposit on the mineral surface initially but are later removed physically, through the vacuum filtration to recover samples between runs, or by further reaction. But it should be noted that this was not the case in the cyanide-only system which is chemically different. It can

therefore be concluded that the reason and mechanisms of passivation are different for the different systems.

Table 32 shows the molar ratios of Pt to As in solution for these cyanide-ferricyanide experiments. In the case of the first run for each experiment it stays at 0.5 after levelling off, consistent with no more leaching occurring and with the 2nd and 3rd runs it is still at 0.5 showing not only continuous leaching but consistent leaching of the sperrylite mineral as compared to the preferential leaching of the cyanide-only experiments.

Table 32: Molar ratio of Pt to As in solution for repeated leaching experiments for cyanide-ferricyanide system

	Reactor 1			Reactor 2		
Time (hrs)	1st Run	2nd Run	3rd Run	1st Run	2nd Run	3rd Run
0	0.0	0.1	0.3	0.0	0.3	0.2
1	0.3	0.4	0.4	0.2	0.4	0.4
4	0.4	0.5	0.4	0.3	0.5	0.4
8	0.4	0.5	0.4	0.3	0.5	0.5
16	0.4	0.5	0.4	0.4	0.5	0.5
24	0.4	0.5	0.5	0.4	0.5	0.5
48	0.5	0.5	0.5	0.4	0.5	0.5
72	0.4	0.5	0.5	0.4	0.5	0.5
96	0.4	0.5	0.5	0.4	0.5	0.5
120	0.4	0.5	0.5	0.4		0.5

As seen previously, the leaching patterns of the Pt correspond with the leaching patterns of the As (Figure 61, Figure 62, Figure 63 and Figure 64).

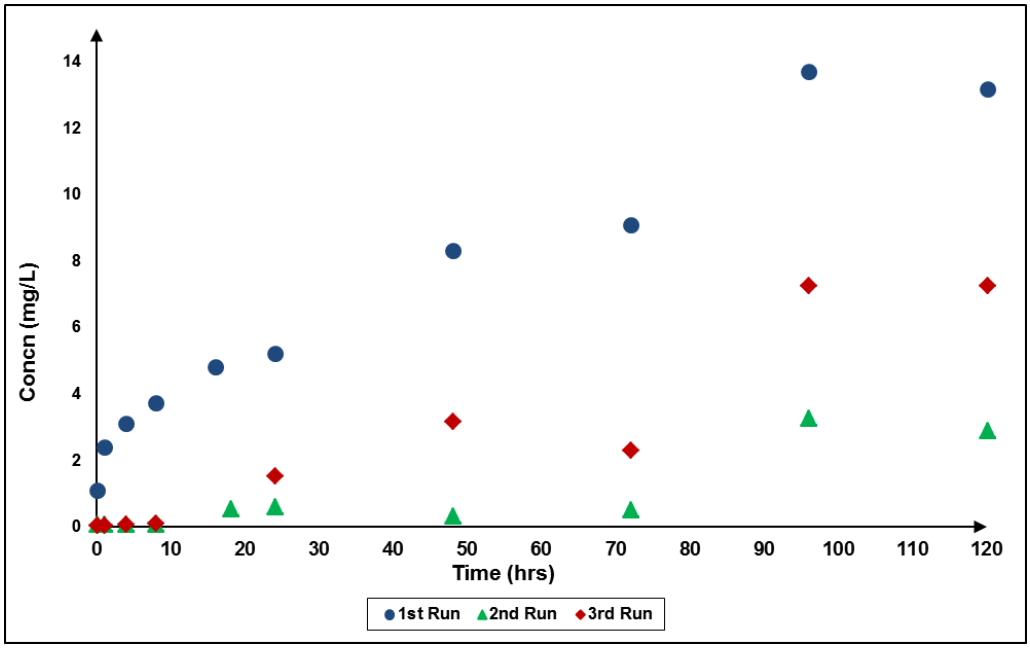

Figure 61: Reactor 1-As leach curves for repeated runs leaching experiments using 5 g/L NaCN and residual sperrylite from each run before, at 50°C, using 500 mL of solution

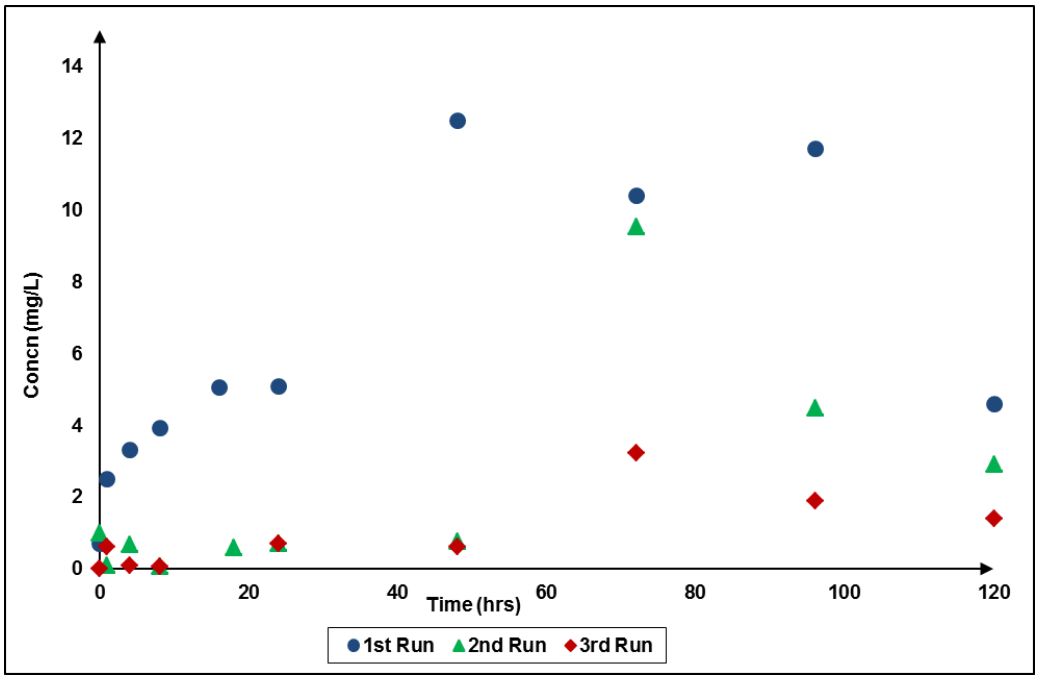

Figure 62: Reactor 2-As leach curves for repeated runs leaching experiments using 5 g/L NaCN and residual sperrylite from each run before, at 50°C, using 500 mL of solution

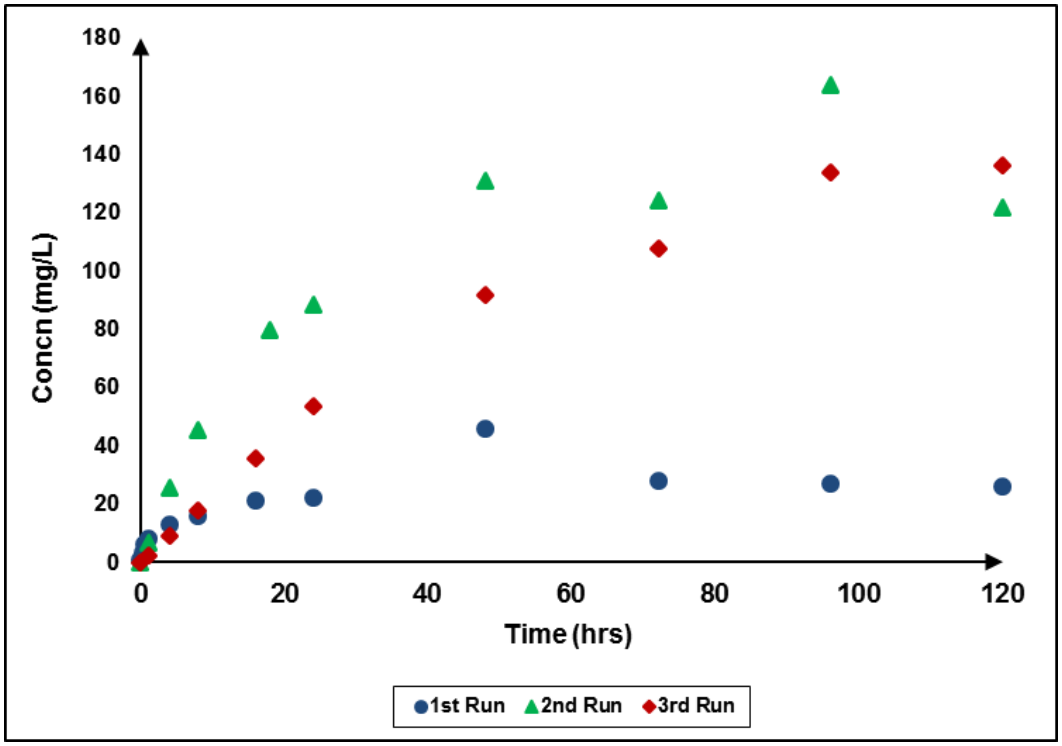

Figure 63: Reactor 1- As leach curves for repeated runs leaching experiments using 5 g/L NaCN, 5 g/L $K_3[Fe(CN)_6]$ and residual sperrylite from each run before, at 50°C, using 500 mL of solution

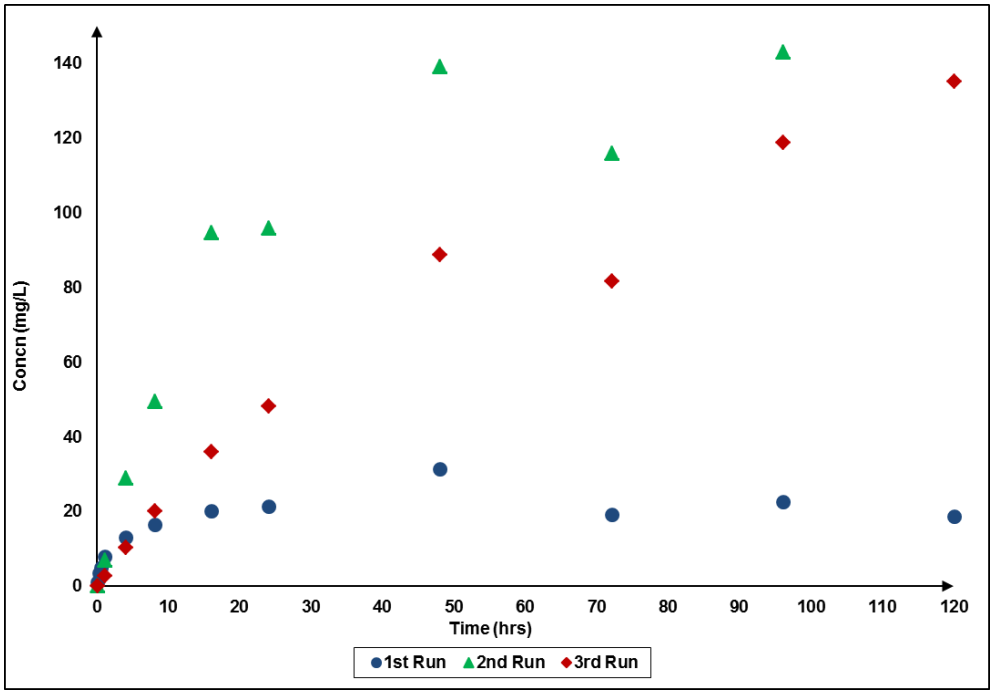

Figure 64: Reactor 2- As leach curves for repeated runs leaching experiments using 5 g/L NaCN, 5 g/L $K_3[Fe(CN)_6]$ and residual sperrylite from each run before, at 50°C, using 500 mL of solution

To further understand the leaching patterns exhibited in these experiments, a sample of the sperrylite untreated (Sample 1), after the third run in reactor 1 of the cyanide-only experiment (Sample 2), after the first (Sample 3) and third (Sample 4) runs of reactor 1 of the cyanide-ferricyanide experiments were analysed using XPS and SEM. Additionally, the pattern in the cyanide-ferricyanide experiments was further explored in a system where solution was continuously fed into the system, using mini-columns without the interruptions to see if a similar or identical pattern would emerge (section 4.3.3.).

Additionally, to further investigate whether or not the improved leaching was connected to the overnight drying of the sample in-between the five day leach runs, a comparison was conducted with two experiments using a freshly micronized sample of sperrylite. The first experiment (Expt 1) was run identical to the previous BSTR experiments (5 g/L NaCN, 5 g/L $K_3[Fe(CN)_6]$, 50°C for 5 days per run) with the sample being left to dry overnight before being leached with fresh solution. A second experiment (Expt 2) was run identical to all BSTR experiments but in-between runs the sperrylite was not dried overnight but immediately leached with fresh solution. As explained earlier, drying the sample was originally done to obtain a sub-sample for XPS and SEM analysis, which was forgone in this experiment.

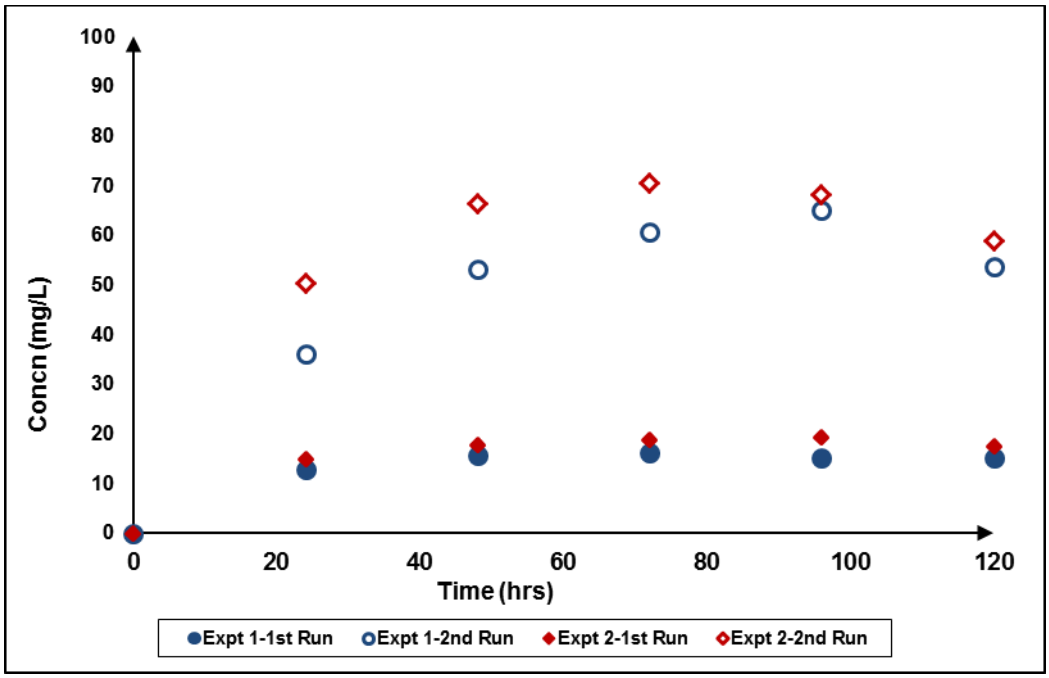

Figure 65: Comparison of Pt leach curves for Expt 1 and Expt 2. Expt 1-1 day interval and over-night drying of sample at room temperature before 2nd run leach. Expt 2-sample immediately leached after 1st run with no interval. Experiments ran at 50°C, 500 mL solution, 1 g sperrylite, 5 g/L NaCN and 5 g/L $K_3[Fe(CN)_6]$

Figure 65 shows that the over-night drying had no influence on the improved leaching of the Pt but the addition of fresh solution did. The curves in both runs of both experiments are very similar in pattern and level of extraction. However it should be noted that the levels extracted in all runs for both experiments were lower than those achieved in the earlier experiments (Figure 59 and Figure 60) and the 2nd run experiments levelled off much sooner than the previous ones. There is no conclusive explanation for this difference as the samples come from the same bulk sample of sperrylite and every effort was made to ensure that the micronizing process is identical at all times. However the starting sample in all cases is not consistent in terms of particle size distribution and this may have some influence on the extent of leaching in the different experiments.

Another factor that may have played a role in the improved leaching of the Pt was the use of vacuum filtration to recover the sample of sperrylite before the next "run" of leaching. This was common in all BSTR experiments. It can be argued that this step acts as a form of washing in that the vacuum filtration process through suction of the liquid removes the passivation layer from the grains by force and through the filtrate. Hence after the first run in each experiment whatever material that is hindering leaching is removed and hence the 2nd and 3rd runs have much improved leaching. However this does not explain why this passivation does not occur in the 2nd and 3rd runs at the same time it did in the 1st runs as the process conditions were identical. But these observations further support the theory that the passivation is an unknown reaction product or products due to the use of ferricyanide. This product or products are removable through the vacuum filtration of the samples which acts as a form of wash which clears the surface and supports further and improved leaching until it occurs again. It should be noted that even in the earlier cyanide-ferricyanide BSTR experiments (Figure 59 and Figure 60) the 2nd runs 3rd runs showed signs of levelling off eventually. But then the delay in its occurrence still remains to be explained. These observations will be further investigated using the continuously fed reactor (mini-column) as proposed (section 4.3.3.).

4.3.2. XPS and SEM analysis

Figure 66 shows SEM images of sperrylite samples from various batch leach tests as discussed above. There were no visible differences in the appearance of the different samples. Based on the hypothesis, it was decided that perhaps EDS analysis of the different sample may show a

difference in As:Pt atomic ratio between the different samples. More specifically that Sample 1 would have a ratio consistent with literature (Sperrylite, n.d.), approximately 2:1, whereas in Sample 2 it would have one greater than 2:1 with the surface layers perhaps having more arsenic than Sample 1, while Samples 3 and 4 would most likely have a ratio of 2:1 since leaching of both Pt and As had not levelled off in Sample 3 and in Sample 4 it continued for both and the BSTR experiments showed the As to Pt ratio in solution for these systems was 2:1 (Table 32). The EDS analysis (

Table 33) for all samples showed that the As:Pt atomic ratio, approximately 2:1, and the weight percentages more less stayed the same. This shows no change in the As:Pt ratio in the bulk of the sample. Thus the focus turned to the XPS analysis to determine if any changes could be detected at the surface of the samples possibly by scanning a little deeper below the surface.

Table 33: EDS analysis results of the diffrent samples

Sample	Weight %		Atomic %	
	As	Pt	As	Pt
Sample 1 (untreated-fresh)	43.1	56.9	66.3	33.7
Sample 2 (cyanide)	44.2	55.8	67.4	32.6
Sample 3 (cyanide-ferricyanide-1st run)	44.4	55.6	67.5	32.5
Sample 4 (cyanide-ferricyanide-3rd run)	44.3	55.7	67.4	32.6

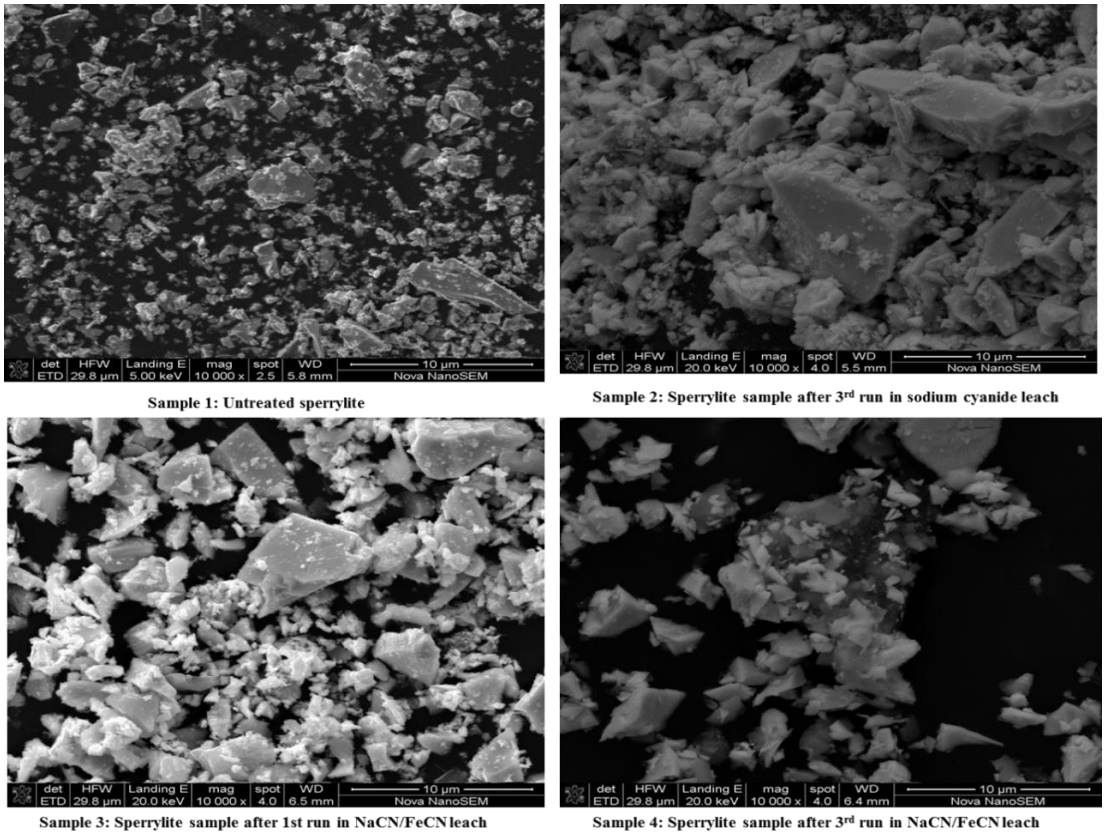

Figure 66: SEM comparative images of various samples in NaCN and NaCN/FeCN leach tests

Using a similar approach to that used in the SEM analysis; the XPS analysis worked on the hypothesis that sperrylite leaching in cyanide is hampered due to the eventual passivation of the mineral surface by an arsenic layer. In this case it was expected that the analysis would reveal that the atomic ratio of As:Pt for Sample 2 was greater than Sample 1 at the surface of the mineral samples. Given the unusual behaviour exhibited by the leach curves producing Sample 3 and Sample 4 (refer to Figure 59, Figure 60, Figure 63 and Figure 64) it was unknown what caused the levelling off in the 1st run and what caused the improved leaching in the 2nd and 3rd runs. An analysis of the surface was warranted given that the SEM analysis of the bulk mineral did not yield any explanations.

Table 34: Atomic ratios of As:Pt in the various samples

Sample	Before survey	2 mins.
Sample 1 (untreated-fresh)	2.2 : 1	1.32 : 1
Sample 2 (cyanide)	2 : 1	1.62 : 1
Sample 3 (cyanide-ferricyanide-1st run)	1.82 : 1	1.89 : 1
Sample 4 (cyanide-ferricyanide-3rd run)	1.75 : 1	0.89 : 1

Table 34 shows some results from the surface scan and depth profiling of the different samples. The second column in Table 34 (Before Survey) refers to a scan/survey of the mineral surface prior to the penetrative or depth scans of the third and fourth columns. A comparison of results shows less As in Sample 2 than Sample 1 which is contrary to the theory that Pt was preferentially leached leaving behind As which gradually passivates the surface. However, given the small quantities of both Pt and As leached in the cyanide-only experiment the theory still holds especially given the analysis of the molar ratios of these elements in solution. On the other hand, this result is consistent with the BSTR experiments which showed As initially leaching out more rapidly than Pt (Figure 53 and Figure 54). Although the differences in As are not large, a comparison between Sample 2 and Samples 3 and 4 supports both the hypotheses to some extent. There is not much leaching of Pt taking place in the cyanide leach as not much As is being oxidised as can be seen by the similar ratios of Sample 1 and Sample 2. But in Sample 3 which leached out more Pt than Sample 2 before levelling off, we see less As because more was oxidised and dissolved. Finally in Sample 4 which corresponds to the curve at a point when Pt leached out the most we see the lowest amount of As at the surface.

The $Pt4f_7$ peaks and binding energies in all 4 samples (Figure 67) from the XPS analysis are identical to those in the Moulder et al. (1995) (Handbook of X-ray Photoelectron Spectroscopy) and the study by Avril et al. (2015) show that the Pt in all 4 samples was Pt^{2+}. The peak for the depth profile for the 36 nm scan shifts to the left quite noticeably in all samples but stays below a binding energy of 75 eV. All compounds with Pt^{2+} in Moulder et al. (1995) (Table 35) have the $4f_7$ peak between 72 and 75 eV, while metallic Pt has a binding energy close to 71 eV and Pt^{4+} has a binding energy of above 75 eV. Whatever the cause for the shift, it is not believed to be Pt being in another oxidation state.

Table 35: Binding energies for Pt4f7 peaks for various compounds taken from Moulder et al. (1995)

$Pt4f_7$	**Binding Energies**	**Likely Oxidation State of Pt**
Pt	71.2	0
PtSi	72.8-73.2	+2
Pt_2Si	72.2-72.7	+4
$PtCl_2$	73.4-73.8	+2
$PtCl_4$	75.4-75.8	+4

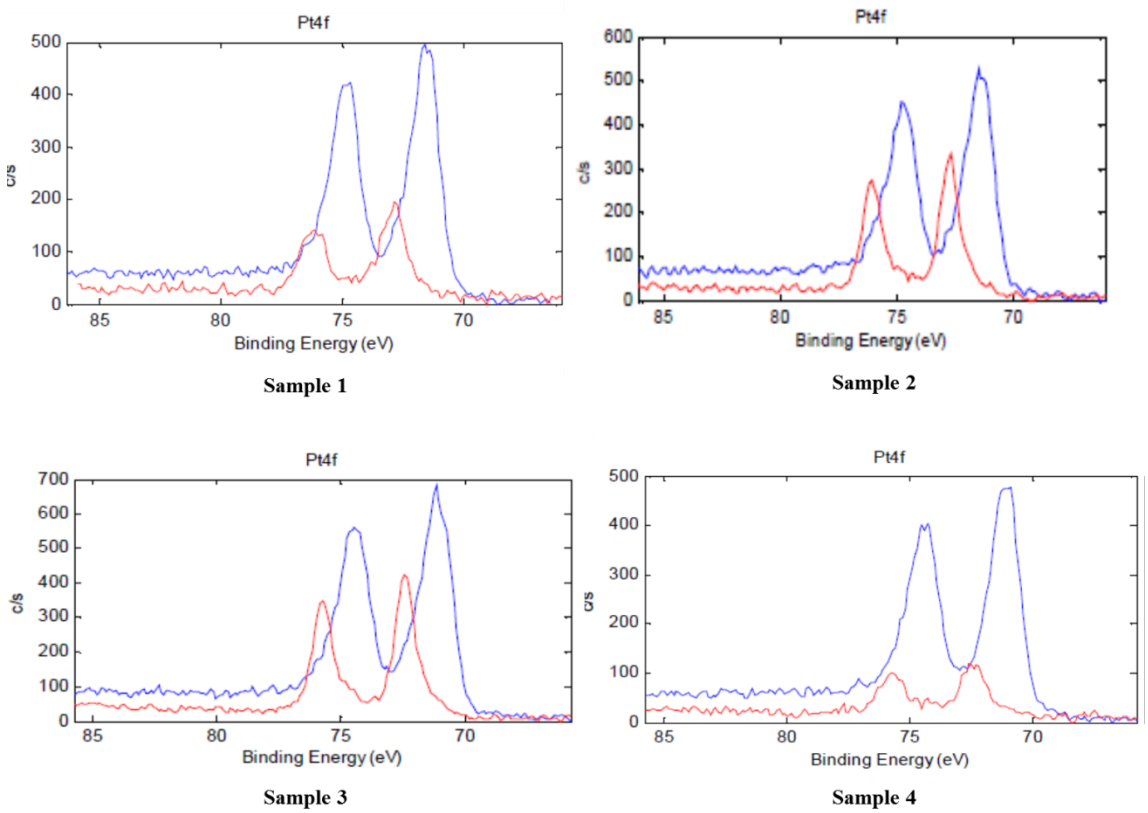

Figure 67: Pt4f XPS peaks for all 4 samples. Red represents survey at the surface of sample and blue survey after 2 minutes of depth profile-penetration of 36 nm

For the most part the As3d peaks (and corresponding binding energies) for all 4 samples (Figure 68) did not match those in Moulder et al. (1995) or any other studies on arsenides and arsenic compounds. Coincidentally, all the data uncovered related to As in the +5, +3 and 0 states and none were found for the lowers states. However a comparison with studies conducted by Nesbitt and Reinke (1999) on NiAs, and Jones and Nesbitt (2002) on $FeAs_2$ using XPS, showed that although their peaks differ from those in Figure 68, they found binding energies between 41-42 eV which is identical to the 41-42 eV range for the As3d peaks in this study specifically for Samples 1, 3 and 4. Arsenic in NiAs and $FeAs_2$ is in the -1 oxidation state (Jones and Nesbitt, 2002; Nesbitt and Reinke, 1999) and hence with those similar binding energies it may also be in the -1 state in $PtAs_2$. This oxidation state represents mixed or multiple oxidation states of As as stated by Henke and Hutchison (2009). It should be noted from Moulder et al. (1995) that As^0 has binding energies 41.3-41.6 (Table 36), but it is not possible that that is the oxidation state of As in $PtAs_2$.

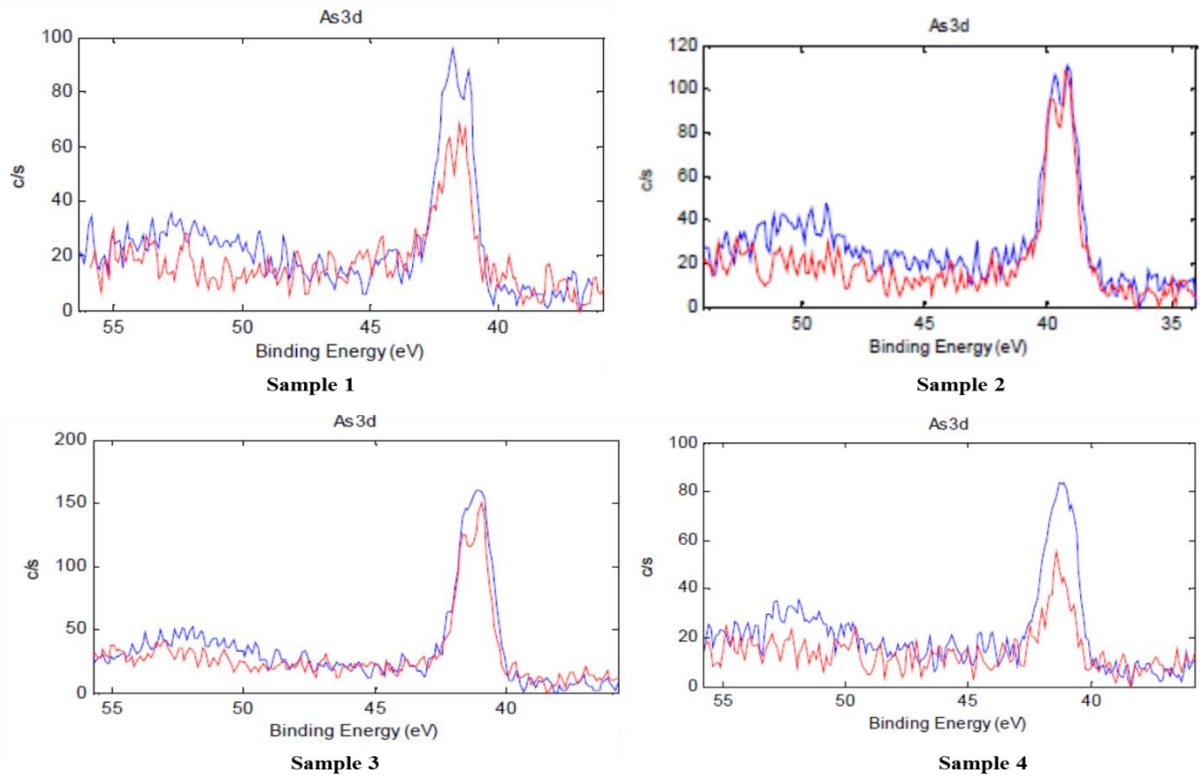

Figure 68: As3d XPS peaks for all 4 samples. Red represents survey at the surface of sample and blue survey after 2 minutes of depth profile-penetration of 36 nm

Table 36: Binding energies for As3d peaks for various compounds taken from Moulder et al. (1995)

As3d	Binding Energies	Likely Oxidation State of As
As	41.3-41.6	0
GaAs	40.6-40.9	-3
Sulphides	43.1-44	mixed
$AsBr_3$	45-45.5	+3
As_2O_3	44.7-45.2	mixed
As_2O_5	45.9-46.2	mixed

From Figure 68, the shift of the peak below a binding energy of 40eV for Sample 2, as compared to the other samples is quite noticeable. As in various compounds, regardless of the oxidation state, is not known to have a binding energy of less than 40eV for its 3d peak based on currently documented compounds (Moulder et al., 1995). Sample 2 was the residue from the plain cyanide leach after 3 runs and reduced Pt and As leaching suggesting a change in surface akin to gradual passivation (Figure 57). In fact the peak for Sample 2 is closer to the 41.3-41.6 eV of As^0 than the other 3 samples. Perhaps this shift from the known range

represents an intermediate or transitional state of As compound in which As is in between negative and positive oxidation states. This new state of As may actually completely change the structure of the sperrylite at the surface resulting in a form of sperrylite that is difficult to leach, which is why in the BSTR experiments some Pt leached out and then it stopped i.e. the change is over a period of time. It is further speculated that the new form of sperrylite is of the form $PtAs_{(X)}$ where x is less than 2 since Pt does not change and the part of the As that is in the higher oxidation is most likely leached out.

4.3.3. Mini-columns

Figure 69 shows the Pt and As leach curves plotted as cumulative amounts in mg extracted versus time. This form of representing the data was chosen over percentage extraction because the percentage extraction was low, amounting to 7-8% extraction for each element. Similar to the BSTR experiments the rates of Pt and As leaching appear similar and follow an almost identical pattern. Even the quantities leached were identical. The leaching pattern is similar to the ones seen in BSTR experiments in that the leaching reduces after sometime. This is observed on the graphs after day 8. Based on the discussion on the last set of BSTR experiments attributed to Figure 65, it was thought that perhaps the extent of leaching in the mini-columns could be improved by subjecting the bed of sperrylite to a wash process similar to the vacuum filtration of the sperrylite samples in the BSTR experiments. Rather than emptying the columns, all traces of the leach solution was pumped out and the distilled water was pumped through for 24 hours at a rate of 2 L/day. This was done on day 18. Then leaching with the leaching solution (cyanide-ferricyanide combination) re-commenced with the first sample point being at day 19.

From Figure 69 the effect of the wash with distilled water can be seen immediately after day 18. From day 19 the jump in the rate and extent of extraction is significant compared to what it was from day 8 to day 18. This does add some credibility to the theory that passivation occurs due to the formation of unknown reaction products which deposit on the surface initially and not due to a change in the surface structure. These products hinder further leaching but can be washed off to allow for continued and improved leaching. It is further postulated that these products could be formed either from reaction with trace elements (Cu, Si and S) or more likely due to the presence of ferricyanide which may react with Pt or the trace elements. It may be possible that once ferricyanide has been reduced to ferrocyanide it complexes with some

elements in solution and adsorbs to the mineral surface. Further proof that the cause of passivation is due to the deposition/formation of reaction products at the surface of the mineral and not a change in the mineral surface due to a lack of As oxidation can be seen in Table 34 from the XPS analysis. Sample 3 which was from the end of the 1st run of the cyanide-ferricyanide leach after the curve levelled off completely has less As at the surface than Sample 2 which was from the end 3rd run of cyanide-only leaching when passivation had set in. This means that Sample 3 was passivated. In this instance however, it appears the passivation starts to occur again after day 30 (Figure 69). This may be because merely pumping distilled water through the sperrylite bed was not as aggressive a wash as the vacuum filtration in the BSTR experiments, and hence the passivation layer may not be completely removed.

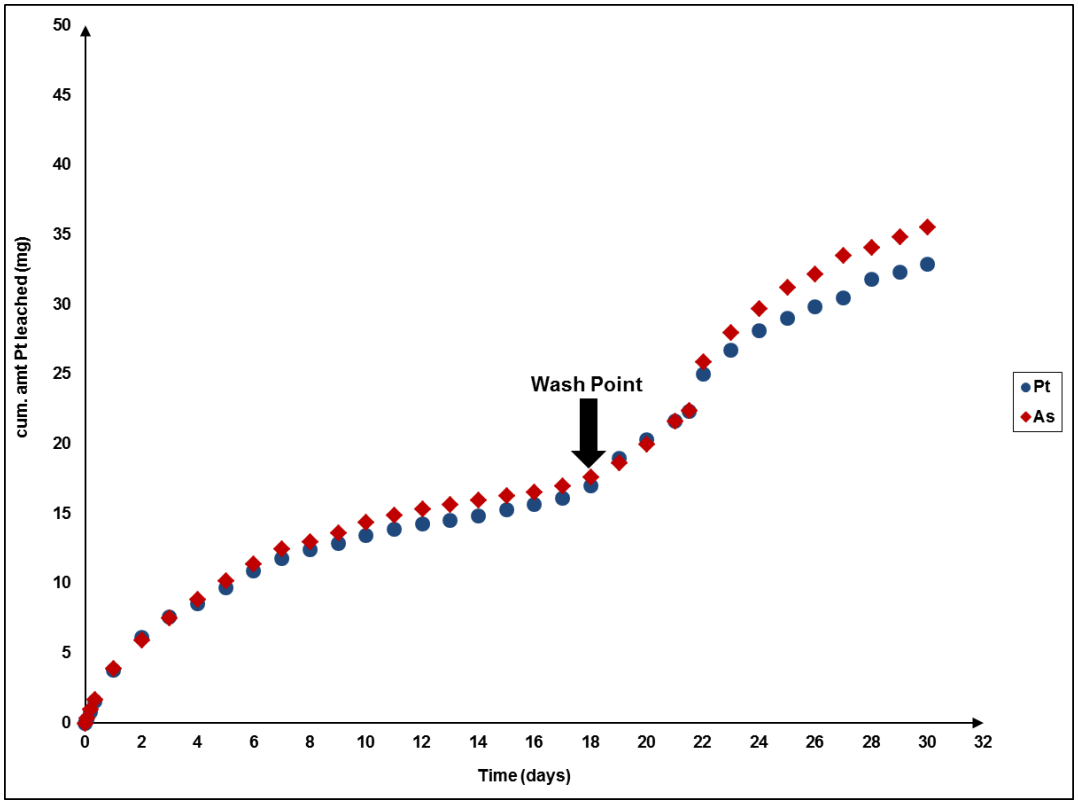

Figure 69: Pt and As leaching curves for mini-column experiment. 5 g/L NaCN, 5 g/L $K_3[Fe(CN)_6]$, 500 mg sperrylite, 50°C, feed rate-2 L/day, pH 10.3-10.6

4.3.4. Electrochemistry Study

Figure 70 shows the results for the OCP experiments on a 5 g/L solution of NaCN at 40°C after just over 17 hours. The potential (vs SCE) starts at -180 mV and -160 mV for the repeat and in both cases drops over time, indicative of gradual establishment of a cathodic reaction balancing

an anodic dissolution of sperrylite, thus shifting the mixed potential. But after an initially rapid decline the potential seems to level off towards -220 mV in both cases perhaps indicating the establishment of a steady state between anodic and cathodic reactions. In this case the cathodic reaction would be the reduction of oxygen, whatever small amount was present in the system. But as noted from the BSTR experiments (section 4.3.1.), oxygen is a poor oxidant hence the poor leaching of Pt in a cyanide-only system due to poor As oxidation. The negative potential is indicative of the minor extent of the anodic reaction. The anodic reaction being the As oxidation which results in the leaching of Pt from sperrylite.

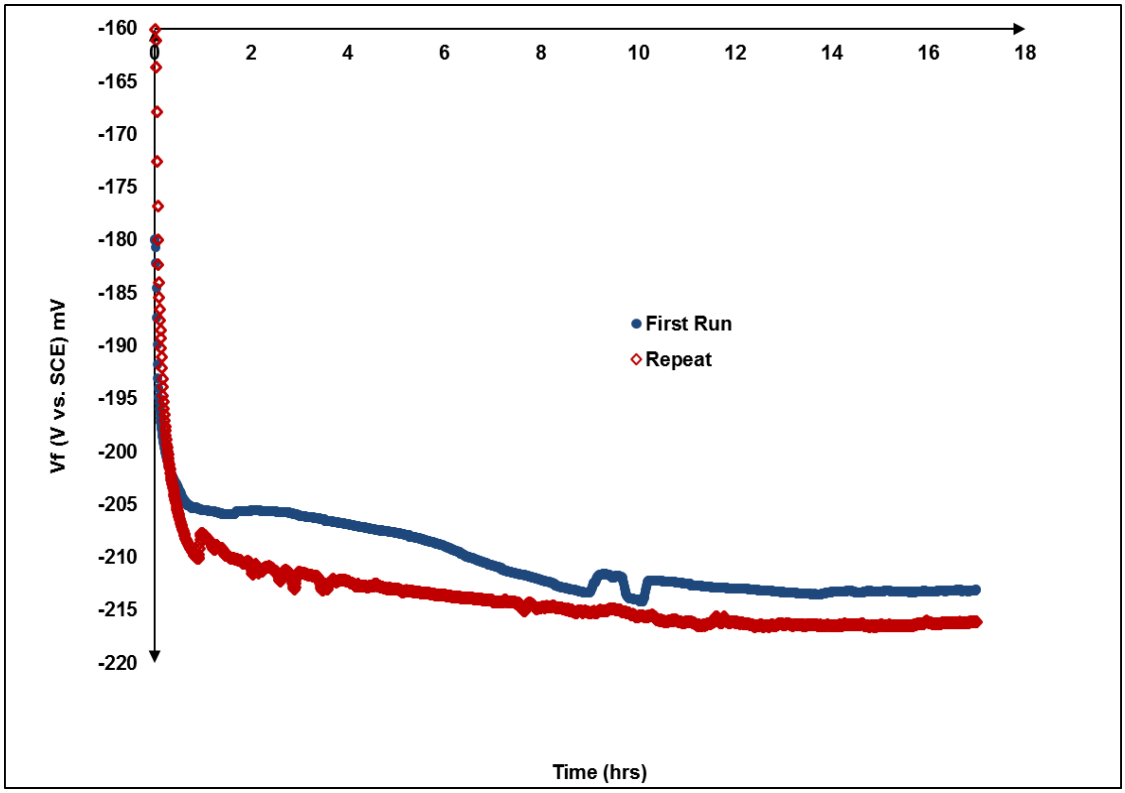

Figure 70: OCP experiments for 5 g/L NaCN solution at 40°C for 17 hours

The experiments were repeated with identical conditions with the exception that varying amounts of $K_3[Fe(CN)_6]$ were added to the solution, more specifically 0.5, 5 and 25 g/L (Figure 71). All the curves had an identical shape and started with a potential of 205 mV indicating that the different quantities of ferricyanide used do not have an effect on the reaction. Analysing Figure 70 and Figure 71 it can be said that the higher potentials of the cyanide-ferricyanide systems as compared to those of the cyanide-only experiments are a sign of the higher extent of the anodic reaction in the cyanide-ferricyanide systems. This is due to the reduction of ferricyanide which creates a cathodic reaction that counterbalances with the anodic reaction

(oxidation of As) at much higher rates. Correlating these results with those from the BSTR experiments of section 4.3.1 specifically Figure 49, it shows that the ferricyanide creates the mixed (reaction) potential needed for the improved leaching of Pt from sperrylite compared to the other systems when only cyanide (whether in the presence of oxygen or compressed air or neither) is used.

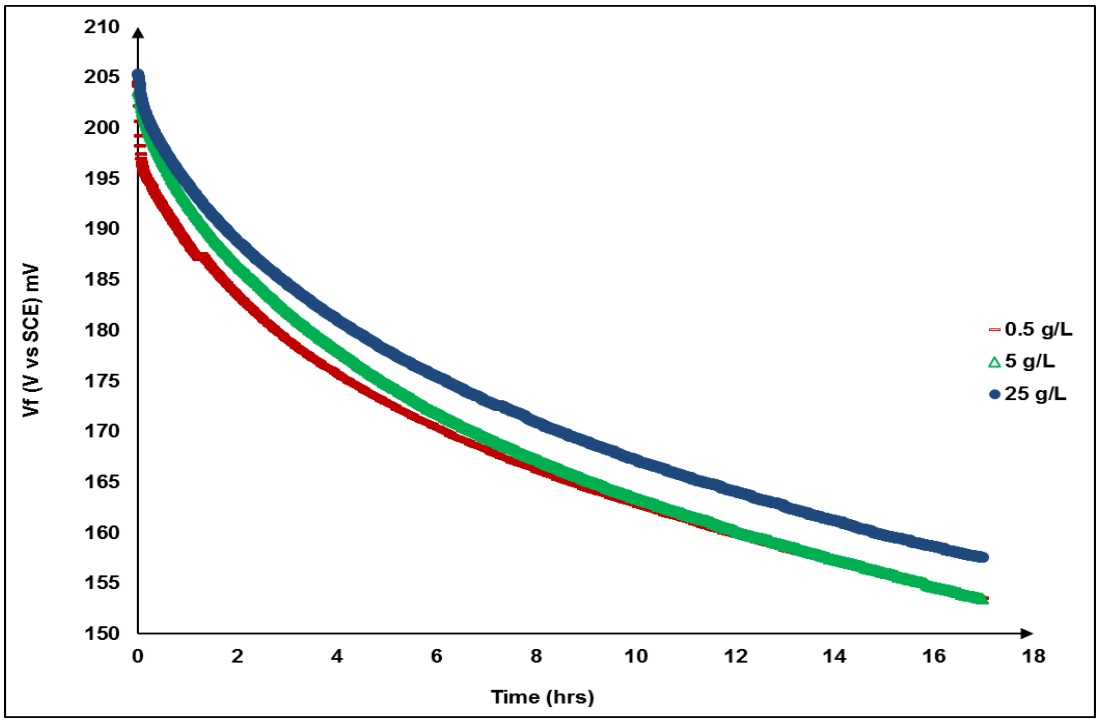

Figure 71: OCP experiment for 5 g/L NaCN and 0.5, 5 and 25 g/L $K_3[Fe(CN)_6]$ solution at 40°C for 17 hours

For the cyclic voltammetry experiments the voltage was increased from the initial mixed potential to 450 mV (first forward sweep-dot marker) then decreased to -330 mV (backward sweep-dot marker) and increased again to 450 mV (second forward sweep-diamond marker with no fill). The pattern in Figure 72 for the cyanide experiment is such that at higher potentials an anodic reaction is supported, but when the potential is reduced, as expected the current drops to zero indicating no cathodic reaction. But when the voltage is increased again on the reverse sweep, the current starts to increase and this happens in the 160-180 mV range, which is the equivalent but opposite of the initial electrode potential. It continues to increase but not as high as during the first forward sweep as seen from the red curve. This is likely because there was no cathodic reaction to produce cathodic products that are re-oxidised during the forward sweep to boost the current to initial or higher levels. The first forward sweep shows no signs of passivation as seen in the cyanide-only BSTR experiments where the amount of Pt leached

generally reduced over time regardless of the introduction of fresh solution (Figure 57 and Figure 58).

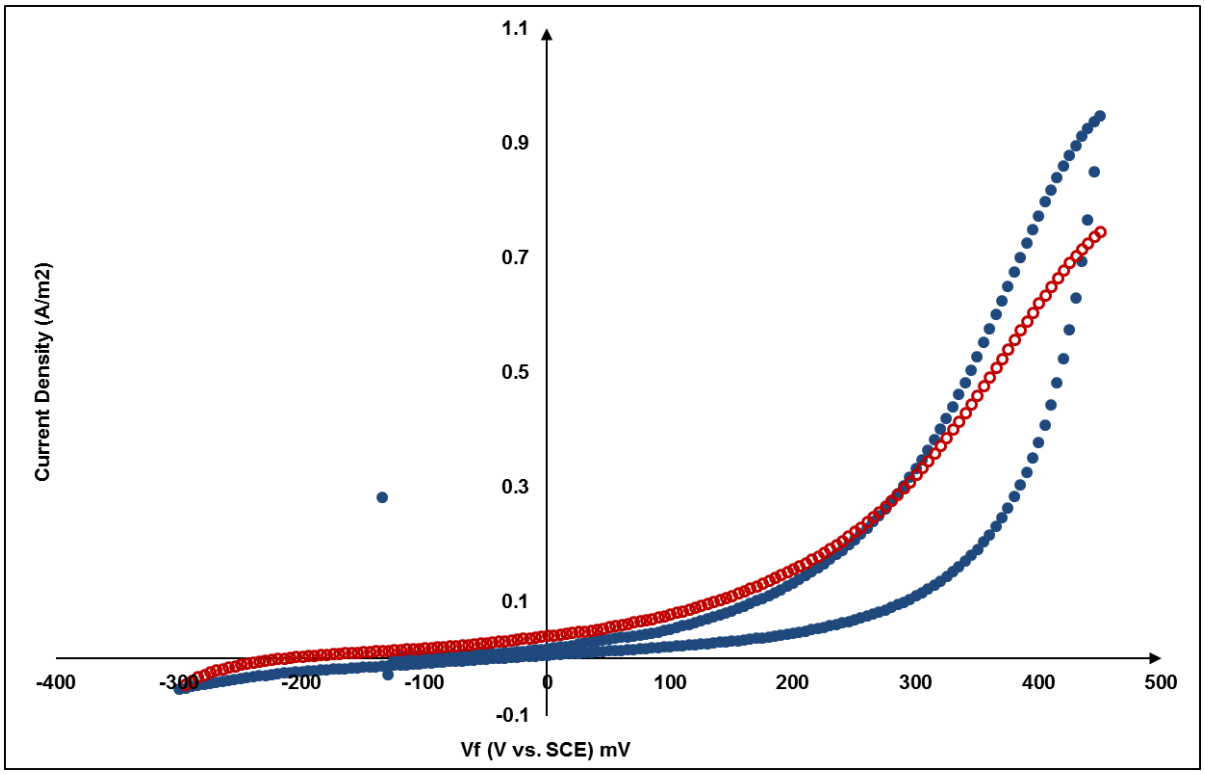

Figure 72: Cyclic voltammogram for sperrylite in 5 g/L NaCN at 40°C between 450mV and -300mV

When ferricyanide is added to the system (Figure 73, Figure 74 and Figure 75) we see much higher anodic currents generated, specifically for the 5 and 25 g/L experiments, than in the cyanide-only experiment; an indication of increased oxidation activity. In all experiments an increase in anodic current is observed with increase in voltage, but in the 0.5 g/L experiment it appears the increase is still ongoing as compared to the 5 and 25 g/L experiments where the currents appear to be approaching the limiting current. This is the current which is independent of potential and is determined by the speed at which oxidizing species can be transported to the electrode surface. This in turn depends on the convection conditions at the electrode surface which are controlled by the rotation speed of the electrode (Power and Ritchie, n.d.). In this case it may be due to a build-up of unknown reaction products first discussed in 4.3.3. Whatever the cause it limits but does not stop the As oxidation. Perhaps the larger amounts of ferricyanide in the 5 and 25 g/L experiments help reach this limiting current faster than in the 0.5 g/L experiment.

This was followed by an expected drop in current with decrease in voltage and it proceeds to go to negative (cathodic) currents which are an indication of the reduction of ferricyanide to ferrocyanide. When the potential is increased again, an increase in current (red curve) is observed and it is slightly higher than the current from the first sweep in all three cases (0.5, 5 and 25 g/L $K_3[Fe(CN)_6]$). This may be an indication of an improved/increased rate of anodic reaction or perhaps it may just be oxidation of some of the cathodic products (ferrocyanide) resulting in an added boost in current. Relating these results to the results of the BSTR experiments (section 4.3.1.), in which the cyanide/ferricyanide system produced significantly better Pt extraction than the cyanide only system. It is evident from the presence of cathodic curves in the cyanide/ferricyanide systems show that it is a redox reaction. By contrast, in the cyanide-only system no cathodic reaction took place and the higher anodic currents in the cyanide/ferricyanide systems are an indication of higher rates of As oxidation in these systems than the cyanide only system.

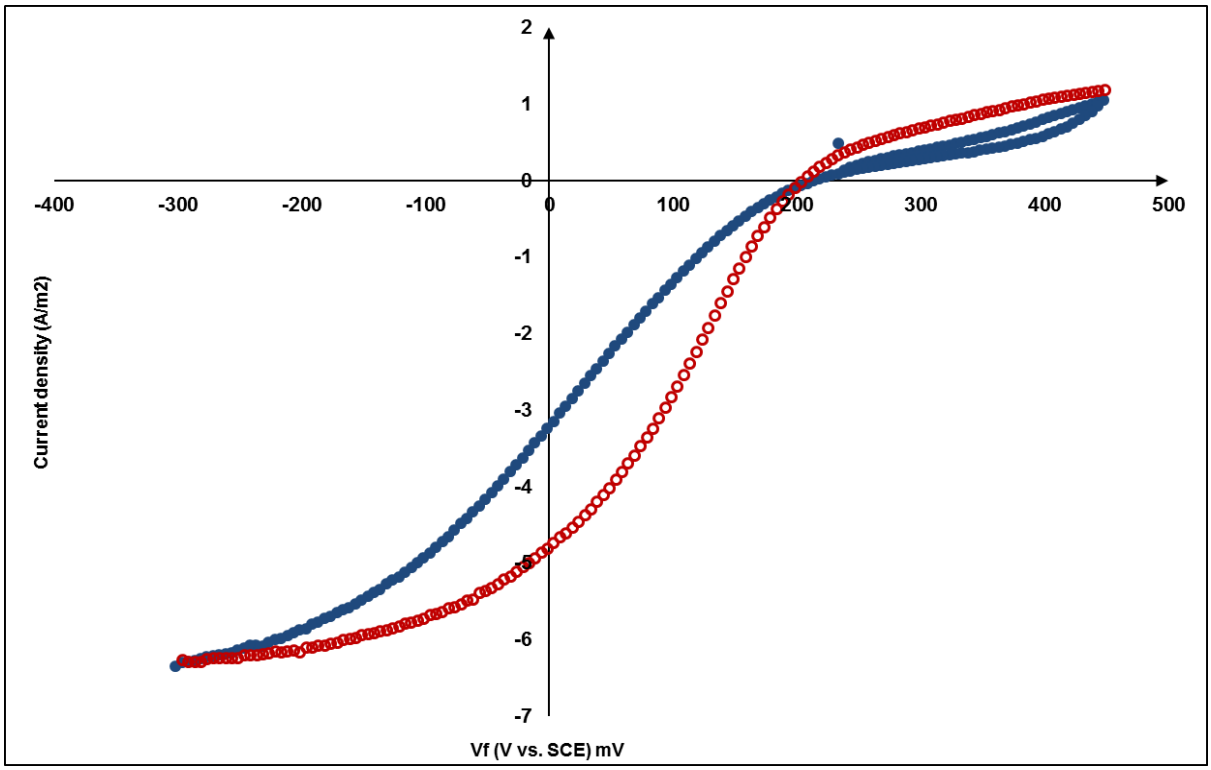

Figure 73: Cyclic voltammogram for sperrylite in 5 g/L NaCN and 0.5 g/L $K_3[Fe(CN)_6]$ at 40°C between 450mV and -300mV

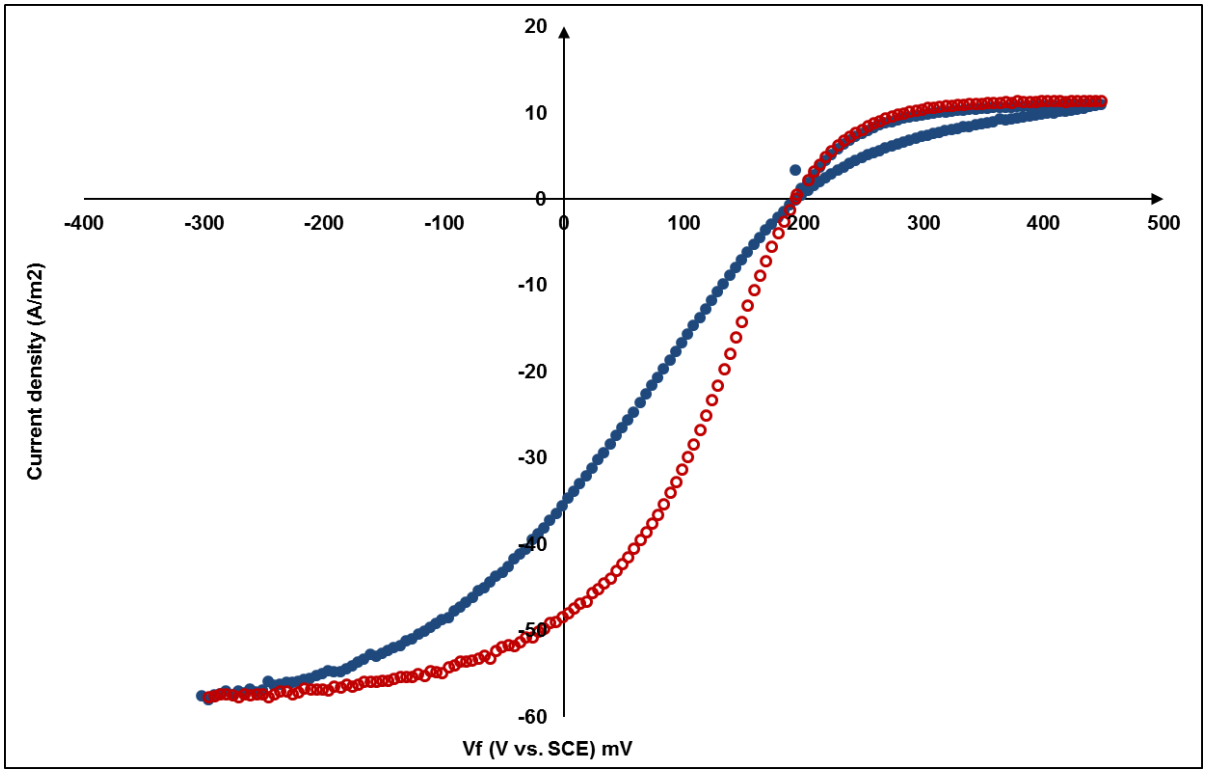

Figure 74: Cyclic voltammogram for sperrylite in 5 g/L NaCN and 5 g/L $K_3[Fe(CN)_6]$ at 40°C between 450mV and -300mV

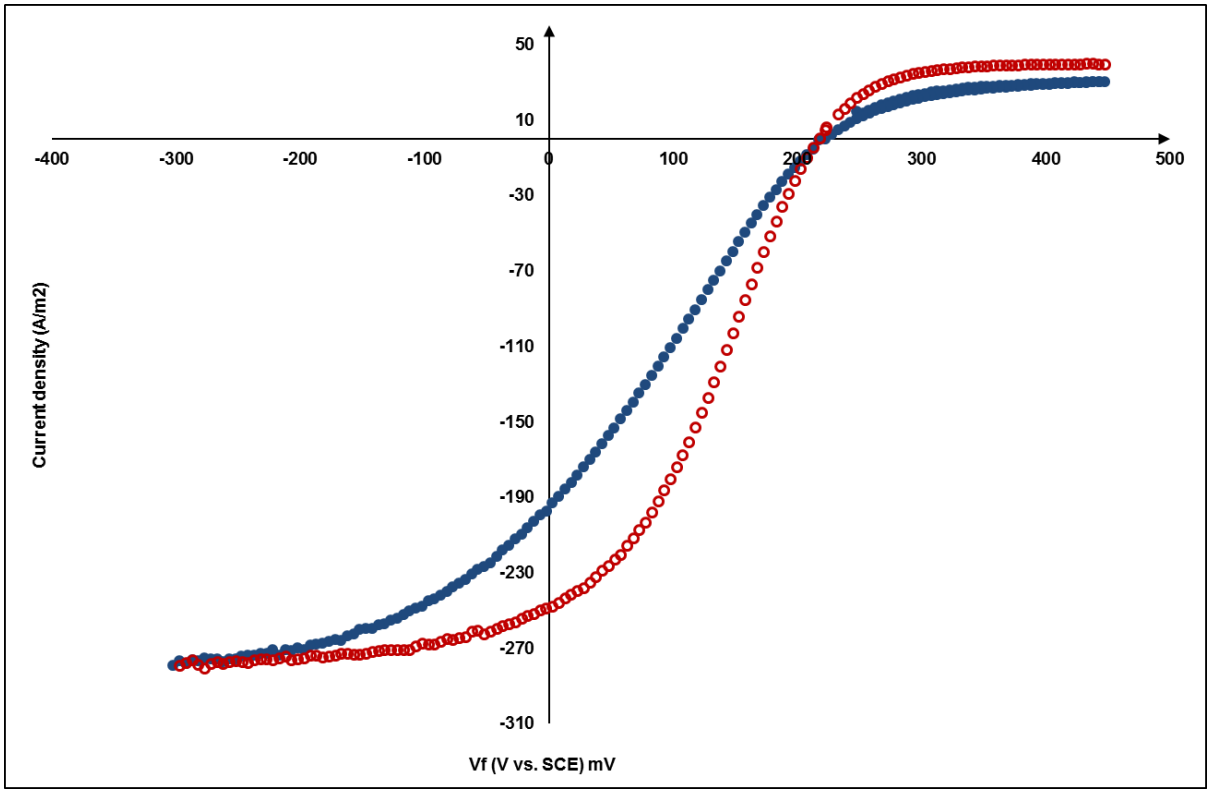

Figure 75: Cyclic voltammogram for sperrylite in 5 g/L NaCN and 25 g/L $K_3[Fe(CN)_6]$ at 40°C between 450mV and -300mV

The experiments were repeated but the forward sweep limit was increased from 450 to 600 mV, and the backward sweep limited to 100 mV as the cathodic reaction was no longer the primary focus. In Figure 76 the current increases with voltage and reaches a maximum or peak anodic current at a potential of 470 mV after which it starts to drop. This drop can be attributed to a hindrance in the rate at which the oxidising species are reaching the electrode which in turn may be caused by gradual passivation of the surface. In the backward sweep the current declines as with the previous cyanide-only experiment and in the forward sweep the current only begins to increase noticeably after 400 mV, unlike the previous experiment where it increased much earlier at around 160-180 mV after the cathodic episode. The increase in current is also much less than what was observed in the previous experiment. Since the potential was not taken into the net cathodic region there were no cathodic products to re-oxidise and provide a boost in current. But even in the first cyanide-only experiment (Figure 72) when the reaction was taken to a negative potential no cathodic reaction took place. Thus the much lower current generated in this case may be due to both gradual passivation of the crystal surface and lack of cathodic products to re-oxidise.

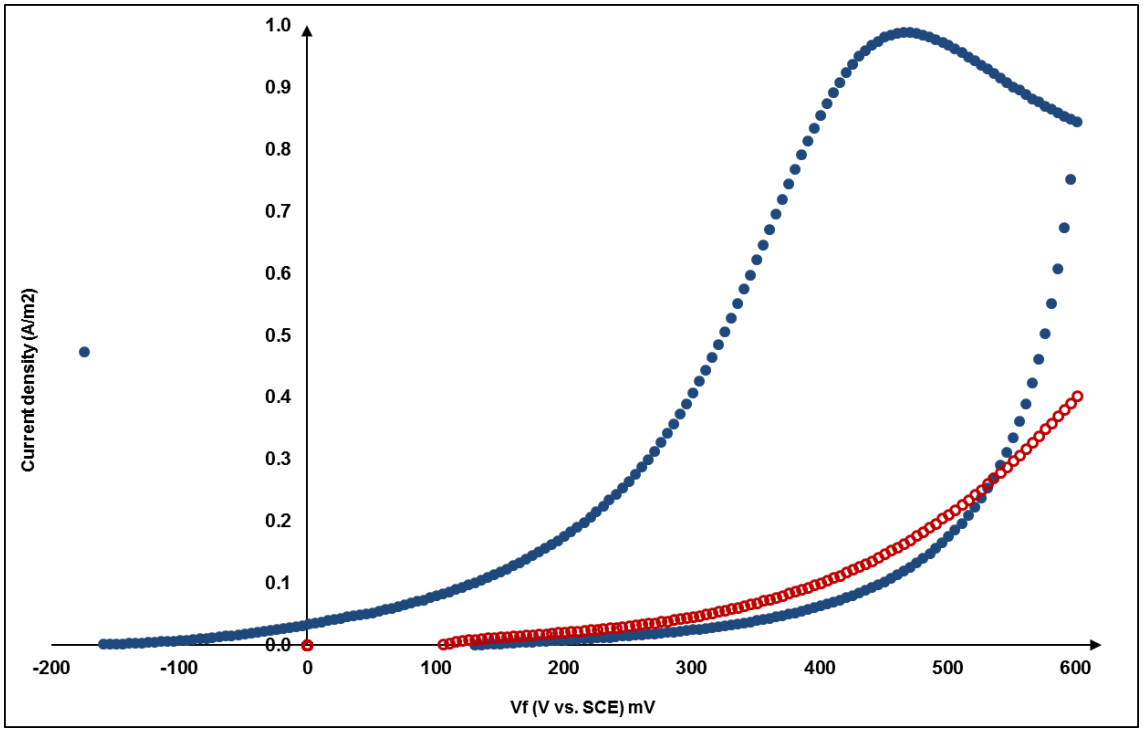

Figure 76: Cyclic voltammogram for sperrylite in 5 g/L NaCN at 40°C between 100mV and 600mV

Identical experiments were conducted for systems with 5 and 25 g/L of $K_3[Fe(CN)_6]$ added to the 5 g/L NaCN. In Figure 77 it can be seen that an increase in voltage lead to an increase on

current as expected, but at around 450-470 mV a maximum was reached before a gradual decrease in current was observed similar to what was observed in the cyanide experiment (Figure 76). This effect may be similar to the effect observed in the cyanide/ferricyanide BSTR experiments (Figure 55 and Figure 56) in which leaching stopped after some time, appearing to have been halted either by passivation or an equilibrium constraint. The backward sweep saw a decrease in current going below 0 A again an indication of the cathodic reaction of ferricyanide being reduced to ferrocyanide. The second forward sweep saw the current rise but not equal or go beyond that of the initial forward sweep as seen in the previous experiment where the potential went up to 400 mV (Figure 74). However the curve appears to be still increasing and may reach an anodic current peak over a longer time period and higher potential. This resistance may be due to passivation.

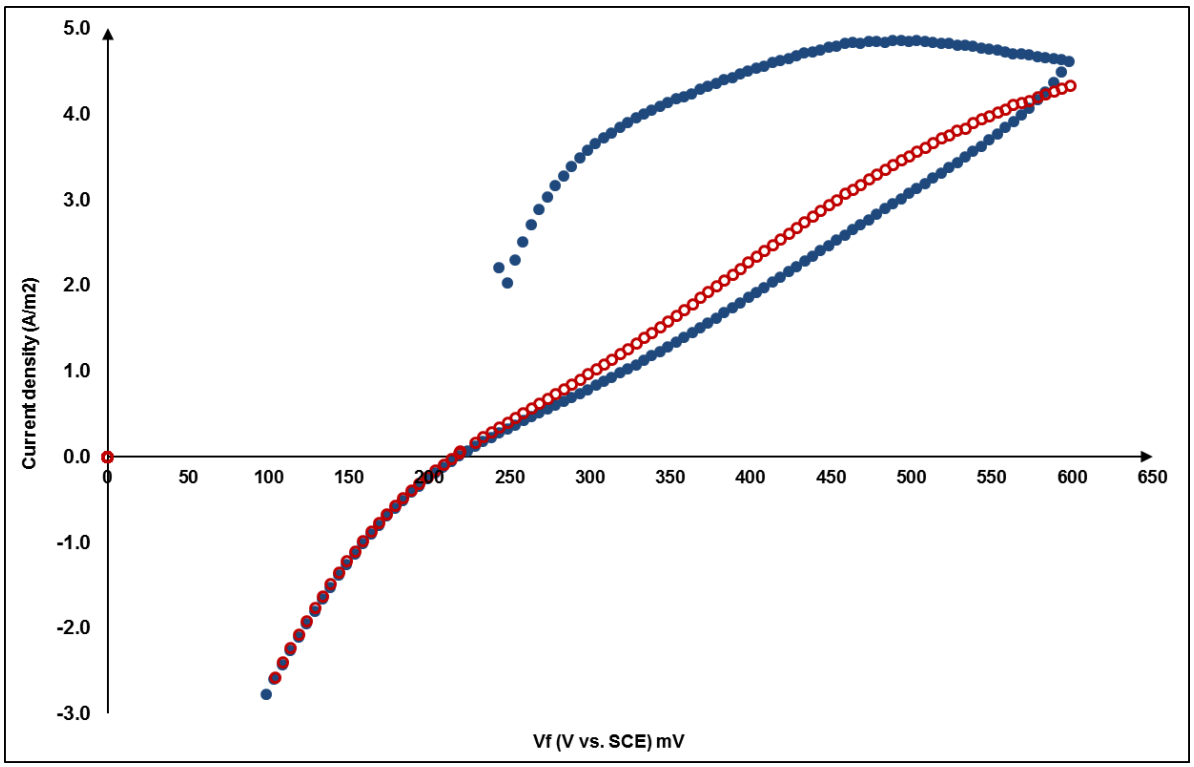

Figure 77: Cyclic voltammogram for sperrylite in 5 g/L NaCN and 5 g/L $K_3[Fe(CN)_6]$ at 40°C between 100mV and 600mV

The voltammogram for the 25 g/L system (Figure 78) on closer examination has an identical pattern to Figure 77, with the exception that in the forward sweep the curve is still increasing and hence will approach peak anodic current at a potential slight past 600 mV. In the backward sweep the current eventually drops below 0 A, but in the second forward sweep unlike the 5 g/L system, the current achieved is higher than the first forward sweep but also looks to be

approaching a peak anodic current just after 600 mV. The cyclic voltammetry experiments with the larger quantities of ferricyanide namely 25 g/L (Figure 75 and Figure 78) produced much higher anodic currents than the ones with less, 5 g/L (Figure 74 and Figure 77). By the second hypothesis these higher anodic currents should be an indication of higher As oxidation and hence increased Pt leaching; but Figure 52 for the cyanide-ferricyanide BSTR experiments shows that this is not the case since the 25 g/L test leached far less Pt than the 5 g/L test. It is possible that the excess ferricyanide simply oxidises the As already present in solution to its highest oxidation state of +5, and does not oxidise the As in the sperrylite hence the much higher anodic currents but no resultant higher leaching of Pt. Additionally, the excess ferricyanide may also oxidise Pt in solution to its highest state of +6 which may not complex with cyanide as well as the states of +2 and +4. This would also contribute to the higher anodic currents; hence the 25 g/L test leaches less Pt than the other tests with less ferricyanide (Figure 52).

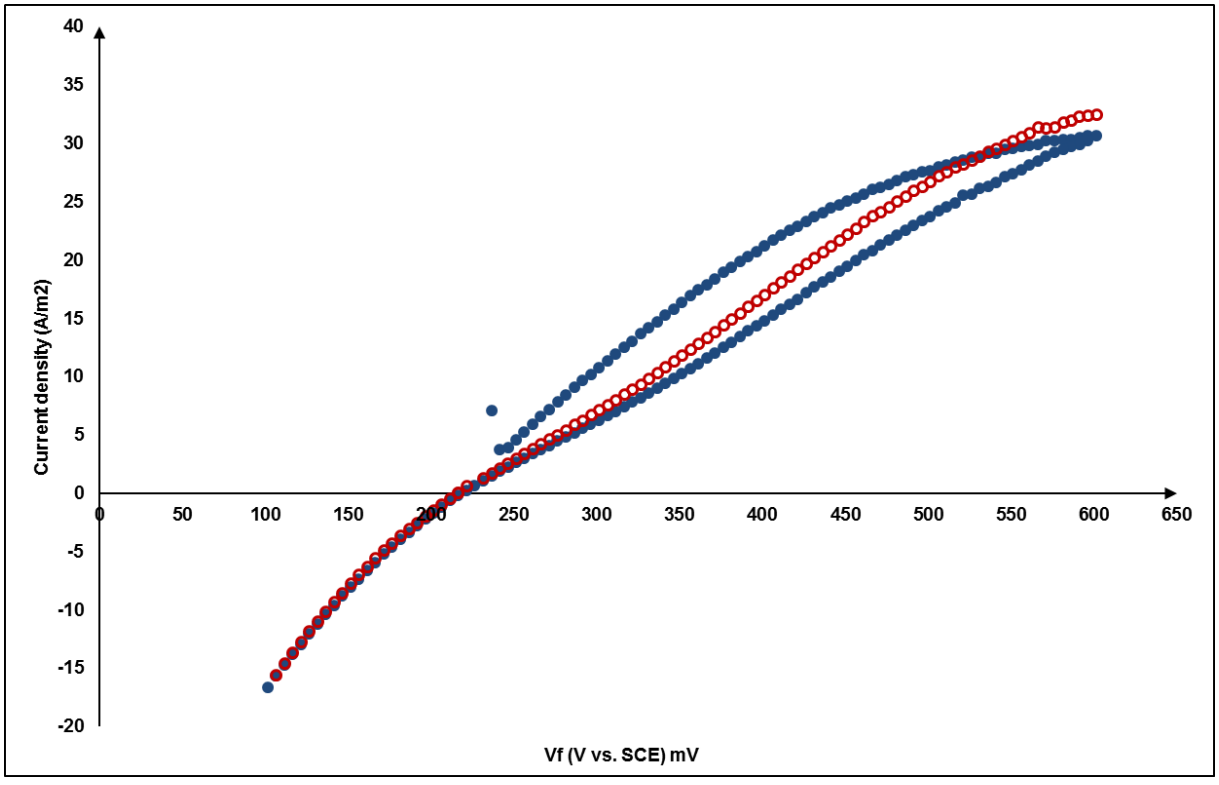

Figure 78: Cyclic voltammogram for sperrylite in 5 g/L NaCN and 25 g/L $K_3[Fe(CN)_6]$ at 40°C between 100mV and 600mV

It should be noted that technically As^{3+} could act as a reducing agent to Pt^{2+} taking it to Pt^{+}. However, if this reaction does occur in this system then it is most likely a minor side reaction.

These ions have to go into solution first and this is achieved by the ferricyanide which has been shown to be the main driving force for this to happen. Then the reduction has to occur before the Pt^{2+} complexes with the cyanide. Additionally, the cyclic voltammetry experiment with cyanide solution and sperrylite only would have had a reduction curve but it didn't, hence this reaction doesn't happen or is insignificant. Additionally, passivation should produce very characteristic current density - potential curves, and standard potentials and also Eh-pH diagrams should be used in a discussion of these results. But in the absence of this data for the Pt-cyanide system, these tools could not be used in the discussion. Further, although standard potentials for oxidation of As from +3 to +5 are available as well as Eh-pH diagrams, the main reaction involves the oxidation of As from the lower states. For this, standard potentials and Eh-pH diagrams are not available.

From the cyclic voltammetry experiments for both cyanide and cyanide/ferricyanide systems, it was observed that the rate of reaction seemed to be highest at around 380 mV. Thus a chronoamperometry experiment was run at 380 mV for 2 days with the hope of achieving high enough dissolution of As in solution to measure confidently and therefore use the Faraday equation to calculate the amount of electrons transferred and thus have some more understanding of the leaching stoichiometry. In this experiment only cyanide solution was used without ferricyanide. Setting and fixing the potential at 380 mV, with the aid of the Pt wire (counter electrode) would in theory recreate the conditions that the ferricyanide facilitates to encourage oxidation of As and improved Pt leaching.

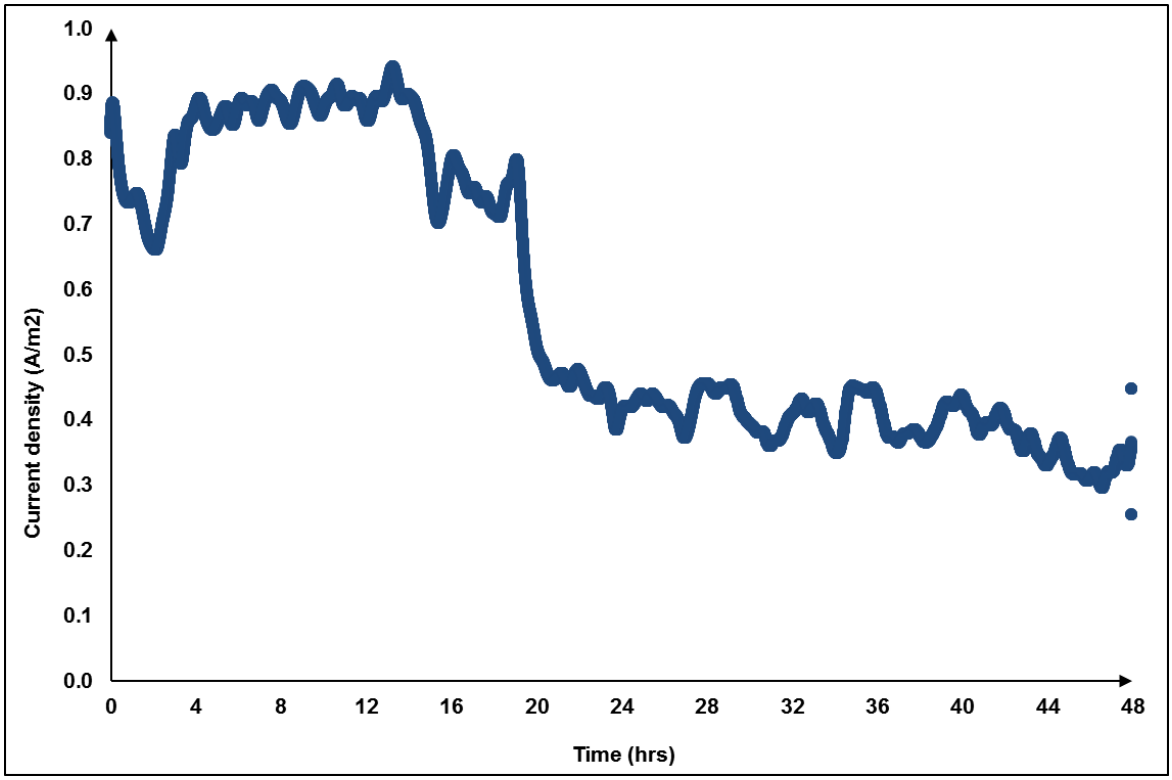

Figure 79: Chronoamperometry for 5 g/L NaCN running at 380 mV at 40C for 2 days

Figure 79 shows the current versus time curve from the experiment. Towards the end of the first day the current drops suddenly again pointing towards passivation and a decrease in the rate of As oxidation, although in this case the onset was sudden and not gradual. It is also noted that the current profile remains very erratic with fluctuations of as much as 20% about the average. The plot in Figure 79 also shows a sudden drop in current after 24 hours which is consistent with all the cyanide-ferricyanide BSTR experiments where the leach curves levelled off at 24 hours. Unfortunately even after running for 2 days the levels of Pt and As in solution were not accurately detectable by ICP-OES. These low levels are not surprising given the extremely low currents generated in all the electrochemistry experiments from the onset. Without this information it was not possible to proceed with calculating the electron transfer of the reaction. This also prevented the plotting of Tafel slopes.

It is acknowledged that there are some studies (Arena et al., 2016; Olvera et al., 2015; Yang et al., 2015; Khoshkhoo et al., 2014) that have used electrochemistry and XPS to explain the phenomenon of passivation in chalcopyrite leaching. Although passivation also occurs in chalcopyrite leaching it is not a similar system to the one explored in this study. It is a sulphide mineral in acidic media and to date there are actually different theories on the cause of this

passivation with no widely accepted consensus. That is why a comparison was not made between those studies and this study.

4.4. Conclusion: Sperrylite Leaching

Based on the results of the BSTR experiments on sperrylite in cyanide solution, the slow leaching of sperrylite in cyanide can be attributed to a form of passivation. This was observed in tests in which fresh solution was applied when the leaching of Pt levelled off, and with each fresh application less Pt was leached (Figure 57 and Figure 58), pointing towards passivation. This was further confirmed by the results of the cyclic voltammetry experiment using a sperrylite electrode in cyanide solutions. Although not conclusive, the drop in current at the potential of 470 mv in this voltammogram (Figure 76) supports the occurrence of passivation. Arsenic in sperrylite is in a mixed oxidation state resulting in it having positive and negative oxidation sates. The part of the As which is in the lower (negative) oxidation state is the most insoluble form of As (Anderson, 2010; Vladmir and Moran, 2006). Combined with the absence of enough oxidant (oxygen, air, or any suitable oxidant) to oxidise it to a higher oxidation (and hence more soluble) state, an eventual build-up of As results at the surface of the mineral which acts as a passivation layer causing slow leaching of Pt. XPS analysis further suggested that the As remaining behind was in an oxidation state close to 0 (Figure 68) suggesting that in a cyanide-only system the limited oxidant does not completely oxidise As but leaves it in an intermediate/transitional oxidation state. Further this may change the entire sperrylite structure at the surface forming a less cyanide soluble compound of the form $PtAs_{(X)}$ where x is less than 2. Additionally, through XPS analysis, peaks from test samples were compared with the peaks from similar studies and pointed to Pt being in the +2 state and As have a multiple oxidation states resulting in a net valence of -1. BSTR experiments also showed that the amount of cyanide present had almost no effect on the amount of Pt leached.

Identical BSTR experiments conducted with the addition of ferricyanide as an oxidant conclusively proved the second hypothesis. The presence of ferricyanide significantly improved the leaching of Pt and As, leaching 12-16 times more than what was leached in the experiments that used only cyanide solution, even with compressed air or pure oxygen sparged into the solution. The tests clearly showed that ferricyanide acted as an oxidant in conjunction with free cyanide but on its own was ineffective. The presence of air or pure oxygen did not

significantly increase the amounts of Pt and As leached in the cyanide-ferricyanide experiments. Further, the BSTR experiments showed that certain amounts of $K_3[Fe(CN)_6]$ between 1 and 5 g/L were more effective in leaching Pt, while a concentration of less than 1 and more than 5 resulted in lower Pt extractions. This observation combined with cyclic voltammetry experiments with 25 g/L $K_3[Fe(CN)_6]$, suggested that perhaps higher concentrations of ferricyanide only served to oxidise As in solution and not in sperrylite and possibly Pt to an oxidation state at which it could not combine with cyanide, resulting in reduced leaching.

Samples of sperrylite that were leached in cyanide and the cyanide-ferricyanide combination were analysed by XPS and the comparison showed that As:Pt ratio at the surface of the samples leached with cyanide was greater than that at the surface of the samples leached with the cyanide-ferricyanide system. This further supports the first hypothesis that the slow leaching of Pt from sperrylite in cyanide is due to passivation due to As build-up at the surface.

In the chronoamperometry experiments the quantities of Pt and As leached were not confidently detectable through ICPS, hence the exact amount of electrons transferred in the process could not be determined. Based on what is known in the literature about sperrylite and the results from the experiments, the mechanism for the successful sperrylite leaching is described as follows:

The ferricyanide oxidises the part of the As in sperrylite that is in a lower oxidation state to a higher oxidation state thus breaking the chemical bonds of the sperrylite to release Pt into solution to be complexed with cyanide. In doing so the ferricyanide is reduced to ferrocyanide, representing a cathodic reaction to the anodic reaction of the As oxidation. The part of the As that is in lower oxidation state is most likely in the -3 state. This is the most common lower state of the As and is most likely oxidised to +3. The whole mechanism is represented by the following equations:

$$As^{3-} \rightarrow As^{3+} + 6e \quad (4.1)$$

$$Fe(CN)_6^{3-} + e \rightarrow Fe(CN)_6^{4-} \quad (4.2)$$

$$Pt^{2+} + 4CN^{-} \rightarrow PtCN_4^{2-} \quad (4.3)$$

The results show that a combination of cyanide-ferricyanide is a potential solution to the low Pt extractions using cyanide in Platreef ore heap leaching. It must be evaluated using laboratory column test work prior to pilot scale test work. However, a phenomenon which is yet to be fully explained in the cyanide-ferricyanide system is the initial passivation observed in both BSTR and mini-column tests. At present, the passivation is believed to be a deposition of unknown reaction products that are adsorbed at the surface of the sperrylite. Through a water wash of the sperrylite sample, the passivation layer was removed and this resulted in improved leaching of Pt but with signs that the passivation would occur but at a much later time than the previous occurrence. The passivation was observed again in the mini-column experiment where the washing was not as thorough as the BSTR experiments. This may point to the need to use a form of intermittent leaching, in which the use of the leaching solution and water are applied alternatively to achieve maximum extraction of Pt from the sperrylite component of the Platreef ore. This would require a reserve of water to be used over and over again for washing only.

5. Chapter 5: Conclusion

This study, through lab-scale column test work, has shown that cyanide-based heap leaching of PGMs from Platreef ore is a viable technology to further explore at pilot scale. The high extractions of 96.5-66.9% Cu, 83.4-56.6% Ni and 61.2-35.8% Co, 94.3-79.3% Pd and 92.3-80.6% Au combined with the more moderate 59.8-41.0% Pt extractions mean that it may still be viable given the relatively lower capital and operating costs of heap leaching as compared to conventional technologies. Heap leaching is a technology that is not currently used in the PGM industry and therefore unfamiliarity may present itself as an economic risk. However it is a decades-old technology in the copper and gold industry and hence there is a wealth of information on best practices regarding operations, environmental and risk management, especially around the use of cyanide. This information can be tapped into to reduce the risk of initial failure. Cyanide-based heap leaching thus presents a lower cost, lower energy intensive and environmentally manageable option to conventional methods in the face of rising operational costs in the PGM industry.

The use of high temperature bioleaching to pre-treat the ore has shown to be a critical step in extracting valuable BMs, and to oxidize sulphur to prevent high consumption of cyanide via conversion to thiocyanate. Critical to evaluating a new leaching technology is the mineralogy of the ore to be treated. Test work on the Platreef materials has shown that heap leaching of PGM ores differs from Au and Cu heap leaching. Pt which is the most valuable metal of the PGMs, and is usually the most abundant does not occur as a single mineral in PGM ores, but as variety and in varying quantities, unlike in Au and Cu ores that are presently heap leached. In Au and Cu heap leaching the metals are present as mostly one primary mineral which is amenable to the chemical treatment or not, making the decision to process the ore via heap leaching more straight forward. But with the Platreef ore, the test work and analyses has shown that the different Pt minerals leach at different rates in cyanide and hence the success of the process is dependent on the vast majority being cyanide soluble at a rate which is commercially viable. This is a critical factor in applying this technology to other PGM ores and materials locally and globally.

Although the presence of sperrylite has proven a challenge to heap leaching Platreef ore, there are other significant PGM ore bodies that do not have these levels of sperrylite and hence have

the potential to yield higher Pt extractions through cyanide heap leaching. Further, there are a number of secondary or waste materials produced by the conventional process such as tailings which may yield value through heap leaching by coating them on support media. Surface ore bodies that have been oxidised resulting in low sulphide content and hence poor flotation performance might also be processed by direct cyanide heap leaching. There is no doubt left that the two-stage heap leaching process (as a whole or through direct cyanide leaching) presents options for the PGM industry to potential exploit a number of unexplored opportunities for increased production and growth with the addition of new producers.

An investigation using samples of pure sperrylite mineral showed that the addition of ferricyanide to a cyanide leach significantly improves the leaching of Pt from sperrylite thus presenting a possible route to improve Pt extractions in heap leaching. However it was observed that initially the leaching was inhibited by some form of passivation suspected to be products of the reaction. Through a suitable wash of the material this layer can be removed allowing the leaching to proceed with improved results. In practice this would require a reserve of water to be used over and over again for washing only.

It is recommended that further column test work, using a combination of cyanide-ferricyanide, should be conducted prior to pilot testing. A critical matter to be addressed in this is the initial passivation observed in the cyanide-ferricyanide system in both BSTR and the mini-column experiments. This phenomenon could signal the need for a form of intermittent leaching in which the use of the leaching solution and water are applied alternatively to achieve maximum extraction of Pt from the sperrylite component of the Platreef ore. Further, if possible BSTR and electrochemical experiments must be conducted in the vicinity of XPS equipment to allow for immediate analyses. XPS analysis in this study was limited to scanning for the elements Pt and As. Future analyses must scan for all elements in the leaching system to give more insight into the cause of passivation in both the cyanide and cyanide-ferricyanide systems.

6. References

Acevedo, F. 2002. “Present and future of bioleaching in developing countries”, Electronic Journal of Biotechnology, ISSN: 0717-3458, Vol.5 No.2, Issue of August 15, 2002.

Acevedo, F. 2000. “The use of reactors in biomining processes”. Electronic Journal of Biotechnology, vol. 3, no. 3.

Adams, M., Lawrence, R., Bratty, M., 2008. “Biogenic sulfide for cyanide recycle and copper recovery in gold–copper ore processing”. Minerals Engineering 21 (6), pp 509–517.

Adams, M., Liddell, K., Holohan, T. 2011. “Hydrometallurgical processing of Platreef flotation concentrate”, Minerals Engineering 24, pp 545-550.

Arena, F.A., Suegama, P.H., Bevilaqua, D., dos Santos, A.L.A, Fugivara, C.S., Benedetti, A.V. 2016. "Simulating the main stages of chalcopyrite leaching and bioleaching in ferrous ions solution: An electrochemical impedance study with a modified carbon paste electrode”, Minerals Engineering, Volume 92, pp 229-241.

Aylmore, M.G., Muir, D.M. 2001. “Thiosulfate leaching of gold-a review”, Minerals Engineering 14, no. 2, pp 135-174.

Andserson, C.G. 2010. “The treatment of arsenic bearing ores, concentrates and materials with alkaline sulfide hydrometallurgy”. Retrieved June 2011 from: http://www.camp-montanatech.net/_Documents/Published/Articles_Papers/the_treatment_of_arsenic_bearing_ores_concentrates_and_materials_with_alkaline_sulfide_hydrometallurgy.pdf.

Aswegen, P.C., Van Niekerk, J., Olivier, W. 2007. “The BIOX™ process for treatment of refractory gold concentrates”, In Rawlings, D.E., Johnson, D.B. (Eds.) 2007. “Biomining”, Springer-Verlag, Berlin, Heidelberg.

Avril, L., Bourgeois, S., Simon, P., Domenichini, B., Zanfoni, N., Herbst, F., Imhoff, L. 2015. “Nanostructured Pt–TiO2 composite thin films obtained by direct liquid injection metal

organic chemical vapor deposition: Control of chemical state by X-ray photoelectron spectroscopy", Thin Solid Films 591, pp 237-244.

Baghalha, M., Khosravian Gh., H., Mortaheb, H.R. 2009. "Kinetics of platinum extraction from spent reforming catalysts in aqua-regia solutions", Hydrometallurgy 95, pp 247-253.

Barratt, D., Sherman, M. 2002. "Factors which influence the selection of comminution circuits". In Mular, A.L., Halbe, D.N., Barratt, D.J. (Eds.) 2002. Minerals Processing Plant design, Practice, and Control-Proceedings. Volume 1, Society for Mining, Metallurgy, and Exploration, Inc. (SME).

Becker, M., Ramonotsi, M., Wiese, J.G. 2014. "Investigation into the mineralogy and flotation performance of oxidised PGM ore". Minerals Engineering 65, pp 24-32

Becker, M., Ramonotsi, M., Petersen, J. 2011. Effect of alteration on the mineralogy and flotation performance of PPM platinum ore. In Broekmans, M.A.T.M. (editor), 10th International Congress for Applied Mineralogy (ICAM), (pp 63-71), Trondheim, Norway.

Bernadis, F.L., Grant, R.A., Sherrington, D.C. 2005. "A review of methods of separation of the platinum group metals through their chloro-complexes", Reactive & Functional Polymers 65, pp. 205-217.

Bharathi, K., Lakshmi, M., Ravindra, P. 2008. "Role of galvanic interaction in selective leaching of nickel from copper flotation concentrate", Advances in Natural and Applied Sciences, vol. 2, issue 2, pp 68-72.

Biswas, J., Jana, R.K., Kumar, V., Dasgupta, P., Bandyopadhyay, M., Sanyal, S.K. 1998. "Hydrometallurgical processing of anode slime for recovery of valuable metals", Environmental and Waste Management, pp 216-224.

Botz, M. 1999. "Overview of cyanide treatment methods". Reprinted with permission of The Gold Institute, 1112 16th Street N.W., Suite 240, Washington, D.C. (USA) 20036.

British Geological Survey. 2009. “Platinum”, retrieved 12 January 2016 from https://www.**bgs**.ac.uk/downloads/start.cfm?id=1401

Bruckard, W.J., McDonald, K.J., McInnes, C.M., Sparrow, G.J., Woodcock, J.T. 1992. “Platinum, palladium, and gold extraction from Coronation Hill ore by cyanidation at elevated temperatures”, Hydrometallurgy 30, pp 211-227.

Bryson, M. 2008. “Review of metallurgical characteristics of Akanani ore”, Mintek restricted presentation, 22 January 2008.

Bruckard, W.J., McDonald, K.J., McInnes, C.M., Sparrow, G.J., Woodcock, J.T. 1992. “Platinum, palladium, and gold extraction from Coronation Hill ore by cyanidation at elevated temperatures.” Hydrometallurgy volume 30, pp 211-227.

Bushell, C.J. 2006. “PGM grains detected by MLA in borehole core samples from Afriore”, Mintek restricted report.

Cabri, L.J. 2002. “The Platinum-Group Minerals”, In Cabri, L.J. (Editor). 2002, “The Geology, Geochemistry, Mineralogy and Mineral Beneficiation of Platinum-Group Elements”, CIM Special Volume 54, Canadian Institute of Mining, Metalurgy and Petroleum, Quebec, Canada.

Cao, Y., Harjanto, S., Shibayama, A., Naitoh, I., Nanami, T., Kasahara, K., Okumura, Y., Fujita, T. 2006. “Kinetic study on the leaching of Pt, Pd and Rh from automotive catalyst residue by using chloride solutions”, Materials Transactions, Vol. 47, No. 8, pp 2015-2024.

Cawthorn, R.G., Hochreiter, R.C. 2000. Global Platinum and Palladium Deposits. In Proceedings, 2nd Bi-Annual World Platinum Congress, p 20.

Chamberlain, P.G., Pojar, M.G. 1984. “Gold and Silver leaching practices in the United States”; Bureau of Mines Information Circular/1984, United States Department of the Interior IC 8969.

Chang-Li, L., Jin-Lan, X., Yang Yi, Y., Zhen-Yuan, N, Xiao-Juan, Z., Lei, Z., Chen-Yan, M., Yi-Dong, Z. 2011. “Characterization of the thermo-reduction process of chalcopyrite at 65 °C by cyclic voltammetry and XANES spectroscopy”, Hydrometallurgy 107 p13-21.

Chaponda, B. 2011. “Effect of operating variables on IsaMill™ performance using platinum bearing ores”. MSc thesis, Department of Chemical Engineering, University of Cape Town.

Chen, J., Huang, K. 2006. “A new technique for extraction of platinum group metals by pressure cyanidation”, Hydrometallurgy in China Journal, Volume 82, Issues 3-4, Pages 164-171.

Cole, S., Joe Ferron, C. 2002. A Review of the Beneficiation and Extractive Metallurgy of the Platinum Group Elements, Highlighting Recent Process Innovations. SGS
Minerals Services Technical Paper 2002-03.

Costa, R. S., Torres, V. M.1997. “Recovery and production of gold and platinum-group metals by using cyanidation under pressure”, Braindex online database, Retrieved online 2 July 2007 from http://www.braindex.com/patent_pdf/

Crundwell F.K., Moats, M.S., Ramachandran, V., Robinson, T.G., Davenport, W.G. 2011. “Extractive metallurgy of nickel, cobalt and platinum-group metals”, Elsevier, Kidlington, Oxford, UK.

De Lange, B., Reinecke, J. 2012. “Prefeasibility of Solar Process Heat for Heap Leaching Process for Lonmin Pty (Ltd)”, Restricted report, Centre for Renewable and Sustainable Energy Studies, Stellenbosch University.

Department: Minerals and Energy, Republic of South Africa. 2003. Platinum-Group Metal Mines in South Africa. Directorate: Mineral Economics (Minerals Bureau).

Desmond, D. P., Atkinson, G. B., Kuczynski, R. J., Walters, L. A. 1991. “High-temperature cyanide leaching of platinum group metals from automobile catalysts-laboratory tests”, Bureau of Mines Report of Investigation, RI 9384, United States Department of the Interior.

Dew, D.W., Van Buuren, C., McEwan, K., Bowker, C. 2000. “Bioleaching of base metal sulphide concentrates: A comparison of high and low temperature bioleaching”, The Journal of The South African Institute of Mining and Metallurgy, vol. 100 no. 7, pp 409-414.

Dew, D.W., Rautenbach, G.F., van Hille, R.P., Davis-Belmar, C.S., Harvey, I.J., Truelove, J.S. 2011. "Method of evaluation and process model evaluation", The Southern Africa Institute of Mining and Metallurgy, International Conference, Percolation leaching: The status globally and in southern Africa, Symposium Series S69, pp. 201-220, 7-9 November 2011.

Dixon, D.G. 2000. "Analysis of heat conservation during copper sulphide heap leaching", Hydrometallurgy, vol. 58, issue 1, pp 27-41.

Dixon, D.G., Petersen, J. 2003. "Comprehensive modelling study of chalcocite column and heap bioleaching", In P.A. Riveros, D. Dixon, D. Dreisinger and J. Menacho, (eds.), Copper 2003-Hydrometallurgy of Copper (Book 2), vol. 6, CIM, 2033, pp 493-516.

Dhawan, N., Safarzadeh, M. S., Miller, J. D., Rajamani, R. K., Moats, M. S. 2012. "Insights into heap leaching technology", SME Annual meeting, Feb. 19 - 22, 2012, Seattle, WA, Preprint 12-119.

Dorfling, C., Akdogan, G., Bradshaw, S.M., Eksteen, J.J. 2010. "Determination of the relative leaching kinetics of Cu, Rh, Ru and Ir during the sulphuric acid pressure leaching of leach residue derived from Ni-Cu converter matte enriched in platinum group metals", Minerals Engineering 24(6), pp 583-589.

Dreisinger, D., 2012. Hydrometallurgical extraction of base, rare, and precious metals from complex and low grade resources. In: XXVI International Mineral Processing Congress (IMPC) 2012 Proceedings/New Delhi, India/24–28 September 2012.

Du Plessis, C. A., Batty, J.D., Dew, D.W. 2007. "Commercial applications of thermophile bioleaching", In Rawlings, D.E., Johnson, D.B. (Eds.) 2007. "Biomining", Springer-Verlag, Berlin, Heidelberg.

Ekmekci, Z., Demirel, H. 1997. "Effects of galvanic interaction on collectorless flotation behaviour of chalcopyrite and pyrite", International Journal of Mineral Processing 52, pp 31-48.

Eksteen, J.J., Mwase, J.M., Petersen, J.P. 2012. “Energy efficient recovery of precious metals and base metals”, International Patent Number WO 2012/114165 A1, 30 August 2012.

Eksteen, J.J. 2010. “Heap leach options for Akanani and Platreef type ores”. Presentation to board of executives.

Els, E.R., Lorenzen, L., Aldrich, C. 2000. “The adsorption of precious metals and base metals on a quaternary ammonium group ion exchange resin”, Minerals Engineering 13, no. 4, pp 401-414.

Evans, T. 2007. “Comments on Bioleaching of PGMs to accompany Report Nos. 102/CON/MS0006/SB and 111/MS030/SB”, Lonmin Platinum.

Ferron, C.J., Hamilton, C.C., Valeyev, O., McKay, N., 2006. “The effect of the mineralogy of the platinum group metals on their leachability during the Platsol™ leach process”. SGS Minerals Services Technical Paper 2006-03. Retreived 25 March 2015 from http://www.sgs.co.za/~/media/Global/Documents/Technical%20Documents/SGS%20Technical%20Papers/SGS%20MIN%20TP2006%2003%20PGM%20Mineralogy%20in%20PLATSOL%20Leachability.pdf

Fleming, C.A. 2002. “PLATSOL™ process provides a viable alternative to smelting”, SGS Mineral Services Technical Paper 2002-01. Retrieved 25 March 2015 from http://www.sgs.co.za/~/media/Global/Documents/Technical%20Documents/SGS%20Technical%20Papers/SGS%20MIN%20TP2002%2001%20Platsol%20Process%20Alternative%20to%20Smelting.pdf.

Free, M.L. 2013. “Hydrometallurgy: Fundamentals and Applications”, John Wiley & Sons Inc., Hoboken, New Jersey, USA.

Gentina, J.C and Acevedo, F. 2013. “Application of bioleaching to copper mining in Chile”. Electronic Journal of Biotechnology, vol. 6, Issue 3, Retrieved 15 January 2014 from http://www.ejbiotechnology.info/index.php/ejbiotechnology/issue/view/86/showToc

Ghorbani, Y., Franzidis, J-P., Petersen, J. 2015. "Heap leaching technology-current state, innovations and future directions: A review”, Mineral Processing and Extractive Metallurgy

Review. Retrieved 23 January 2016 from http://www.tandfonline.com/doi/pdf/10.1080/08827508.2015.1115990.

Giandomenico, C.M. 2000. "Platinum-group metals, compounds", Kirk-Othmer Encyclopedia of Chemical Technology-Online. Published online: 4 December 2000, Retrieved online 22 September 2007 From http://onlinelibrary.wiley.com/doi/10.1002/0471238961.1612012007090114.a01/pdf

Gold Fields. 2013. "Integrated annual review 2013", Retrieved from https://www.goldfields.co.za/reports/annual_report_2013/minerals/reg-grow-arctic-level.php.

Gonzalez, R., Gentina, J.C., Acevedo, F. 2004. "Biooxidation of a gold concentrate in a continuous stirred tank reactor: mathematical model and optimal configuration", Biochemical Engineering Journal, vol. 19, pp 33-42.

Green, B.R., Smit, D.M.C., Maumela, H., Coetzer G. 2004. "Leaching and recovery of platinum group metals from UG-2 concentrates", The Journal of The South African Institute of Mining and Metallurgy, pp 323-332. Retrieved online 25 March 2015 from http://www.saimm.co.za/Journal/v104n06p323.pdf.

Greenwood, N.N., Earnshaw, A. 1997. "Chemistry of elements", second edition, Pergamon Press plc, Elsevier Butterworth-Heinemann, Burlington, MA.

Grosse, A.C., Dicinoski, G.W., Shaw, M.J., Haddad, P.R. 2003. "Leaching and recovery of gold using ammoniacal thiosulfate leach liquors (a review)", Hydrometallurgy Vol. 69, pp1-21.

Grumet, P. 2003. "Precious metal recovery from spent catalysts", Platinum Metals Review, 47 (4), 163-166.

Gupta, C.K., Mukherjee, T.K. 1990. "Hydrometallurgy in Extraction Processes Volume I", CRC Press, Boston.

Habashi, F. 1999. “Hydrometallurgy, textbook of”, Second edition, Metallurgie Extractive Quebec, Quebec City, Canada.

Hackl, R.P., Dreisinger, D.B., Peters, E., King, J.A. 1995. “Passivation of chalcopyrite during oxidative leaching in sulfate media”, HydrometaIlurgy 39, pp 25-48.

Harvey, T.J., Holder, N., Stanek, T. 2002. “Thermophilic bioleaching of chalcopyrite with GEOCOAT® Process”, Presented at Alta 2002 Nickel/Cobalt 8-Copper 7 Conference, Perth, Australia.

Henke, K.J. and Hutchison, A. 2009. “Arsenic Chemistry”. Chapter 2 in Henke, K.J. (Ed). 2009. “Arsenic: Environmental chemistry, health threats and waste treatment”, John Wiley & Sons Ltd, Great Britain, Chippenham, Wiltshire

Hewitt, D., Breuer, P., Jeffery, C. n.d. “Cyanide detoxification of cyanide tails and process streams”. Retrieved 18 August 2015 from https://publications.csiro.au/rpr/download?pid=csiro:EP123765&dsid=DS3

Huang, K., Chen, J., Chen, Y., Zhao, J., Li, Q., Yang, Q., Zhang, Y. 2006. “Enrichment of platinum group metals (PGMs) by two-stage selective pressure leaching cementation from low-grade Pt-Pd sulphide concentrates”, Metallurgical and Materials Transactions B, Volume 37B, pp 697-701

Jha, M.K., Lee, J., Kim, M., Jeong, J., Kim, B., Kumar, V. 2013. “Hydrometallurgical recovery/recycling of platinum by the leaching of spent catalysts: A review”, Hydrometallurgy 133, pp 23-32.

Jergensen, G.V. (editor). 1999. “Copper leaching, solvent extraction, and electrowinning technology”, Society for Mining, Metallurgy, and Exploration, Inc. USA

Johnson Matthey. 2015. “Summary of Platinum: supply & demand in 2014”, PGM market report May 2015. Retrieved 14 January 2016 from http://www.platinum.matthey.com/documents/new-item/pgm%20market%20reports/pgm%20market%20report%20may%202015.pdf

Jones, R.A., Nesbitt, H.W. 2002. “XPS evidence for Fe and As oxidation states and electronic states in loellingite ($FeAs_2$)”, American Mineralogist, Volume 87, pp 1692-1698

Jones, R.T., 2009. “Towards commercialisation of Mintek’s ConRoast process for platinum smelting”. Retrieved online 10 July 2015 from http:// http://www.mintek.co.za/Pyromet/Files/2009Jones-ConRoast.pdf

Kappes, D.W. 2002. Precious metal heap leach design and practice. In Mular, A.L., Halbe, D.N., Barratt, D.J. (Eds.) 2002. Minerals Processing Plant design, Practice, and Control-Proceedings. Volume 2, Society for Mining, Metallurgy, and Exploration, Inc. (SME).

Kelly, G., Ahlborn, G., Carretero, E., Gunn, M., Harvey, P. 2008. “Laboratory and Demonstration Scale Optimization of the Quebrada Blanca Heap Leach Bacterial Regime Using Geoleach™”, II taller Internacional de Procesos Hidrometalurgicos-HydroProcess 2008, Mayo 14-16, 2008, Hotel Sheraton, Santiago, Chile.

Khoshkhoo, M., Dopson, M., Shchukarev, A., Sandstrom, A. 2014. “Chalcopyrite leaching and bioleaching: An X-ray photoelectron spectroscopic (XPS) investigation on the nature of hindered dissolution”, Hydrometallurgy, Volume 149, pp 220-227.

Klauber, C., Parker, A., Van Bronswijk, W., Watling, H.R. 2001. “Sulphur speciation of leached chalcopyrite surfaces as determined by X-ray photoelectron spectroscopy”, International Journal of Mineral Processing 62, pp 65–94

Kononova, O.N., Melnikov, A.M., Borisova, T.V., Krylov, A.S. 2011. “Simultaneous ion exchange recovery of platinum and rhodium from chloride solutions”, Hydrometallurgy 105, Issues 3-4, pp 341-349.

Kruyswijk, L. 2009. “Electrorefining of base metal refinery residue copper alloy for platinum metal group metal recovery”, MSc thesis, Department of Chemical Engineering, University of Cape Town.

Kuczynski, R. J., Atkinson, G. B., Walters, L. A. 1992. “High-temperature cyanide leaching of platinum group metals from automobile catalysts-process development unit”, Bureau of Mines Report of Investigation, RI 9428, United States Department of the Interior.

Leahy, M.J., Schwarz, M.P. 2009. “Modelling jarosite precipitation in isothermal chalcopyrite bioleaching columns”, Hydrometallurgy 98, pp 181-191.

Liddell, K.S., Adams, M.D., 2012. “Kell hydrometallurgical process for extraction of platinum group metals and base metals from flotation concentrates”, J. South.
Afr. Inst. Min. Metall., 112

Liebenberg, C.J., Dorfling, C., Akdogan, G., Bradshaw, S.M., Eksteen, J.J. 2013. “The recovery of copper from pregnant sulphuric acid bioleach solution with developmental resin Dow XUS43605”, The Journal of the Southern African Institute of Mining and Metallurgy, vol. 113, no. 5, pp 389-397.

Lien, L. 2008, “H W Process technologies’ Engineered Membrane Separation® (EMS®) systems for hydrometallurgical applications”, Proceedings for Hydrometallurgy 2008-6th International Symposium, Society of Mining, Metallurgy and Exploration , 17-20 August, J W Marriot Desert Ridge Resort, Phoenix, Arizona.

Luthy, R.G., Bruce, S.G. 1979. “Kinetics of reactions of cyanide and reduced sulphur species in aqueous solution”, Environmental Science and Technology, vol. 13, no. 12, pp 1481-1487.

Marinov, A.M., Brebbia, C.A. 2010. “Water Polution”, WIT Press, Great Britain.

Marsden, J., House, I. 2006. “The Chemistry of Gold Extraction. Society of Mining, Metallurgy and Exploration”, Second Edition, Colorado, USA

Mason, L.J., Rice, N.M. 2002. “The adaptation of Thiobacillus ferrooxidans for the treatment of nickel-iron sulphide concentrates”, Minerals Engineering 15, pp 795-808.

McInnes, C.M., Sparrow, G.J., Woodstock, J.T. 1994. “Extraction of platinum, palladium and gold by cyanidation of Coronation Hill ore’, Hydrometallurgy 35, pp 141-159.

Merkle, R.K.W., McKenzie, A.D. 2002. “The Mining and Beneficiation of South African PGE Ores – An Overview”. In Cabri, L.J. (Editor). 2002. “The Geology, Geochemistry, Mineralogy and Mineral Beneficiation of Platinum-Group Elements.” CIM Special Volume 54, Canadian Institute of Mining, Metalurgy and Petroleum, Quebec, Canada, pp 793-809.

Milbourne, J., Tomlinson, M., Gormely, L., 2003. Use of hydrometallurgy in direct processing of base metal/PGM concentrates. Hydrometallurgy, 625.

Miller, P., Brown, A. 2005. “Bacterial oxidation of refractory gold concentrates”, in Adams, M.D. (editor). 2005. “Advances in gold ore processing”, Developments in mineral processing, Elsevier, Mutis Liber Pty Ltd., Guildford, Western Australia.

Mintek. n.d. CYNOPROBE: Online, in Process Cyanide Analysis, Retrieved July 2012 from: http://www.mintek.co.za/wp-content/uploads/2011/09/Cynoprobe-Brochure_en.pdf

Mogosetsi, D. 2006. “Scoping flotation work on sample from the Akanani platinum project”, External Mintek restricted report, no. 4272.

Mogase, B.M.S. 2012. “An electrochemical study of the oxidation of platinum employing ozone as oxidant and chloride as complexing agent”, MSc Thesis, Department of Chemistry, North-West University.

Moulder, J.F., Stickle, W.F., Sodol, P.E., Bomben, K.D. 1995. “Handbook of X-ray Photoelectron Spectroscopy”, Physical Electronics, Inc, Eden Prairie, Minnesota 55344, USA.

Mountain, B. W., Wood, S. A. 1987. “Solubility and transport of platinum-group elements in hydrothermal solutions: thermodynamic and physical chemical constants”, Prichard, H. M. Geo-platinum 87, Open University, pp57-82.

Mpinga, C.N., Eksteen, J.J., Aldrich, C., Dyer, L. 2015. “Direct leach approaches to Platinum Group Metal (PGM) ores and concentrates: A review”, Minerals Engineering 78, pp. 93-113.

Mpinga, C.N., Bradshaw, S.M., Akdogan, G., Snyders, C.A., Eksteen, J.J., 2014a. "The extraction of Pt, Pd, and Au from an alkaline cyanide simulated leachate by granular activated carbon", Minerals Engineering 55 pp. 11-17.

Mpinga, C.N., Bradshaw, S.M., Akdogan, G., Snyders, C.A., Eksteen, J.J., 2014b. "Evaluation of the Merrill-Crowe process for the simultaneous removal of platinum, palladium and gold from cyanide leach solution", Hydrometallurgy 142, pp 36-45.

Mwase, J.M., Petersen, J., Eksteen, J.J. 2012a. "A conceptual flowsheet for heap leaching platinum group metals (PGMs) from a low-grade ore concentrate", Hydrometallurgy 111-112, pp. 129-135.

Mwase, J.M., Petersen, J., Eksteen, J.J. 2012b. "Assessing a two-stage heap leaching process for Platreef flotation concentrate", Hydrometallurgy, 129-130, pp74-81.

Mwase, J.M. 2009. "Hydrometallurgical extraction of platinum group metals from a low-grade ore concentrate", MSc dissertation, Department of Chemical Engineering, University of Cape Town.

Mycroft, J.R., Nesbitt, H.W., Pratt, A.R. 1995. "X-ray photoelectron and Auger electron spectroscopy of air-oxidized pyrrhotite:Distribution of oxidized species with depth", Geochimica et Cosmochimica Acta, vol. 59, no. 4, pp 721-733.

Neale, J. 2012. "The application of bioleaching to base metals in Southern Africa: Prospects and opportunities", Bio-mining & Acid Rock Drainage in S.A. seminar, University of Cape Town, Cape Town, 23 November.

Nesbitt, H.W., Reinke, M. 1999. "Properties of As and S at NiAs, NiS and $Fe_{1-x}S$ surfaces, and reactivity of niccolite in air and water", American Mineralogist, Volume 84, pp 639-649.

Newell, A.J.H. 2008. "The processing of platinum group metals (PGMs)-Part 1", Pincock Perspectives, Consultants for mining and financial solutions, Issue no. 89-March 2008, Retrieved online 12 February 2010 From http://pincock.com/perspectives/Issue89-PGM-Processing-Part1.pdf

Norris, P.R., Owen, J.P. 1993. “Mineral sulphide oxidation by enrichment cultures of novel thermoacidophilic bacteria”, FEMS Microbiology Reviews, vol. 11, Issues 1-3, pp 51-56.

Nsimba, E.B. 2009. “Cyanide and cyanide complexes in the gold-mine polluted land in the East and Central Rand Goldfields, South Africa”, MSc dissertation, University of Witwatersrand, Johannesburg, South Africa.

Oberthür, T. 2002. “Platinum-group element mineralization of the Great Dyke, Zimbabwe”, In Cabri, L.J. (Editor). 2002, *“The Geology, Geochemistry, Mineralogy and Mineral Beneficiation of Platinum-Group Elements”,* CIM Special Volume 54, Canadian Institute of Mining, Metalurgy and Petroleum, Quebec, Canada.

Oberthür, T., Weiser, T.W., Gast, L., Lodziak, J., Klosa, D., Wittich, C. 1998. “Detrital platinum group minerals in rivers along the Great Dyke, and the Somabula gravels, Zimbabwe”, In 8th International Platinum Symposium. South African Institute of Mining and Metallurgy, Symposium Series S18, pp 289-292.

Oblonsky, L.J., Ryan, M.P., Isaacs, H.S. 2000. “In situ XANES study of the formation and reduction of the passive formed on Fe in acetate solution”, Corrosion Science 42 p229-241.

Ojumu, T.V., Petersen, J., Hansford, G.S. 2008. “The effect of dissolved cations on microbial ferrous-iron oxidation by Leptosprillum ferriphilum in continuous culture”. Hydrometallurgy 94, pp 64-76.

Olvera, O.G., Rebolledo, M., Asselin, E. 2015. “Atmospheric ferric sulfate leaching of chalcopyrite: Thermodynamics, kinetics and electrochemistry”, Hydrometallurgy, In press, available online 25 September 2015.

Ozkaya, B., Sahinkaya, E., Nurmi, P., Kaksonen, A.H., Puhakka, J.A. 2007 “Iron oxidation and precipitation in a simulated heap leaching solution in a Leptospirillum ferriphilum dominated biofilm reactor”, Hydrometallurgy, vol. 88, pp 67-74.

Parker, A., Klauberb, C., Kougianosa, A., Watling, H.R., Van Bronswijk, W. 2003. "An X-ray photoelectron spectroscopy study of the mechanism of oxidative dissolution of chalcopyrite", Hydrometallurgy 71, pp 265-276.

Petersen, J. and Dixon, D.G. 2002. "Thermophilic Heap Leaching of A Chalcopyrite Concentrate", Minerals Engineering 15 (11), pp 777-785.

Petersen, J. and Dixon, D.G. 2007. "Modelling zinc heap leaching", Hydrometallurgy, vol. 85, 2-4, pp 127-143.

Plumb, J.J., Hawkes, R.B., Franzmann, P.D. 2007. "The microbiology of moderately thermophilic and transiently thermophilic ore heaps", In Rawlings, D.E., Johnson, D.B. (Eds.) 2007. "Biomining", Springer-Verlag, Berlin, Heidelberg.

Plumb, J.J., Gibbs, B., Sttot, M.B., Robertson, W.J., Gibson, J.A.E., Nichols, P.D., Watling, H.R., Franzmann, P.D. 2002. "Enrichment and characterisation of thermophilic acidophiles for the bioleaching of mineral sulphides", Minerals Engineering 15, pp 787-794.

Polinares EU Policy on Natural Resources. 2012. "Fact Sheet: Platinum Group Metals", working paper no. 35 Retrieved 23 January 2016 from http://www.polinares.eu/docs/d2-1/polinares_wp2_annex2_factsheet1_v1_10.pdf.

Power, G.P., Ritchie, I.M. n.d. "Mixed Potentials: Experimental illustrations of an important concept in practical electrochemistry", Journal of Chemical Education.

Pradhan, N., Nathsarma, K.C., Srinivasa Rao, K., Sukla, L.B., Mishra, B.K. 2008. "Heap bioleaching of chalcopyrite: A review", Minerals Engineering 21, pp 355-365.

Pratt, A.R., Muir, I.J., Nesbitt, H.W. 1994. "X-ray photoelectron and Auger electron spectroscopic studies of pyrrhotite and mechanism of air oxidation", Geochimica et Cosmochimica Acta, vol. 58, no. 2, pp 827-841.

Qin, W., Zhen, S., Yan, Z., Campbell, M., Wang, J., Liu, K., Zhang, Y. 2009. "Heap bioleaching of a low-grade nickel-bearing sulfide ore containing high levels of magnesium as olivine, chlorite and antigorite". Hydrometallurgy, vol. 98, pp 58-65.

Ream, B.P., Schlitt, W.J., 1997. "Kennecott's Bingham Canyon heap leach program, part 1: the test heap and SX-EW pilot plant", In: ALTA, Copper Hydrometallurgy Forum, Brisbane, Australia.

Rapson, W.S. 1997. "New chloride leaching process for gold extraction from refractory ores". Gold Bulletin 1997, 30(1).

Ramanotsi, M. 2011. "Evaluation of selected treatment strategies to improve the flotation performance of altered Merensky platinum ore". MSc thesis, University of Cape Town.

Riekkola-Vanhanen, M. 2010. "Production Technologies: Talvivaara Mining Company Plc", Talvivaara Technical Seminar May 2010 presentation.

Roxburgh, B. 2011. "Exeter reports progress on the Caspiche stand-alone oxide pre-feasibility study", Retrieved online October 2012 from http://www.exeterresource.com/pdf/2011_news/Exeter_news_110315.pdf

Saari, P., Riekkola-Vanhanen, M. 2011. "Talvivaara bio-heap leaching process", The Southern Africa Institute of Mining and Metallurgy, International Conference, Percolation leaching: The status globally and in southern Africa, Symposium Series S69, pp. 145-164, 7-9 November 2011.

Sasaki, K., Takatsugi, K., Ishikura, K., Hirajima, T. 2010. "Spectroscopic study on oxidative dissolution of chalcopyrite, enargite and tennantite at different pH values", Hydrometallurgy 100, pp 144-151.

Schay, S. 2009. "Drill core characterization and flotation test work on 13 drill cores from the Akanani depost", Mintek external report 5392.

Schoeman, E., Bradshaw, S.M., Akdogan, G., Eksteen, J.J. 2012. “The recovery of platinum, palladium and gold from heap solution with use of ion exchange resins”, Proceedings of the 5th International Platinum Conference, 18-20th September, Sun City, South Africa, Vol. II, pp 729-742.

Scheffel, R.E. 2002. “Copper heap leach design and practice”, in Mular, A.L., Halbe, D.N., Barratt, D.J. (Eds.) 2002. “Minerals Processing Plant design, Practice, and Control-Proceedings”, vol. 2, Society for Mining, Metallurgy, and Exploration, Inc. (SME).

Schouwstra, R., P.; Kinloch, E., D. 2000, “A short geological review of the Bushveld Complex”, Platinum Metals Review, vol. 44, Issue 1, pp33-39.

Schultz, K.J., Chandler, V.W., Nichilson, S.W., Piatak, N., Seal II, R.R., Woodruff, L.G., Zientek, M.L. 2010. “Magmatic sulphide-rich nickel-copper deposits related to Picrite and/or Tholeiitic Basalt Dike-Sill Complexes: A preliminary deposit model”, Open-file report 2010-1179, U.S. Department of the Interior, U.S. Geological Survey. Retrieved online 12 January 2016 from http:// http://pubs.usgs.gov/of/2010/1179/pdf/ofr2010-1179.pdf

Searby, G.E. 2006. “An investigation of the kinetics of thermophilic microbial ferrous iron oxidation in continuous culture”, PhD thesis, Department of Chemical Engineering, University of Cape Town.

Seymour, R.J., O'Farrelly, J.I. 2001. “Platinum Group Metals”, Kirk-Othmer Encyclopedia of Chemical Technology-Online. Published online: 13 July, 2001, Retrieved online 22 September 2007 From http://www.mrw.interscience.wiley.com/emrw/9780471238966/kirk/article/platseym.a01/current/pdf.

Shackleton, N.J., Malysiak, V., O’Connor, C.T. 2007a. “Surface characteristics and flotation behavior of platinum and palladium arsenides”, International Journal of Mineral Processing 85, 25-40.

Shackleton, N.J., Malysiak, V., O’Connor, C.T. 2007b. “Surface characteristics and flotation behavior of platinum and palladium tellurides”, Minerals Engineering 20, 1232-1245.

Shamaila, S., O'Connor, C. T. 2008. "The role of synthetic minerals in determining the relative flotation behaviour of Platreef PGE tellurides and arsenides", Minerals Engineering 21, pp 899-904.

Sibrell, P.L., Atkinson, G.B., Walters, L.A. 1994. Cyanide leaching chemistry of Platinum Group Metals. United States Department of the Interior, Bureau of Mines, RI 9507, ISSN 1066-5552.

Smith, M.E. 2004. "Applying the "Seven Questions" to heap leaching". The Mining Record, Denver, CO, USA, June, 2004.

Snyders, C.A., Mpinga, C.N., Bradshaw, S.M., Akdogan, G., Eksteen, J.J. 2013. "The application of activated carbon for the adsorption and elution of platinum group metals from dilute cyanide solutions", The Journal of the Southern African Institute of Mining and Metallurgy, vol. 113, no. 5, pp 381-388.

Solomon, N. 2010. "Effect of HPGR on platinum bearing ores and the flotation response as compared to the conventional ball mill". MSc thesis, Department of Chemical Engineering, University of Cape Town.

Song, C., Zhang, J. n.d. "Electrocatalytic oxygen reduction reaction" Retrieved 9 April 2016 from
http://www.springer.com/cda/content/document/cda_downloaddocument/9781848009356-c1.pdf?SGWID=0-0-45-602204-p173838515.

Sperrylite. n.d. Handbook of Mineralogy Retrieved 8 March 2016 from http://rruff.info/doclib/hom/sperrylite.pdf.

Stander, G.J., Henzen, M.R., Funke, J.R. 1970. "The disposal of polluted effluents from Mining, Metallurgical and Metal Finishing Industries, their effects on receiving water and remedial measures", Journal of the South African Institute of Mining and Metallurgy, December 1970, 95-103.

Stewart, M., Kappes, D. 2011. "SART for copper control in cyanide heap leaching", The Southern Africa Institute of Mining and Metallurgy, International Conference, Percolation

leaching: The status globally and in southern Africa, Symposium Series S69, pp145-164, 7-9 November 2011.

Stott, M.B., Watling, H.R., Franzmann, P.D., Sutton, D. 2003. "Comparative leaching of chalcopyrite by selected acidophilic bacteria and archaea", Geomicrobiology Journal 20, pp 215-230.

Stott, M.B., Watling, H.R., Franzmann, P.D., Sutton, D. 2000. "The role of iron-hydroxy precipitates in the passivation of chalcopyrite during bioleaching", Minerals Engineering 13, No 10-1, pp1117-1127.

Tempel, K., 2003. "Commercial biooxidation challenges at Newmont'sNevada operations", In: 2003 SME Annual Meeting, Preprint 03-067, Soc Mining, Metallurgy and Exploration, Littleton, Colo.

University of Cape Town-Anglo Platinum. 2007. "Introduction to Hydrometallurgy and Hydrometallurgical Operations at Anglo Platinum". Short Course.

van Rensberg, S.J., Lotz, P.W. 2010. "Kinetic cyanide and arsenic data generation during gold leach tests by MINTEK Advanced Leach Facility", presented at the Precious Metal 10 conference, Falmouth, UK, 15-16 June.

van Zyl, A.W., Harrison, S.T.L., van Hille, R.P. 2011. "Biodegradation of thiocyanate by a mixed microbial population". In: Proceedings of the 11th International Mine
Water Association Congress, pp. 119–123.

van Zyl, A.W., Huddy, R., Harrison, S.T.L., van Hille, R.P., 2015. "Evaluation of the ASTER™ process in the presence of suspended solids". Minerals Engineering 76, pp 72-80.

van Zyl, D., Henderson, M., Cobb, B. 1990. "Economic aspects of pad construction costs on heap leach projects", International Journal of Mining and Geological Engineering 8, 275-286.

Vermaak, M. K. G. 2005. "Fundamentals of the flotation behaviour of palladium bismuth tellurides", PhD thesis, University of Pretoria.

Vladimir, S., Moran, R.E. 2006. “Environmental occurrence and impacts of arsenic at gold mining sites in the western united states”. Mine Water and the Environment, International Mine Water Association 2006, Lisboa 90. Retrieved online June 2011 from: http://www.imwa.info/bibliographie/09_14_181-191.pdf.

Von Gruenewaldt, G. 1977. “The mineral resources of the Bushveld Complex”, Minerals Science Engineering, vol. 9, no. 2, pp 83-95.

Watling, H.R. 2008. “The bioleaching of nickel-copper sulphides”, Hydrometallurgy 91, pp 70-88.

Watling, H.R. 2006. “The bioleaching of sulphide minerals with emphasis on copper sulphides — A review”, Hydrometallurgy 84, pp 81–108.

Xia, J., Yang, Y., He, H., Zhao, X., Liang, C., Zheng, L., Ma, C., Zhao, Y., Nie, Z., Qiu, G. 2010. “Surface analysis of sulfur speciation on pyrite bioleached by extreme thermophile Acidianus manzaensis using Raman and XANES spectroscopy”, Hydrometallurgy 200 p129-135.

Xie, F., Dreisinger, D. 2009. “Use of ferricyanide for gold and silver cyanidation”, Transactions of Nonferrous Metals Society of China 19, 714-718.

Xie, F., Dreisinger, D., Lu, J. 2008. “The novel application of ferricyanide as an oxidant in the cyanidation of gold and silver”, Minerals Engineering 21, 1109-1114.

Xie, F., Dreisinger, D. 2007. “Leaching of silver sulphide with ferricyanide-cyanide solution”, Hydrometallurgy 88, pp 98-108.

Yang, Y., Harmer, S., Chen, M. 2015. “Synchrotron-based XPS and NEXAFS study of surface chemical species during electrochemical oxidation of chalcopyrite”, Hydrometallurgy, Volume 156, pp 89-98.

Yang, Y., Liu, W., Chen, M. 2013. “A copper and iron K-edge XANES study on chalcopyrite leached by mesophiles and moderate thermophiles”, Minerals Engineering 48 p31-35.

Yuzer, H., Dogan, H., Koroglu, J., Kocakusak, S. 2000. “Analysis of sulfide layer on gallium arsenide using X-ray photoelectron spectroscopy”, Spectrochimica Acta Part B 55, pp 991-996.

Zanbak, C. 2012. “ Heap leaching technique in mining” Retrieved online 25 August 2015 from http://www.euromines.org/files/mining-europe/mining-techniques/batforheapleaching-feb2013-c.zanbak-euromines.pdf

Zientek, M.L., Cooper, R.W., Corson, S.R., Geraghty, E.P. 2002. “Platinum-group metal mineralization in the Stillwater Complex, Montana”, In Cabri, L.J. (Editor). 2002, “The Geology, Geochemistry, Mineralogy and Mineral Beneficiation of Platinum-Group Elements”, CIM Special Volume 54, Canadian Institute of Mining, Metalurgy and Petroleum, Quebec, Canada.